AWARD NUMBER:

W81XWH-09-1-0658

TITLE:

New Advanced Technologies in Stem Cell Therapy

PRINCIPAL INVESTIGATOR:

Johnny Huard, Ph.D.

CONTRACTING ORGANIZATION:

University of Pittsburgh

Pittsburgh, PA 15260

REPORT DATE:

September 2012

TYPE OF REPORT:

Annual

PREPARED FOR: **U.S. Army Medical Research and Materiel Command**
Fort Detrick, Maryland 21702-5012

DISTRIBUTION STATEMENT:

Approved for public release; distribution unlimited

The views, opinions and/or findings contained in this report are those of the author(s) and should not be construed as an official Department of the Army position, policy or decision unless so designated by other documentation.

REPORT DOCUMENTATION PAGE

Form Approved
OMB No. 0704-0188

1. REPORT DATE	**2. REPORT TYPE**	**3. DATES COVERED**
1 September 2012	Annual	1 Sep 2011 – 31 Aug 2012

4. TITLE AND SUBTITLE
New Advanced Technologies in Stem Cell Therapy

5a. CONTRACT NUMBER

5b. GRANT NUMBER
W81XWH-09-1-0658

5c. PROGRAM ELEMENT NUMBER

6. AUTHOR(S)
Johnny Huard, Ph.D.

Email: jhuard@pitt.edu

5d. PROJECT NUMBER

5e. TASK NUMBER

5f. WORK UNIT NUMBER

7. PERFORMING ORGANIZATION NAME(S) AND ADDRESS(ES)
University of Pittsburgh
Pittsburgh, PA 15260

8. PERFORMING ORGANIZATION REPORT NUMBER

9. SPONSORING / MONITORING AGENCY NAME(S) AND ADDRESS(ES)
U.S. Army Medical Research and Materiel Command
Fort Detrick, Maryland 21702-5012

10. SPONSOR/MONITOR'S ACRONYM(S)

11. SPONSOR/MONITOR'S REPORT NUMBER(S)

12. DISTRIBUTION / AVAILABILITY STATEMENT
Approved for Public Release; Distribution Unlimited

13. SUPPLEMENTARY NOTES

14. ABSTRACT
See Next 2 Pages

15. SUBJECT TERMS Project 1: Duchenne Muscular Dystrophy (DMD), human muscle-derived cells (hMDC), myoendothelial cells, pericytes, hMDC transplantation, angiogenesis Project 2: Hepatacyte transplantation, inducible pluripotent stem (iPS)cells, alpha-1-antitrypsin (AT) deficiency, PiZ mice

16. SECURITY CLASSIFICATION OF:			**17. LIMITATION OF ABSTRACT**	**18. NUMBER OF PAGES**	**19a. NAME OF RESPONSIBLE PERSON**
					USAMRMC
a. REPORT	**b. ABSTRACT**	**c. THIS PAGE**			**19b. TELEPHONE NUMBER** *(include area code)*
U	U	U	UU	88	

Standard Form 298 (Rev. 8-98)
Prescribed by ANSI Std. Z39.18

Abstracts

Project 1

Background: We have isolated and characterized a population of skeletal muscle-derived stem cells (MDSCs) that display a greatly improved skeletal and cardiac muscle transplantation capacity when compared to skeletal muscle myoblasts. The MDSCs' ability to withstand oxidative and inflammatory stresses appears to be the single most important factor for their improved transplantation capacity. Although the true origin of MDSCs remains unclear, their high degree of similarity with blood vessel-derived stem cells suggests their potential origin could be from the vascular wall. We have recently isolated two distinct populations of cells from the vasculature of human skeletal muscle known collectively as human skeletal muscle-derived cells (hMDCs). The two populations are myo-endothelial cells and pericytes and both can repair skeletal and cardiac muscles in a more effective manner than myoblasts, as is observed with murine MDSCs.

In the current proposal we intend to evaluate and compare the regeneration capacity of these two hMDC populations after their implantation into the skeletal muscle of immunodeficient/dystrophic (SCID/mdx) mice. We will then investigate the influence that sex has on the regeneration and repair capacity of the hMDCs endowed with the greatest regeneration capacity (either myo-entothelial cells or pericytes). Finally we will investigate the influence that age plays on the regeneration capacity of the cells.

Study Design: We will investigate the effects of cell survival, proliferation, resistance to stress, and neo-angiogenesis on the regeneration capacity of the hMDCs implanted into the skeletal muscle of SCID/mdx mice Since we have observed that female murine MDSCs display an improved transplantation capacity in skeletal muscle when compared to male MDSCs, we will determine the influence that sex has on the hMDCs. Due to the fact that MDSCs isolated from aged mice have a lower skeletal muscle regeneration index than MDSCs isolated from young mice, we will also investigate the influence that donor and host age has on the isolated hMDCs.

Relevance: This project will enable us to further assess the feasibility of using hMDC transplantation to improve the function of skeletal muscle that has been damaged by Duchenne muscular dystrophy (DMD) and other muscle degenerative disorders and injury.

Technical Objective #1: To compare the regeneration capacities of human muscle-derived myo-endo cells and pericytes when implanted in the skeletal muscle of *SCID/mdx* mice and select the optimal cell type to proceed with Technical Objectives 2 and 3.

> *<u>Hypothesis 1</u>: A differential regeneration capacity will be observed in skeletal muscle of SCID/mdx mice between myo-endo cells and pericytes.*

Technical Objective #2: To investigate the influence of sex on the regeneration/repair capacity of the hMDCs implanted in the skeletal muscle of *SCID/mdx* mice.

> *<u>Hypothesis 2</u>: After implantation into skeletal muscle, the hMDCs cells (myo-endo cells or pericytes) endowed with the highest regenerating potential in skeletal muscle will be influenced by the sex of the donor, due to a differential ability to resist stressful conditions.*

Technical Objective #3: To investigate the influence of age on the regeneration/repair capacity of hMDCs implanted in the skeletal muscle of *SCID/mdx* mice.

> *<u>Hypothesis 3</u>: After implantation into skeletal muscle, the hMDCs cells (myo-endo cells or pericytes) endowed with the highest regenerating potential in skeletal muscle will be influenced by the age of the donor due to a differential ability to induce angiogenesis.*

Project 2

Background: Hepatocyte transplantation holds great promise as an alternative to whole organ liver transplantation. Unfortunately, the availability of human hepatocytes is limited. We have shown that functionally normal hepatocytes can be generated from human ES cells (hES). Since human skin fibroblasts can now be genetically modified to produce (iPS) cells with characteristics nearly identical to hES cells, it may be possible to generate hepatocytes from patients using their own cells. We believe the PiZ transgenic mouse model of alpha-1-antitrypsin (AT) deficiency is critical for evaluating the efficacy of stem cell therapies, as hepatocytes without the mutant protein have a selective hepatic repopulation advantage in these mice, and the

PiZ mouse recapitulates the slowly progressing type of disease that affects most patients with chronic liver diseases.

Objective/Hypothesis: Both of the main obstacles to transplantation of stem cells for the treatment of liver disease (the number of livers available and the immunological barrier) might be addressed if liver cells could be generated de novo from precursor cells of the individual to be treated.

Study Design: We will determine the extent to which human patient-specific, inducible pluripotent stem (iPS) cells can be differentiated into primary human hepatocytes. We will then determine the extent to which the PiZ mouse model of AT deficiency can be developed as a platform for pre-clinical testing of hepatic stem cells. Finally, we will identify specific molecules responsible for regenerative and fibrotic signals in the PiZ mouse model of liver disease.

Relevance: This project will determine the extent to which patient-specific hepatic stem cells can be used for regeneration and repair of injuries to the liver and liver failure. A more complete understanding of the mechanisms by which donor stem cells can reduce liver injury and toxin and/or cancer risk should enhance the number of areas where hepatic stem cell transplantation might be effectively applied.

Technical Objective #1: *Determine the extent to which human patient-specific, inducible pluripotent stem (iPS) cells can be differentiated into primary human hepatocytes.*

> **Hypothesis:** Protocols that successfully differentiate mouse and human embryonic stem (ES) cells toward a hepatocyte phenotype will be effective in differentiating human skin cell-derived iPS cells into liver cells.

Technical Objective #2: Determine the extent to which the PiZ mouse model of alpha-1-antitrypsin (AT) deficiency can be developed as a platform for pre-clinical testing of hepatic stem cell transplantation as a treatment for severe liver injury and disease.

> ***Hypothesis:*** *iPS cells differentiated toward a hepatocyte phenotype can engraft and respond normally to proliferative signals in the livers of PiZ mice.*

Technical Objective #3: Utilize laser-capture microdissection, coupled with high-density oligonucleotide array techniques as well as double-label immunofluorescence techniques to identify specific molecules responsible for regenerative and fibrotic signals in the PiZ mouse model of liver disease.

> ***Hypothesis:*** *Transplantation of donor stem cells can ameliorate liver injury and cancer risk in liver disease.*

Table of Contents

Project 1: Muscle stem cell transplantation for Duchenne muscular dystrophy

A) Introduction…….6

B) Body……..7

C) Key Research Accomplishments……23

D) Reportable Outcomes……..24

E) Conclusions……...25

F) References……...26

G) Appendices…….26

H) Manuscripts/Reprints/Abstracts……..26

Project 2: Generation of human hepatocytes from patient-specific stem cells for treatment of life-threatening liver injury

A) Introduction……28

B) Body……..28

C) Key Research Accomplishments……...35

D) Reportable Outcomes……..35

E) Conclusions…….36

F) References……36

Appendices

2: Published Manuscripts, 1 Manuscript under review, 8: Abstracts.....37

Sub-Project 1: Muscle stem cell transplantation for Duchenne muscular dystrophy
PI: Johnny Huard

INTRODUCTION:
We have isolated and characterized a population of skeletal muscle-derived stem cells (MDSCs) that display a greatly improved skeletal and cardiac muscle transplantation capacity when compared to skeletal muscle myoblasts. The MDSCs' ability to withstand oxidative and inflammatory stresses appears to be the single most important factor for their improved transplantation capacity. Although the true origin of MDSCs remains unclear, their high degree of similarity with blood vessel-derived stem cells suggests their potential origin could be from the vascular wall. We have also isolated two distinct populations of cells from the vasculature of human skeletal muscle known collectively as human skeletal muscle-derived cells (hMDCs). The two populations are myoendothelial cells and pericytes and they both can repair skeletal and cardiac muscles in a more effective manner than myoblasts, as is observed with murine MDSCs. In the current proposal we have evaluated and compared the regeneration capacity of these two hMDC populations in vitro and after their implantation into the skeletal muscle of immunodeficient/dystrophic (SCID/*mdx)* mice. We are now in the process of investigating the influence that sex has on the regeneration and repair capacity of the hMDCs endowed with the greatest regeneration capacity which we have determined to be the myoentothelial cell population. Finally we will investigate the influence that age plays on the regeneration capacity of the cells. We will investigate the effects of cell survival, proliferation, resistance to stress, and neo-angiogenesis on the regeneration capacity of the hMDCs implanted into the skeletal muscle of SCID*/mdx* mice Since we have observed that female murine MDSCs display an improved transplantation capacity in skeletal muscle when compared to male MDSCs, we will determine the influence that sex has on the hMDCs. Due to the fact that MDSCs isolated from aged mice have a lower skeletal muscle regeneration index than MDSCs isolated from young mice, we will also investigate the influence that donor and host age has on the isolated hMDCs. This project will enable us to further assess the feasibility of using hMDC transplantation to improve the function of skeletal muscle that has been damaged by Duchenne muscular dystrophy (DMD) and other muscle degenerative disorders and injury.

Over the 1st two years of this grant we were involved with the characterization of 2 populations of hMDCs, myoendothelial cells and pericytes and demonstrated that the myoendothelial cells and pericytes could repair skeletal and cardiac muscle more effectively than myoblasts. As reported 2 years ago, several aspects of the first aim of the project were completed, namely the fluorescent-activated cell sorting (FACS) of the myoendothelial cells, pericytes and myoblasts from cryopreserved human progenitor skeletal muscle cells (hPSMCs); comparisons of the *in vitro* myogenic potential of these populations; and the transplantation of the populations into cardiotoxin-injured skeletal muscle of SCID mice to assess their *in vivo* regenerative capacity. The results showed that the myoendothelial cells possessed a better in vitro myogenic differentiation capacity, as well as, a better in vivo engraftment capacity when transplanted into cardiotoxin injured skeletal muscle using an antibody against human spectrin. The 2nd year of the grant was devoted to in vitro experiments and preliminary in vivo experiments to establish protocols for completing the SOW. During this period we demonstrated on a minimal number of experimental animals that proliferation and myogenic differentiation capacities were greater in the younger experimental animals and that oxidative stress resistance is reduced in MDC's isolated from older individuals. We were also involved with optimizing the media type for MDC expansion and were attempting to identify an optimal dystrophin antibody to use for the in vivo detection of human MDCs in our mouse model of DMD that is also immunocompromised (mdx/SCID). Unfortunately, all but one of the antibodies tested continued to have high levels of background. More importantly was the fact that even after identifying an antibody with reduced background, preliminary studies, where we injected hMDSs into mdx/SCID mice, showed levels of engraftment that were not significantly higher than what is typically observed in control muscles that show myofiber revertant fibers. Two additional tangential studies performed during year 2's performance period showed that immunomodulary properties of MDCs is associated with a reduction in NF-kB/p65 signally and that MDCs with reduced p65 expression could improve the histopathology of a model of DMD that has no dystrophin or utrophin expression known as the dKO (double Knock-Out) mouse when

injected IP. The current year's major focus was to determine why we were experiencing the transplantation difficulties with the mdx/SCID mice. It was imperative to determine why the mdx/SCID mice were generating such high levels of background when injected with hMDCs and whether the hMDCs were actually engrafting or if they were being rejected by this model. We have been aging this colony of mice for 2 years in order to carry out the 3rd aim of this grant, which outlined experiments to compare the transplantation efficiency of old and young hMDCs injected into old and young host mdx/SCID animals.

BODY:

As outlined in our Statement of Work, this Progress Report for "**Sub-Project 1:** Muscle stem cell transplantation for Duchenne muscular dystrophy" will describe our current results related to Technical Objective 1 which is to be completed in Years 1 and 2.

Statement of Work:

Technical Objective #1: To compare the regeneration capacities of human muscle-derived myoendothelial cells and pericytes when implanted in the skeletal muscle of *SCID/mdx* mice and select the optimal cell type to proceed with Technical Objectives 2 and 3.

Hypothesis 1: A differential regeneration capacity will be observed in the skeletal muscle of SCID/mdx mice between myoendothelial cells and pericytes.

Technical Objective #2: To investigate the influence of sex on the regeneration/repair capacity of the hMDCs implanted in the skeletal muscle of *SCID/mdx* mice.

Hypothesis 2: After implantation into skeletal muscle, the hMDCs cells endowed with the highest regenerating potential in skeletal muscle will be influenced by the sex of the donor, due to a differential ability to resist stressful conditions.

Technical Objective #3: To investigate the influence of age on the regeneration/repair capacity of hMDCs implanted in the skeletal muscle of *SCID/mdx* mice.

Hypothesis 3: After implantation into skeletal muscle, the hMDCs cells endowed with the highest regenerating potential in skeletal muscle will be influenced by the age of the donor due to a differential ability to induce angiogenesis.

Technical Objective 1 will be performed during the first 2 years of funding. Years 3 and 4 will be devoted to completing **Technical Objectives 2 and 3**. **Objectives 2 and 3** can be performed simultaneously once we have determined the optimal cell type (myo-endo cells vs. pericyctes) as is outlined in **Technical Objective 1**.

Progress made from 9-1-11 to 8-31-12

Mdx/SCID mice skeletal muscle generates high levels of background when immunostained with an antibody against "human dystrophin".

An ongoing problem exists with the animal model that we were intending to utilize for our transplantation efficiency experiments on aged and young animals using aged and young hMDCs. It is a mouse model that is both deficient in murine dystrophin (mdx) and is immune-compromised (SCID, lacking both T and B cell functional activity). The purpose of utilizing this model was to demonstrate muscle regeneration in a dystrophic animal without eliciting a cellular immune response. When originally created this model demonstrated excellent grafting capacities and very little immune response, however, over the past year we have been experiencing a problem with this model, in that all the anti-human dystrophin antibodies we have been using have been giving us very high levels of background in the skeletal muscle of these mice. Originally we thought that it was a cross reactivity with the cells injected, but soon discovered the antibody was binding in vivo even when only PBS was being injected. The following is a summary of the work we performed over the past year to try and elucidate and correct this problem.

In this 1st set of experiments human myoendothelial (myoendo) cells, pericyte, and preplate cells purchased from Cook Myosite, Inc. were injected into 8 week old mdx/SCID mice and compared with mice injected with vehicle alone (PBS) or not injected at all. The mice were sacrificed 2 weeks post-transplantation. The following is the resulting data which shows very limited engraftment overall and no significance between the groups Figure 1.

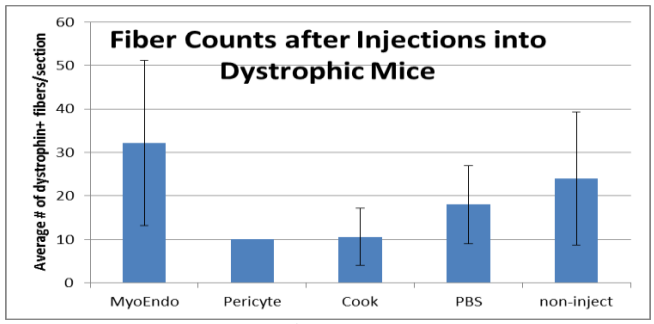

Figure 1 MyoEndo data is taken from 4 separate donor populations injected into 12 separate muscles. Pericyte data is taken from 1 muscle. Cook Myosite data is taken from 1 donor population and 5 muscles. PBS data was taken from 6 separate muscles. Non-injected data was taken from 4 different muscles.

Since previous data indicated that the myoendo populations appeared superior to the pericytes and cells 3 separate populations of the myoendo cells were compared. The data can be seen in Figure 2.

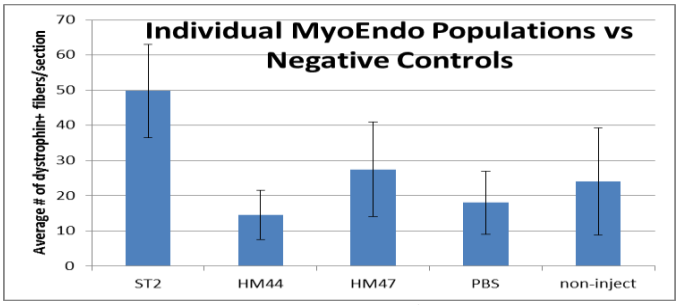

Figure 2: ST2 MyoEndo (69 M) data is taken from 5 separate muscles. HM44 MyoEndo (26 F) data is taken from 4 separate muscle. HM47 MyoEndo (16 M) data is taken from 2 separate muscles. PBS data was taken from 6 separate muscles. Non-injected data was taken from 4 different muscles. Significance between ST2 and PBS ($P > 0.005$); and between ST2 and non-injected ($P > 0.05$) was observed.

Again even when comparing all the populations of myoendo cells we have isolated, only the ST2 population showed any significance in myofiber regeneration; however the number of regenerated myofibers were barely above that observed for revertancy as seen in the PBS and non-injected muscles

Comparison of "dystrophin-positive" myofibers in mdx/SCID after injecting either STS2 myoendo cells in PBS or PBS alone. As is evident in this figure, positive fibers can be seen in both muscles indicating cross reactivity of the antibody with some membrane bound molecule in both the cell injected and PBS injected muscles (Figure 3).

Figure 3

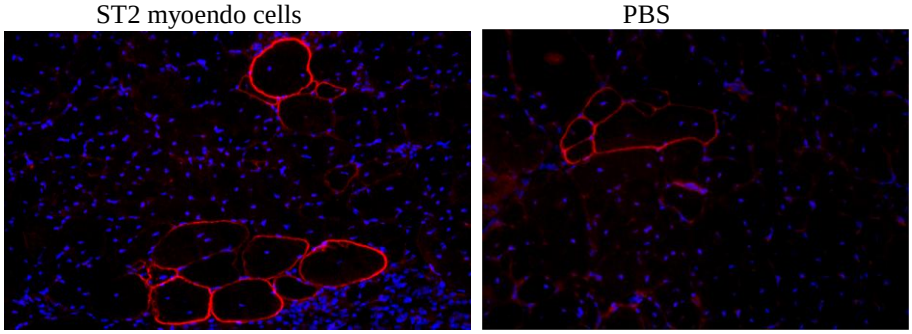

In order to confirm that the cells were actually present in the injected muscle after transplantation we used a retrovirus to label the cells with GFP and 2 days after injecting the cells the mice were sacrificed and the muscles were analyzed for GFP and dystrophin (Figure 4A). Some of the transplanted muscles were allowed to go 14 days prior to harvesting the muscles in order to see if additional time was required for the injected cells to fuse and begin expressing

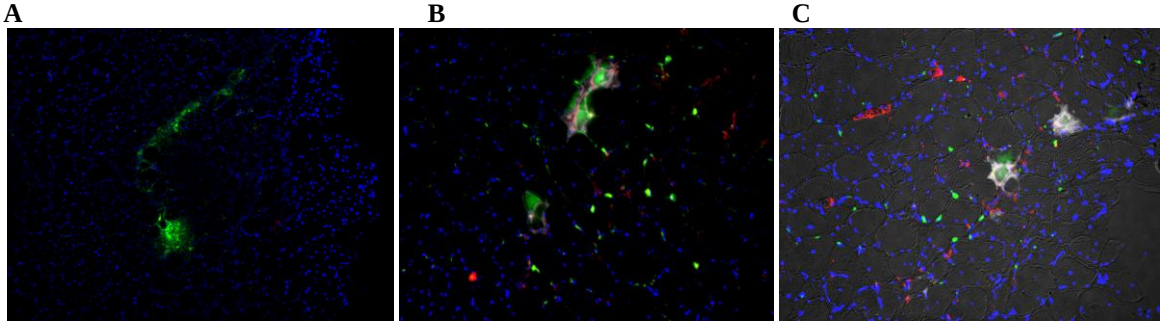

Figure 4: MDCs expressing GFP (green); A and B, anti-GFP (white), C; anti-Dystrophin (red), DAPI (blue)

dystrophin (Figure 4B). To confirm that GFP was truly positive in these sections an anti-GFP antibody was used to detect GFP expression (Figure 4C, white). We have concluded from these data that the injected cells were engrafting but not producing dystrophin; so what are the cells doing?

In order to observe the regenerative processes, if any, in the mdx/SCID skeletal muscle after hMDC injection, we stained the muscles with an antibody against embryonic skeletal myosin heavy chain. Interestingly all the muscles injected, including the PBS injected control, demonstrated a massive amount of myofiber regeneration and there was no difference in the numbers of eMyHC expressing myofibers between any of the groups as can be seen in figure 6.

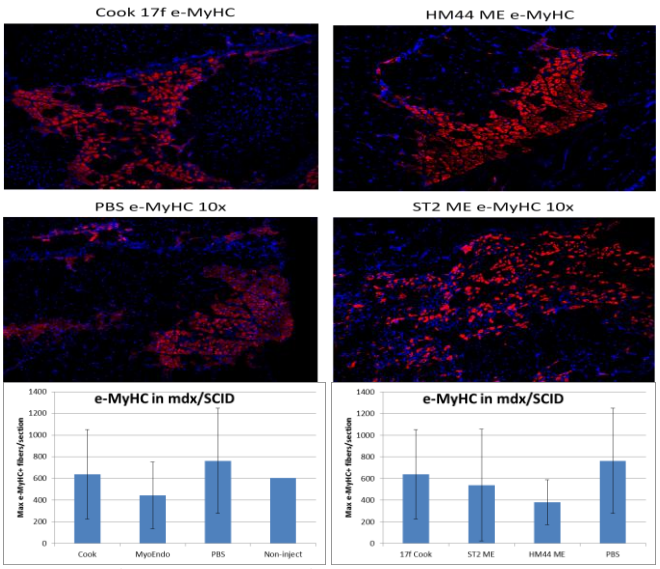

Figure 5: 17f Cook data is taken from 4 separate muscles, ST2 MyoEndo data is taken from 2 separate muscles, HM44, MyoEndo data is taken from 3 separate muscles, PBS data is taken from 4 separate muscles.

In a related set of experiments which confirmed the positive engraftment of the hMDCs and the lack of dystrophin expression, we had injected hMDCs that were being cultured using Platelet-Rich Plasma (PRP) in place of Fetal Bovine Serum (FBS). This experiment was intended to explore the use of an autologously-derived material to expand isolated hMDCs, which would have tremendous benefits for clinical applications of the hMDCs. In this experiment PRP-expanded and FBS-expanded hMDCs were injected into Mdx-SCID mouse muscles damaged with cardiotoxin. 4 weeks after cell injection, human major histocompatability complex I (hMHC-I) positive myofibers (red) could be detected in the injured muscles (**Figure 6**). The human MHC-I (red) expressed both on the membrane and in the cytoplasm of muscle fibers. All populations of hMDCs that were expanded in PRP supplemented medium retained their ability to regenerate myofibers upon extended culture. No significant differences were found between PRP and FBS expanded hMDPCs. From the point of view of mdx/SCID skeletal muscle engraftment, the cells were readily engrafting and producing hMHC-I. This finding supports engraftment occurring, but unfortunately does not explain the lack of dystrophin expression in the transplanted muscles.

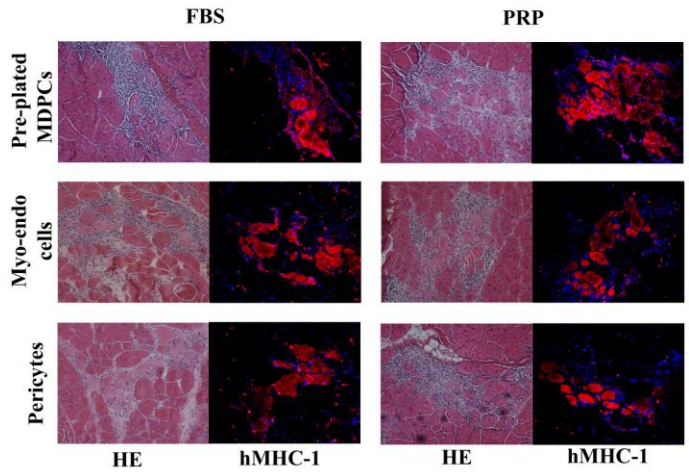

Figure 6. ***In vivo*** **myogenic potential of PRP-expanded hMPDCs.** PRP-expanded and FBS-expanded hMDPCs were also injected into Mdx-SCID mouse muscles damaged with cardiotoxin. 4 weeks after cell injection, HE staining and immuno-fluorescence staining of human MHC- I fluorescence staining of human MHC-n MHC-g and immuno-fluorescence staining human MHC- I MHC- MHC myofibers can be detected in the injured muscles. All populations of hMDPCs that were expanded in PRP supplemented medium retained their ability to regenerate myofibers

In addition to the elucidation of why our mdx/SCID model was not exhibiting good engraftment with the human MDCs we have isolated, we have been performing additional tangential experiments on another model of DMD that is deficient for both dystrophin and utrophin known as the double-knock out (dKO) mouse. This model was being used because its pathophysiology more accurately resembles that of DMD patients and we felt might better accommodate the experiments outline in this grant. The following are results we have obtained using the dKO model.

Progression of muscular dystrophy in dystrophin/utrophin-/- mice is associated with rapid muscle progenitor cell exhaustion

In this study we isolated MPCs from the skeletal muscle of young (2 weeks) and old (6 weeks) dKO (dystrophin/utrophin double knock out) mice, which have a maximum lifespan of 6 to 8 weeks and is a mouse model of DMD that closely recapitulates the disease progression observed in DMD patients. We found that MPCs isolated from old dKO mice have a reduced ability to proliferate and differentiate compared to MPCs isolated from young dKO mice. In addition, Pax7 staining (a muscle progenitor cell marker) indicated that the MPC population significantly decreased during disease progression. These observations suggest that blocking the exhaustion of the MPC pool could be a new approach to improve muscle weakness in DMD patients, despite their continued lack of dystrophin expression.

Figure 1

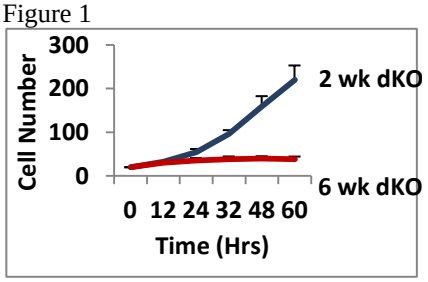

Results:

1. MPCs isolated from aged dKO mice display limited proliferation ability.

We examined the proliferation kinetics of both populations *in vitro* using LCI (3) and we observed a significant reduction in the proliferation capacity of the old dKO MPCs compared to young dKO MPCs (**Figure 1**)

2. Pax7 positive cells undergo a rapid decline in the skeletal muscle of dKO mice during aging and disease progression.

The results from the Pax7 staining showed that there is a rapid statistically significant decline in the population of Pax7 positive cells (red) in the skeletal muscle of dKO mice from 4 to 8 weeks of age in contrast to that observed in *mdx* skeletal muscle ($p<0.05$) (**Figure 2A**).

Figure 2A

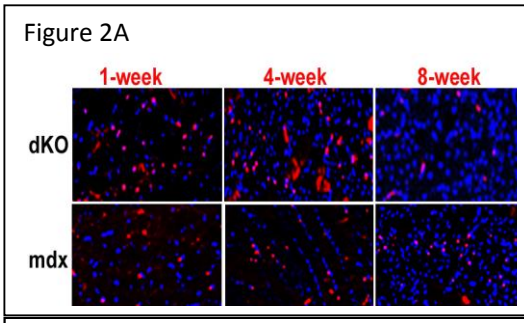

Figure 2B

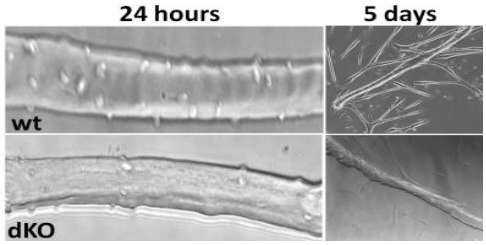

3. Isolated muscle fibers from dKO mice show a reduction in muscle progenitor cells.

The single muscle fibers were isolated from 6 weeks old dKO and WT control mice. We observed that there were more cell nuclei in the WT muscle fibers compared to the dKO muscle fibers. In addition, 5 days post-culturing, the WT muscle fibers were able to release myogenic progenitor cells forming new myotubes, in contrasts to that observed with the dKO muscle fibers. These results support both a reduction in the number and myogenic potential of the MPCs derived from the dKO mice when compared to the WT MPCs (**Figure 2B**)

4. MPCs isolated from aged dKO mice display a limited myogenic differentiation ability.

We observed that the MPCs isolated from young dKO mice formed numerous, large multi-nucleated myotubes compared to the MPCs isolated from the old dKO mice. The degree of myogenic differentiation was significantly reduced in the old dKO MPCs relative to the MPCs isolated from young dKO mice ($P < 0.001$).(**Figure 3**)

Figure 3

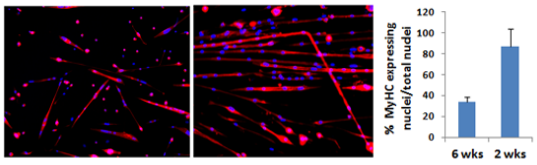

It is interesting to note that despite the lack of dystrophin at birth, the initiation of any signs of muscle weakness does not occur in DMD patients until later in childhood which happens to coincide with the exhaustion of the muscle progenitor cell pool (1). In this study we demonstrated that MPCs isolated from the skeletal muscle of old dKO mice have a reduced ability to proliferate and differentiate compared to MPCs isolated from young mice. Moreover, the numbers of Pax7 positive cells *in vivo* undergo a rapid decline in the skeletal muscle of dKO mice during aging and disease progression. Since dKO mice can only live 6-8 weeks, stem cell exhaustion could represent the main mechanism for the rapid progress of this disease. Blocking

the exhaustion of muscle progenitor cells and stem cell-mediated therapy may represent a potential strategy for treating these muscle diseases. This study suggested that the exhaustion of stem cells contributes to the histopathology associated with DMD and that blocking the exhaustion of muscle progenitor cells and stem cell-mediated therapy could be used as a potential clinical strategy to treat muscle disease.

Muscle-derived cells (MDCs) responsible for myogenesis differ from MDCs involved in adipogenesis in dystrophin/utrophin-/- mice

DMD is characterized by progressive weakening of the skeletal and cardiac muscles. The predominant symptoms seen in advanced cases of DMD are sarcopenia and pseudohypertrophy with fatty infiltration in skeletal muscle. Ectopic fat accumulation in skeletal muscle can be seen not only in myopathies but also in several disorders, including obesity and ageing-related sarcopenia; however, the origin of ectopic adipocytes, nor the stimulus that trigger their formation in disease, is known. In our lab, we utilize utrophin/dystrophin double knockout (dys-/-utro-/-, dKO) mice, which better emulates the phenotype seen in DMD patients. Several types of cells, including satellite cells, can be isolated from skeletal muscle and based on a previously published preplate technique we isolated two types of cells; rapidly adhering cells (RACs) ,which are PDGFRα + mesenchymal progenitor cells, and slowly adhering cells (SACs), which are Pax7+ myogenic progenitor cells, from skeletal muscle of dKO and wild type (wt) mice. Previously, we have shown that dKO-SACs have reduced proliferation and myogenic and adipogenic differentiation abilities compared to wt-SACs. These observations suggested that SACs in dKO mice are exhausted and potentially are the main mechanism for the rapid progress of sarcopenia; however, the cells involved in pseudohypertrophy in dKO mice remains unclear. In this study, we examined the proliferation and adipogenic differentiation capabilities of RACs since adipose cells are thought to be derived from mesenchymal stem cells. We observed increased proliferation and adipogenic differentiation capabilities in dKO-RACs compared to wt-RACs. Our results suggest that muscle progenitor cells, SACs, may be more involved in muscle fiber regeneration or degeneration while mesenchymal progenitor cells, RACs, may be the origin of the cell population that is involved in adipogenesis in dKO muscle.

RESULTS:

dKO-RACs had increased PDGFRα expression compared to dKO-SACs. Flow cytometry analysis was used to evaluate the expression of PDGFRα, a marker for mesenchymal cells, of the RACs and SACs from both dKO and wt mice. dKO-RACs were about 98% positive for the PDGFRα surface protein, while much lower expression levels were detected in the SACs (Figure 1).

Figure 1. Flow analysis of PDGFRα surface protein expression in RACs and SACs from wt and dKO mice.

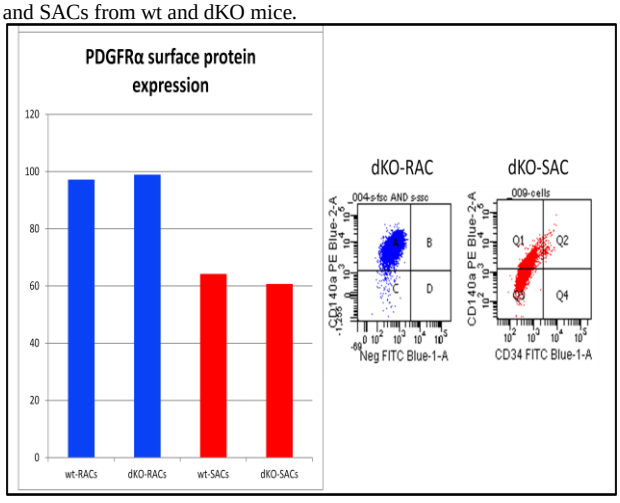

dKO-RACs displayed increased proliferation ability. The proliferation of the RACs and SACs were examined in vitro using an LCI system and MTT assay. We observed a significant increase in the proliferation of the dKO-RACs compared to the wt-RACs.

Increased in vitro adipogenic potential was detected in dKO-RACs. RACs and SACs from both dKO and wt mice were cultured in adipogenic differentiation medium for 21 days. AdipoRed staining was observed in the cytoplasm of the cells, around the nuclei. The degree of adipogenic differentiation was significantly increased in PDGFRα+ dKO-RACs compared to the dKO-SACs (Figure 2).

In dKO mice, an animal model of DMD, we observed severe peri-muscular adipose tissue on the surface of the gastrocneminus muscles (GM) as well as lipid accumulation inside of skeletal muscle myofibers. Intramyocellular lipid accumulation could be observed in the cardiac muscle of dKO mice; however, the source of the ectopic fat tissue within the skeletal muscle is unknown. In this study, we provide evidence that the RACs, PDGFRα + mesenchymal progenitor cells, are responsible for increased fat cell formation in the skeletal muscle of dKO mice. We observed that dKO-RACs had increased proliferation and adipogenic differentiation capabilities. This result suggests that dKO-RACs are prone to form adipocytes in skeletal muscle. This study suggests that dKO-RACs, mesenchymal progenitor cells in skeletal muscle, may contribute to adipogenesis and are responsible for ectopic fat cell formation within skeletal muscle in pathological conditions such as DMD. Therefore, targeting RACs to block adipogenesis in skeletal muscle may open new opportunities to treat muscle diseases.

Figure 2. Adipogenesis of RACs and SACs. Bright field pictures and AdipoRed staining. Quantification of AdipoRed assay is shown.

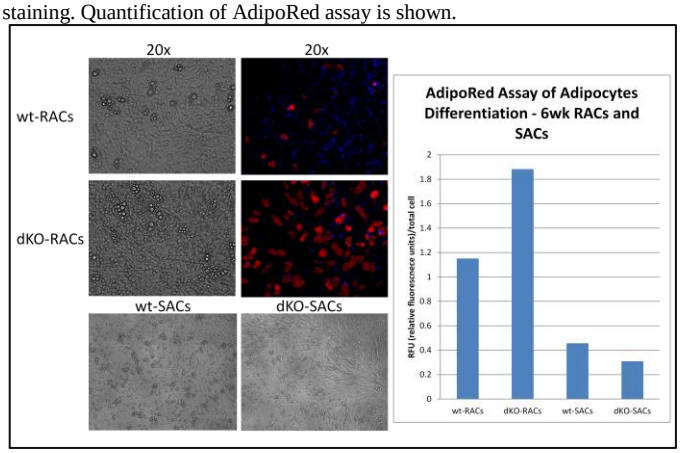

RhoA signaling regulates heterotopic ossification and fatty infiltration in dystrophic skeletal muscle

Frequent heterotopic ossification (HO) or fatty infiltration is observed in the dystrophic muscle of many animal models of human Duchenne muscular dystrophy (DMD); however, little is known about the correlated molecular mechanisms involved in the process. The RhoA-Rho kinase (ROCK) signaling pathway has been shown to function as a commitment switch of the osteogenic and adipogenic differentiation of mesenchymal stem cells (MSCs). Activation of RhoA-ROCK signaling in cultured MSCs in vitro induces their osteogenesis but inhibits the potential of adipogenesis, while the application of Y-27632, a specific inhibitor of ROCK, reversed the process. Inflammation has been shown to be one of main contributors to HO, while the role of RhoA signaling in inflammation reaction has been demonstrated. The objective of the current study is to investigate the potential role of RhoA signaling in regulating HO *and* fatty infiltration in dystrophic skeletal *muscle.*

Results:

1. Skeletal muscle of dKO mice features more HO but less fatty infiltration than mdx mice (Fig. 1). Both μ-CT scan of animals (Fig. 1A) and Alizarn Red stain (Fig. 1B) of the muscle tissues revealed greatly enriched HO in the dystrophic muscles of the dKO mice. While, Oil Red O stain (Fig. 1C) and Trichrome stain (Fig. 1D) of the muscle tissues revealed reduced fatty infiltration and a number of normal muscle fibers in the muscle of dKO mice.

Figure 1

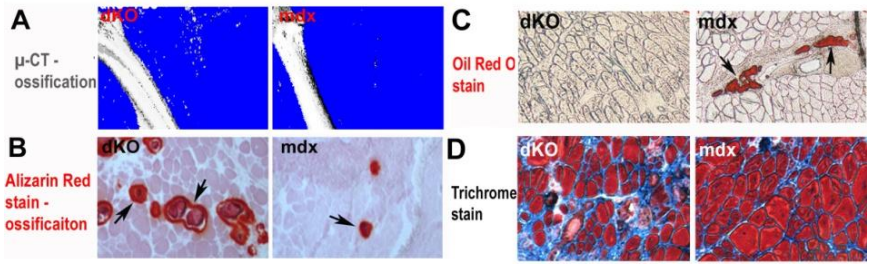

2. RhoA signaling is more activated in both skeletal muscle and muscle-derived stem cells (MDSCs) from dKO mice. Both semi-quantitative PCR and immunohistochemistry study demonstrated that RhoA signaling is more activated in the muscles of dKO mice, as well as dKO MDSCs.

Figure 2

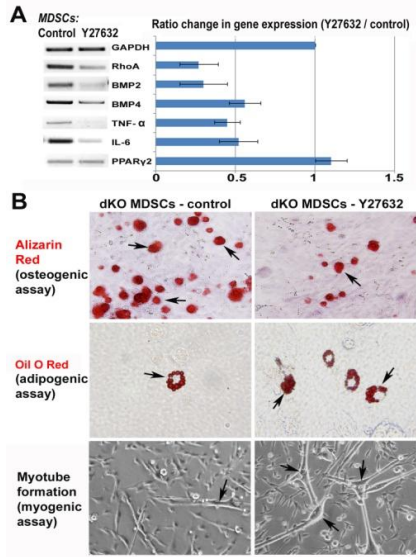

3. *In vitro* RhoA inactivation of cultured MDSCs from dKO mice decreases the osteogenesis potential and increases adipogenesis and myogenesis potential (Fig. 2). Semi-quantitative PCR study showed that Y27632 treatment *(10 μM)* of dKO-MDSCs down-regulated the expression of RhoA, BMP2 and 4, and inflammatory factors such as TNF-α and IL-6 (Fig. 2A). Osteogenesis potential was repressed while the adipogenesis and myogenesis potential of the dKO-MDSCs were increased by Y27632 (Fig. 2B).

4. RhoA inactivation in the skeletal muscle of dKO mice decreased HO and increased both fatty infiltration and muscle regeneration. GM muscles of 6 dKO mice were injected with Y27632 (5mM in 20μL of DMSO) (left limb) or control (20μL of DMSO) DMSO (right limb). Injections were conducted 3 times a week for 3 weeks. The skeletal muscles that received Y27632 injection demonstrated much slower development of HO and improved muscle regeneration, as well as reduced fibrosis formation.

These results revealed that DMD mouse models featuring different severity of muscular dystrophy may have varied potentials for developing HO or fatty infiltration in the dystrophic muscle, and RhoA signaling might be a critical mediator of the determining these differential fates, including the progression towards HO, fatty infiltration, or normal muscle regeneration. RhoA inactivation is shown to have a great potential to repress HO and improve the phenotypes of dystrophic muscle. The status of RhoA activation in the skeletal muscle of human DMD patients and the potential effect of RhoA inactivation in human dystrophic muscle requires further investigation. This data reveals the involvement of RhoA signaling in regulating the process *of* heterotopic ossification, and indicates that RhoA may serve as a potential target for repressing injury-induced and congenital heterotopic ossification in humans.

Suppression of skeletal muscle inflammation by muscle stem cells is associated with hepatocyte growth factor in wild type and mdx;p65$^{+/-}$ mice

Persistent, unresolved inflammation can lead to secondary tissue damage. Recently, we reported that intramuscular (i.m.) injection of muscle-derived stem cells (MDSCs) heterozygous for the NF-kB subunit p65 (p65$^{+/-}$) reduced host inflammation and fiber necrosis seven days following muscle injury, relative to wild type (WT) MDSC injection [1]. In this investigation, we looked closer at the role of secreted factors in this observation. Using a murine cardiotoxin muscle injury model, we observed that delivery of p65$^{+/-}$ MDSCs accelerated the resolution of inflammation, relative to WT MDSCs. *In vitro* inflammation assays demonstrated that MDSCs secrete factors that modulate cytokine expression in LPS-activated macrophages, and genetic reduction of p65 enhanced this effect. Finally, deletion of one p65 allele in a murine model of Duchenne muscular dystrophy (mdx) increased the expression of the anti-inflammatory factor hepatocyte growth factor (HGF) and was associated with disease improvement.

Figure 1.

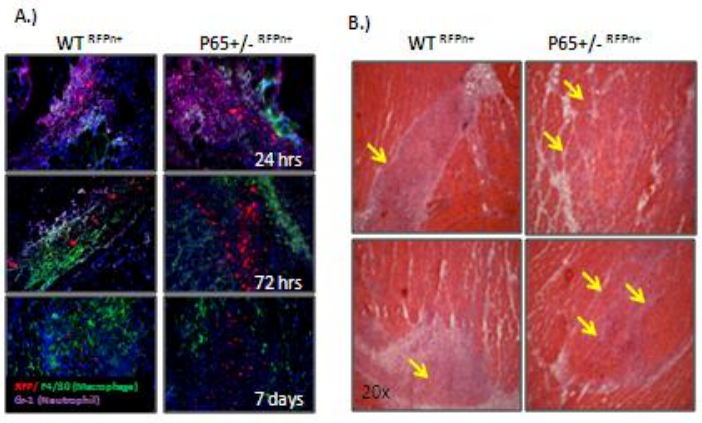

RESULTS

Confirming our previous report [1], we found that by 7 days, p65$^{+/-}$ cell engraftments were associated with reduced numbers of F4/80+ cells, compared to WT cell engraftments (Fig 1A). This can be further demonstrated histologically by H&E staining, revealing a reduction in mono-nuclear cells at sites of injury one week post injection (Fig 1B).

To look at the direct effects of MDSC-secreted factors, we performed *in vitro* inflammation assays. Briefly, RAW264.7 macrophages were activated with LPS (100ng/mL) in normal PM or WT or $p65^{+/-}$ conditioned medium (CM) (Fig 2A). The expression of the cytokines IL-1β and IL-6 was determined by real time (RT-PCR). Our results demonstrated that MDSC-CM significantly attenuates cytokine expression (Fig 2B). Although WT and $p65^{+/-}$ CM had a similar effect, we found that $p65^{+/-}$ CM exerted a stronger suppression of IL-6 expression. Previous reports have found that the activation of inflammatory macrophages is attenuated by the phosphorylation and subsequent inactivation of GSK3β [3]. By western blot, we found that upon treatment with LPS in WT-CM, the fraction of pS9-GSK3beta modestly increased within 30mins and was maintained through 24 hours. Furthermore, $p65^{+/-}$-CM demonstrated an even stronger induction of phosphorylation (Fig 2C).

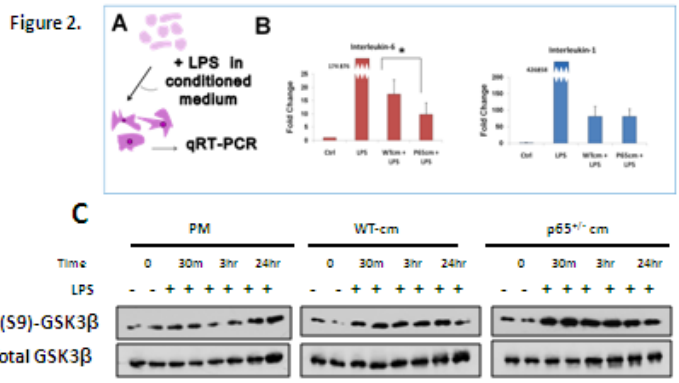

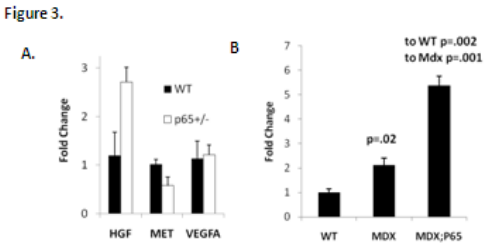

Hepatocyte growth factor (HGF) is one of the factors previously demonstrated to modulate inflammation via pS9-GSK3beta. We examined HGF expression in MDSCs and found elevated levels in $p65^{+/-}$ cells compared to the WT cells (Fig 3A). Acharyya and colleagues have reported that haploinsufficiency of p65 in an mdx background improves dystrophic pathology [4]. As we had hypothesized, HGF expression was significantly increased (Fig 3B). Based on our *in vitro* and *in vivo* inflammatory studies, HGF could be one of the contributing factors to disease improvement.

These findings indicate that NF-kB has a broader role in muscle stem and progenitor cells than previously thought, and that the anti-inflammatory molecules secreted by stem cells, such as HGF, could potentially be harnessed to control secondary pathologies of muscle diseases such as DMD.

Improved muscle histology in old dystrophic mice exposed to young dystrophic peripheral circulation: a parabiotic paring study

Researchers have observed that in Duchenne muscular dystrophy (DMD), despite the lack of dystrophin at birth, the histopathological signs of muscle weakness do not become apparent until patients reach 4-8 years of age. This happens to coincide with the exhaustion of the muscle progenitor cell (MPC) pool. Our previous results demonstrated that MPCs isolated from old dystrophin/utrophin double knock-out (dKO) mice (a reliable mouse model of DMD), are defective in their proliferation and differentiation capacities, however, it remains unclear if the disease-related loss of adult stem cell function is primarily driven by cell autonomous (a direct stem cell defect) and/or non-autonomous mechanisms (aged microenvironment or circulating factors). The parabiotic approach has been useful for revealing the striking ability of circulating factors in young mice to rejuvenate the muscle regenerative potential in old animals. In this study, we preformed heterochronic parabiosis between old dKO-hetero with young mdx mice. We tested whether muscle histopathology can be improved by blood-borne factors in vivo using a parabiotic system to enable constant exchange of peripheral blood between the mice. We found that there was decreased fibrosis, calcium deposition and improved histology of skeletal muscle, and decreased intramyocardial lipid accumulation in the old dKO-hetero mice after parabiotic pairing for 3 months. The results suggested that the defect in the MPCs might be related to the dystrophic microenvironment or circulating factors. These observations suggest that changing the dystrophic microenvironment could be a new approach to improve muscle weakness in DMD patients, despite their continued lack of dystrophin expression.

Results:

1. Peripheral blood cross-circulation and the redistribution of circulating cells were established between the two parabiotic mice. To verify the development of cross-circulation between animals, we examined the distribution of an intravascular dye (Evan's Blue) across the adjoining wounds. After injecting one of the paired mice, the Evan's Blue dye immediately flushed the same animal and progressively spread through the common vascular tree at the junction to its partner, as shown in Figure1. We also found that MPCs could travel from one mouse to its parabiotic partner by the intravenous injection of GFP positive MPCs (Figure1).

Figure 1

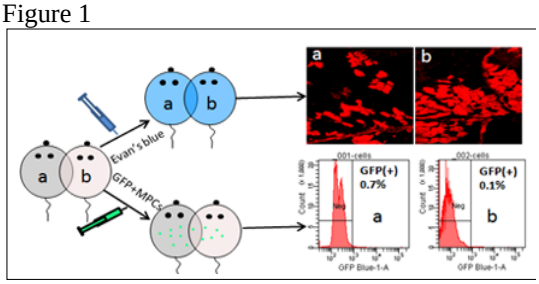

2. *Improved muscle histology in old dKO-hetero mice exposed to young mdx peripheral circulation.* We performed parabiosis between young mdx mice (3-5 months) and old dKO- hetero mice (12-14 months)**.** These heterochronic pairs were compared to the old isochronic paired mice. The H&E results indicated that the skeletal muscles were greatly improved in their histopathological appearance in the old dKO-hetero mice sutured with young mdx mice when compared to old isochronic paired mice. Alizarin red and Trichrome results also showed there was less calcium deposition and decreased fibrotic muscle fibers in the old heterochronic mice compared to old isochronic paired mice (Fig.2A).The AdipoRed staining of the cardiac muscle of the parabiotic mice also revealed reduced intramyocardial lipid accumulation in the cardiac muscle cells of the old heterochronic mice compared to the old isochronic paired mice (Fig.2B).

Figure 2

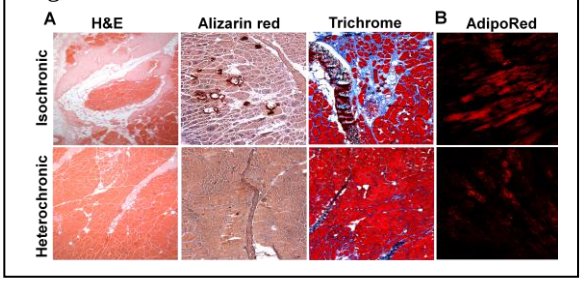

In order to determine if disease-related loss of MPCs function is primarily driven by cell autonomous and/or non-autonomous mechanisms and to further develop a new approach to improve the quality of life of DMD patient's without restoring dystyophin. These experiments were motivated by the question of whether blood-borne factors from young healthy mdx mice could influence the dystrophic microenvironment and improve the histopathology of old dKO-hetero mice. Our results indicated that the skeletal muscles were greatly improved in their histopathological appearance in the old dKO-hetero mice and decreased intramyocardial lipid accumulation in cardiac muscle when sutured with young mdx mice compared to old isochronic paired mice. These parabiosis results provided some evidence which suggested that the defect in the MPCs is driven by the dystrophic microenvironment which might be, in part, attributable to changes in the blood-borne factors passed on from the young mdx mice to the old dKO-hetero mice. Moreover, these histological improvements may relate to a beneficial effect on the dystrophic MPCs due to circulating factors in the blood of the young mdx mice. These observations demonstrated that changes to the dystrophic microenvironment could be a new approach to improving muscle weakness in DMD patients, despite their continued lack of dystrophin expression. We believe that the information gained from these experiments highlight potential treatment regimes that could rescue the stem cell defect in muscular dystrophy and could prove to be highly successful in delaying the disease progression in DMD.

Progress made from 9-1-10 to 8-31-11

Myogenic and proliferation capacity of young vs. old myoendothelial cells

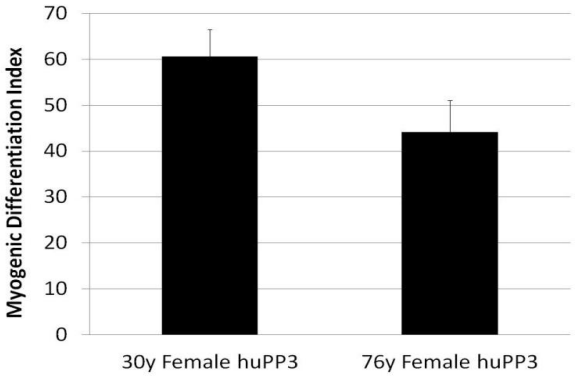

Figure 1: The MDI of two populations of human female myoendothelial cells. The MDI shows the cells isolated from the 30 year old female donor have a greater myogenic capacity than cells isolated from the 76 year old donor ($p < 0.05$).

In vitro assays to look at differences in myogenic capacities of young and old human myoendothelial cells were conducted using two cell populations one from a 30 year old female and the other from a 76 year old female. Both cell populations were derived from human skeletal muscle and isolated using our lab's pre-plate technique for stem cell isolation. Cells isolated from the latest preplate, preplate 3(PP3), were utilized in the current experiments (which means that the isolated cells adhered to the collagenated flasks between 24-48 hours after the initial muscle biopsy isolation and dissociation. For murine cell isolations, PP6 cells are able to be isolated and possess the highest multipotency and engraftment capacities as compared to PP1-PP5. To compare the myogenic capacities of the young and old cells in vitro, the cells were promoted to differentiate by placing them in low (2%) serum media for five days after which the cells were fixed and then stained for their expression of myosin heavy chain (MHC) and DAPI. The myogenic differentiation index (MDI) for each cell type was calculated by counting the number of nuclei inside MHC-stained differentiated myotubes and dividing this number by the total number of nuclei. The results shown in figure 1 indicated that the older female PP3 cells had a reduction in their myogenic potential (myotube formation) *in vitro* compared the cells isolated from the younger female biopsy. These results are being confirmed and the experiment is being repeated with human male myoendothelial cells, as well.

In another set of experiments we isolated myoendothelial cells via FACS from the skeletal muscle of a 76 year old female (HM53) and a 14 year old female (HM8) patient. The cells were studied for their proliferative and oxidative stress resistance (exposure to 400uM hydrogen peroxide) capacities. In this study the cells were found to not differ in their proliferative capacity between HM53 and HM8 (Figure 2A); however there was a significant difference in their resistance to oxidative stress capacities at 24, 32 and 48 hrs post-exposure (Figure 2B, older cells displaying a reduction to stress resistance).

Additional studies are currently underway to increase the number of populations of young and old myoendothelial and PP3 cells (and sex) studied for their proliferation, myogenic and their stress resistance capacities.

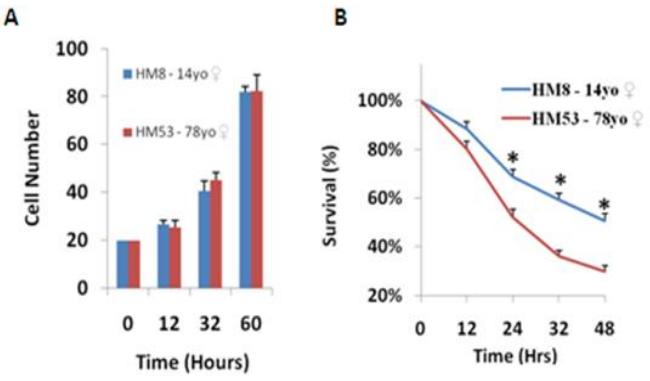

Figure2 Myoendothelial cells isolated from skeletal muscle biopsies taken from 78 year old (HM53) or 14 year old (HM8) female patients exhibit no differences in cell proliferation (A). However, aged cells are significantly less resistant to hydrogen peroxide induced (400uM) oxidative stress (B). ($p<0.05$, data represented as mean +/- s.e.m.)

Optimizing the culture conditions for expanding myoendothelial cells

It is of critical importance that the myoendothelial cells isolated from human skeletal muscle can be maintained in a "stem" like state when expanded in a cell monolayer. A media formulation of 10% fetal bovine serum, 10% horse serum, 1% penicillin/streptomycin and 1% chick embryo extract is normally used to culture the cells. This proliferation media (PRO) was combined with Endothelial Growth Media-2 (EGM2) media (Lonza) at a 1:1 mixture and designated PROe media. A 69 year old, male population of human myoendothelial cells (ST2) isolated via FACS were seeded on a 24-well plate at a density of 2000 cells/cm^2 of growth area. The ST2 cells had been maintained in normal proliferation media or PROe media since the cell isolation and were designated ST2 and ST2e, respectively. The 12-well plate was place on a Live Cell Imaging system (Kairos Instruments) which can capture images at different coordinates in the well and in all the seeded wells at preprogrammed time intervals, which can then be viewed after a set time as a time- lapsed movie. In the current experiment 100x images were captured every 15 minutes for a period of 108 hours. Images were analyzed using ImageJ and the data are presented in figure 3. Morphologically, the ST2e cells (3B) are smaller and less elongated than the ST2 cells and proliferate at a faster rate than ST2 cells (3C). Next, we wanted to know if the cells were able to differentiate after culture in PROe media and to compare this to cells grown under the usual culture conditions (PRO). A myogenic differentiation assay was performed, as described above, and representative images are shown in figure 4. ST2e cells not only form a greater number of myotubes but a greater number of the myotubes contained more nuclei which indicate a higher degree of maturity. These data suggest the PROe media or another variant may be more ideal for culturing human myoendothelial cells and maintaining them in a stem-like state.

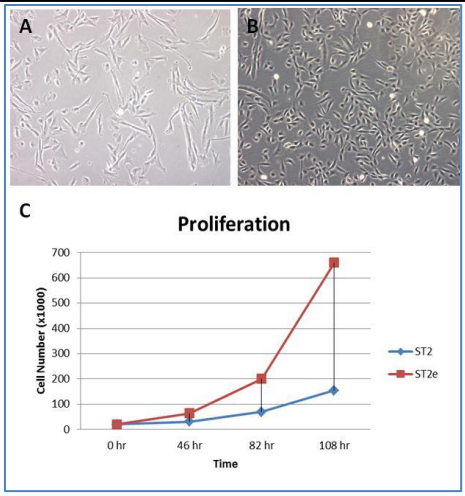

Figure 3: 100x images of human, male myoendothelial cells cultured in PRO media or PROe media. The expected doubling time of 24-36 hours is seen in the ST2 population while the ST2e cells show a doubling time of less than 24 hours (C). The morphologies of the cells are shown in A and B and indicate PROe media maintains the population in a more stem-like morphology.

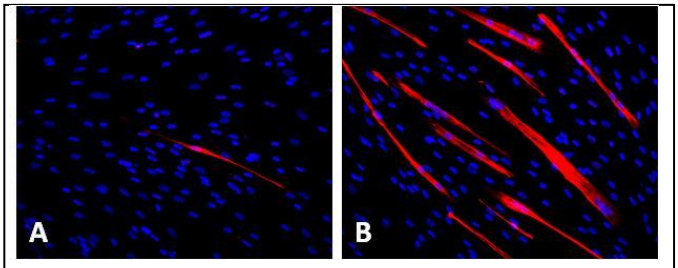

Figure 4: ST2 cells (A) and ST2e cells (B) growth in low (2%) serum media for 5 days. Cells were fixed and stained against DAPI (blue) and myosin heavy chain (red).

Identification of a dystrophin antibody for use in mdx mice

Early analysis of the first mdx/SCID tissues transplanted with human myoendothelial cells revealed a critical problem. Our group was using a polyclonal anti-dystrophin antibody (Abcam #15277) which we use for all our other mouse tissues. The initial staining of the mdx/SCID tissues showed high levels of positive staining in the PBS injected control muscles which should have been completely negative (figure 5C-D). Indeed the PBS groups had higher levels of dystrophin staining than some of the tissues tissues injected with myoendothelial cells (5A-B). It was essential to identify a viable anti-dystrophin antibody to stain *mdx* mouse tissues. Dr. Bing Wang of the Stem Cell Research Center had created four variants (R1R2, R2N, R22R23, R24H4) of a mammalian dystrophin antibody

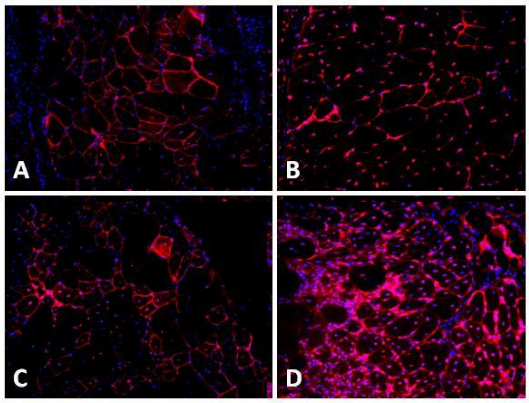

Figure 5: Mdx/SCID muscle sections stained against DAPI (blue) and mammalian dystrophin (red). (A-B) tissue transplanted with human myoendothelial cells. (C-D) tissue injected with PBS.

for testing on these tissues. The results shown in figure 5 suggested variant R1R2 was the best antibody to use on the *mdx/SCID muscle* tissues (Figure 6).

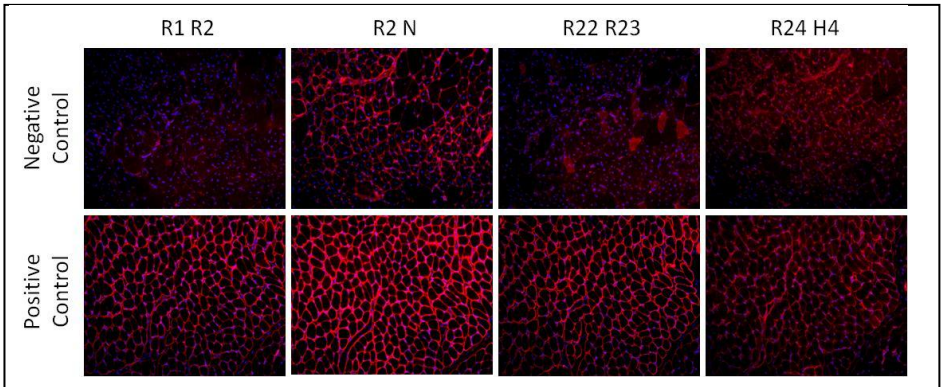

Figure 6: Testing the 4 variants of Dr. Bing Wang's polyclonal dystrophin antibody. Negative control = mdx tissue. Positive control = C57BL6 tissue. Each figure for negative or positive controls shows the identical area of the tissue. Variant R1R2 shows the lowest level of nonspecific staining.

Effect of host sex on the regenerative capacity of old male and female myoendothelial cells

Eight week old mdx/SCID mice, male and female, were randomly assigned to 1 of 5 groups; non-injected (controls), PBS (controls), ST2, ST2e or HM49. All groups, except non-injected controls, received bilateral injections into the gastrocnemius muscles of 20 microliters of PBS or PBS containing $3x10^5$ myoendothelial cells via a 31 gauge insulin syringe. Animals were sacrificed and tissue collected 14 days post-injection. Tissues were cryosectioned and the sectioned tissues stained for dystrophin using the R1R2 variant. Analysis was performed by capturing 100x fluorescent images of the entire stained section and counting the number of positively-stained (for dystrophin) fibers present in the section. The data in figure 7 are not complete as analysis has just begun on these tissues but early evidence suggests ST2 cells (cultured in PRO media) have a greater regenerative capacity than cells grown in PROe media (ST2e). The ST2 (69 year old, male) cells showed no differences when transplanted into male or female hosts (n=3 for both). The trend for ST2e cells is for better regeneration when transplanted into female hosts but the n is low for both conditions (male host, n=1; female host, n=2). This trend is seen in the HM49 again with the HM49 (75 year old, female) injected tissues as greater regeneration is seen when the cells are transplanted into a male host. Again, the n is small (n=1 for both hosts) making further analysis essential for any conclusions to be drawn. More importantly, the numbers of dystrophin positive fibers in female host tissues are all at near-background levels based on the number of revertant myofibers seen in non-injected controls. Analysis has not been performed on non-injected tissues from male hosts. Also, analysis has not yet been performed on non-injected tissues from male hosts.

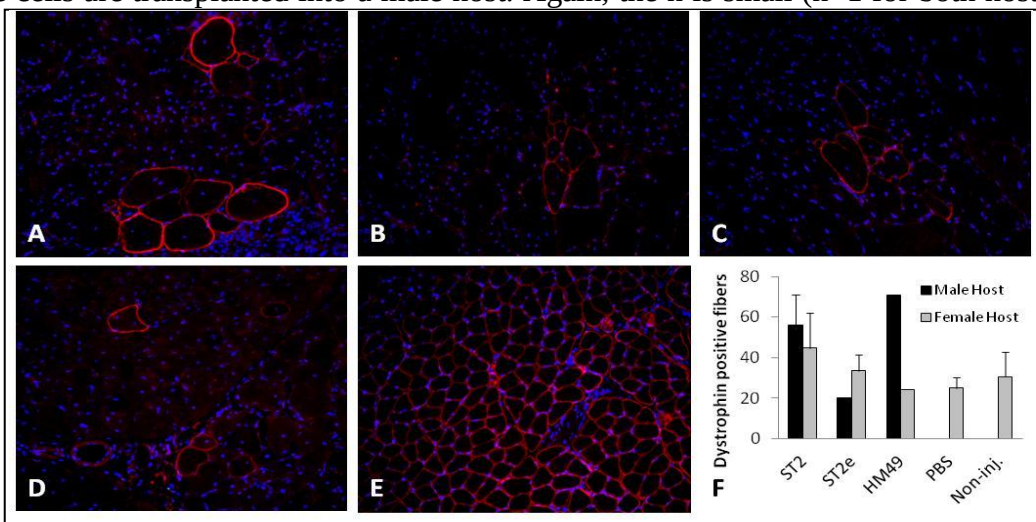

Figure 7: Analysis of tissue cryosections from *mdx/SCID* mice. Dr. Bing Wang's R1R2 dystrophin antibody (red) was used for staining. DAPI (blue) stained for nuclei. A) ST2 injected. B) ST2e injected. C) HM49 injected. D) PBS injected E) wild type (dystrophin positive) control tissue. No significant differences are seen between groups but analysis of tissues is not complete.

Non-invasive behavioral testing to detect functional improvement following stem cell transplantation

Preliminary studies were performed on nine, 12-week old female *mdx/SCID* mice in order to test the potential use of a DigiGait™ system (Mouse Specifics, Inc., Quincy, MA) functional gait analysis system to test the functional improvement of our transplanted mice. The mice received bilateral intramuscular (gastrocnemius) injections of 20uL of PBS or 20uL PBS containing either $3x10^5$ male myoendothelial cells or $3x10^5$ male perivascular cells. This initial experiment was conducted before the determination that myoendothelial cells were the best human cell type for these studies. For non-invasive analysis of muscle function we used the DigiGait™ system (Mouse Specifics, Inc., Quincy, MA). The system consists of a treadmill with a transparent belt which had a high speed digital camera mounted ventral to the test subject. Proprietary software provide by Mouse Specifics used to analyze numerous indices of the animal's gait. A simple schematic of what the software is looking at when calculating these indices is shown in figure 8A. For our study animal gaits were examined at a velocity of 20cm/s and the ratio of the stance time to swing time was calculated. The stance and swing phases are shown in figure 8A and the analysis for the *mdx/SCID* mice is shown in 8B. The data suggest that within 2 weeks of transplantation the myoendothelial-injected mice showed a reduced "running" stride compared to the pericyte-injected mice. Since these mice were forced to move at a constant velocity subjects capable of generating more force via plantar flexion could have a ratio of stance/swing greater than 1. Since the gastrocnemious is partially responsible for plantar flexion and this muscle was the target of the transplantation, these data are encouraging and warrant further use with our other experimental animals.

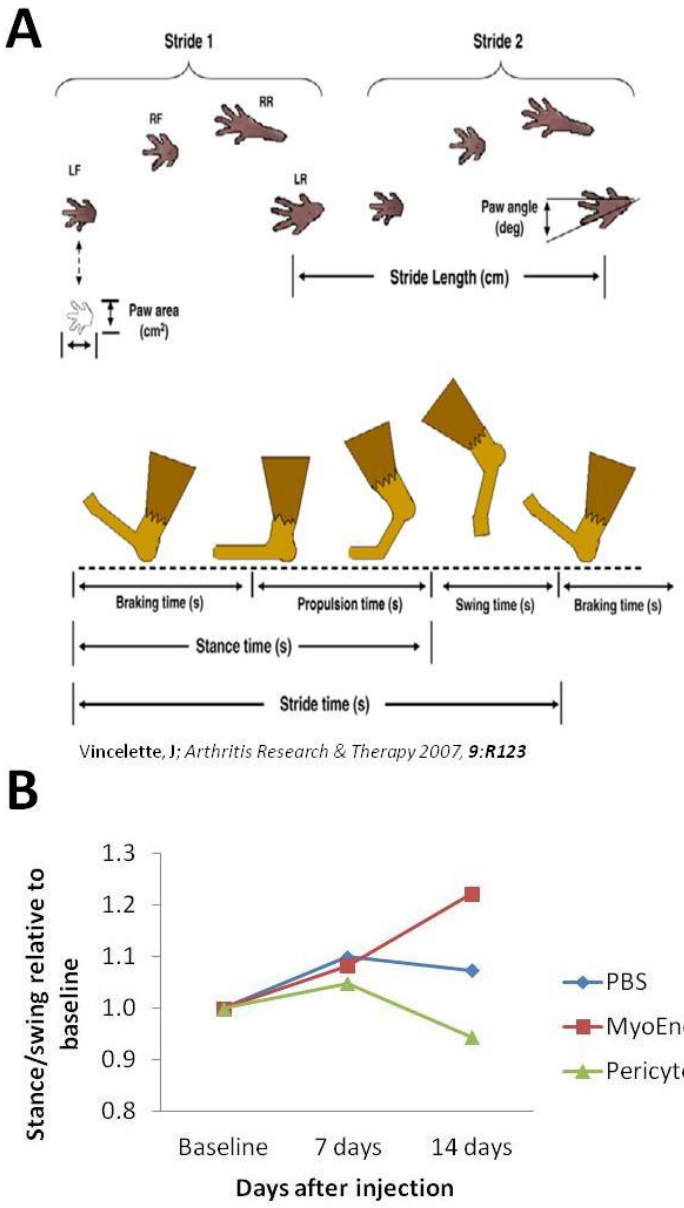

Figure 8: Non-invasive behavioral testing A) schematic of the paw areas detected by the high-speed camera as part of the DigiGait™ system. The diagram below is a visual representation of the 3 phases of a stride; braking, propulsion and swing. B) The stance phase/swing phase ratio for each group at each time point relative to each groups' baseline ratio. An increasing ratio may be indicative of increased muscle function/strength.

Immunomodulatory properties of muscle-derived stem cells associated with reduced NF-κB/p65 signaling

In this study, we examined the role of NF-kB signaling in the regenerative phenotype of muscle-derived stem cells (MDSCs) isolated from the gastrocnemius of p65 deficient mice (heterozygous, *p65*+/-) and wild type littermates (*p65*+/+). We previously found that *p65*+/- MDSCs have enhanced cell proliferation, survival under oxidative stress, differentiation, and muscle regeneration capacity. Furthermore, we have found that *p65*+/- engraftments in wild type skeletal muscle are associated with reduced inflammation and fiber necrosis compared to *p65*+/+ MDSC engraftments. *In vitro* and *in vivo* experiments suggest that reduction of p65 signaling enhances the regenerative phenotype of MDSCs, suggesting this pathway as a candidate target to

improve stem cell-based therapies for muscle disease and injury. The data presented in this study provides evidence supporting that NF-kB inhibition stimulates MDSC-mediated muscle regeneration through multiple mechanisms, including through the expression of anti-inflammatory factors that attenuate inflammation and necrosis. These experiments identify the NF-κB signaling pathway as a potential therapeutic target to enhance muscle regeneration following injury or disease (**Paper in revision. A. Lu et al. Mol. Therapy, Sept. 2011**).

p65 +/- MDSC transplantation improves muscle histology in dKO mice after IP transplantation (Figure 9) -- MDSCs were isolated from 5 month old $p65^{+/-}$ and WT mice as previously described via a modified preplate technique. A total of 5-9 $x10^5$ viable cells or 50µl PBS were injected intraperitoneally into 5-7 day old dKO mice. Four to six weeks after transplantation, the muscles were harvested and cryosections were prepared for staining. Our preliminary data suggest that the regeneration of both the gluteus maximus and diaphragm muscles were more greatly improved in their histopathological appearance in the animals injected IP with p65-deficient MDSCs than the nontreated animals at 4 weeks post-implantation,.

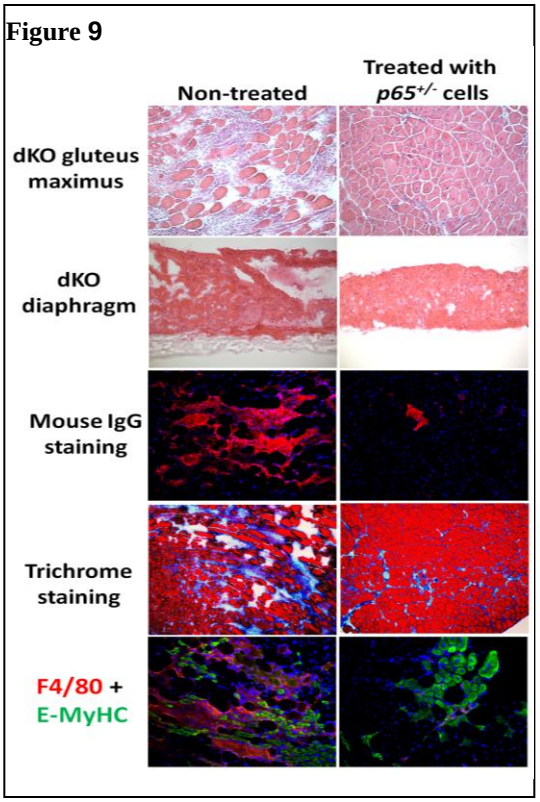

Muscle cryosections were also stained for mouse IgG to determine the extent of muscle fiber necrosis.The results showed that there were less necrotic muscle fibers in the mice injected with $p65^{+/-}$ MDSCs compared to non-treated muscles (**Fig. 9**). Trichrome staining was also preformed according to the manufacturer's instructions and the results showed that there was less muscle fibrosis in the mice injected with $p65^{+/-}$ MDSCs compared to the non-treated muscles (PBS) (**Fig. 9**)

An antibody against embryonic muscle heavy chain (E-MyHC) was used to evaluate muscle regeneration and another antibody against F4/80 (macrophage marker) was used to analyze the extent of inflammation in the regenerated area. These results showed less inflammation (red, F4/80) within the regenerated area (E-MyHC (green) positive myofibers) in the muscles of mice injected with $p65^{+/-}$ MDSCs compared to the untreated muscles (**Fig. 9**). The use of NF-kappa blockade may be useful to improve the regeneration index of hMDCs in the skeletal muscle of MDX/SCID mice.

Progress made from 9-1-09 to 8-31-10

The overall goal of Technical Objective 1 is to identify the optimal human muscle derived cell type for skeletal muscle regeneration. We have completed several aspects of Technical Objective 1, namely – 1)

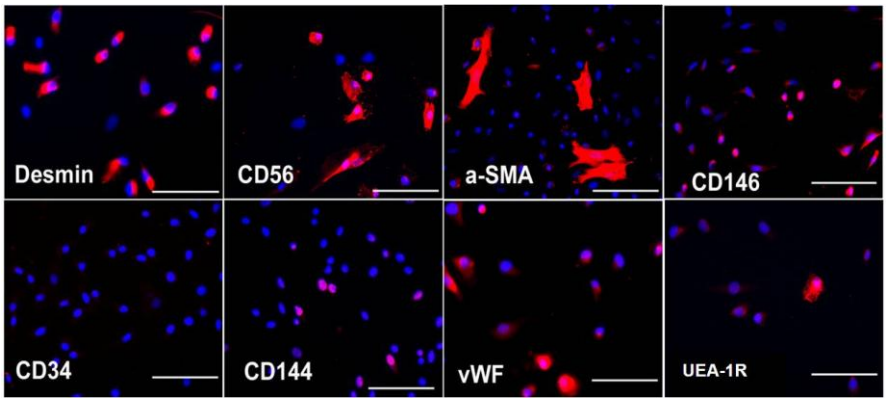

Figure 1. Differential expressions of myogenic and endothelial markers by cryopreserved human skeletal muscle cells. Immunocytochemistry revealed the diverse expressions of various cell lineage markers by cryopreserved skeletal muscle cells after expansion. Nuclei were stained blue with DAPI. (Scale bars = 100µm).

isolation of FACS-defined populations of myoblasts, myo-endothelial cells and pericytes, 2) side-by-side comparison of in vitro myogenic differentiation potential of these populations and 3) transplantation of these 3 populations to mdx/SCID animals and in vivo assessment of skeletal muscle regeneration potential of these cells.

After expansion, the cryopreserved human progenitor skeletal muscle cells (cryo-hPSMCs) were examined by immunocytochemistry for cell surface marker expression. The majority of the cryopreserved skeletal muscle cells expressed desmin and CD56, and to a lesser extent, CD146 (Figure 1). Only a fraction of cells expressed α-SMA, CD144, vWF or UEA-1R. As expected with cultured human cells, cells lacked CD34 expression. Our flow cytometry analysis quantitatively confirmed the diverse expressions of cell lineage makers by the cells: 77.1±5.7% $CD56^+$, 66.9±8.1% $CD146^+$, 11.2±2.5% $UEA\text{-}1R^+$, 0.3±0.1% $CD144^+$, 0.1% vWF^+, and no expression of CD34 and KDR (Figure 2A). Surprisingly, the number of cryo-hPSMCs positive for CD56, CD146 or UEA-1R decreased dramatically after passage 10 as compared to expression prior to passage 10 (Figure 2B).

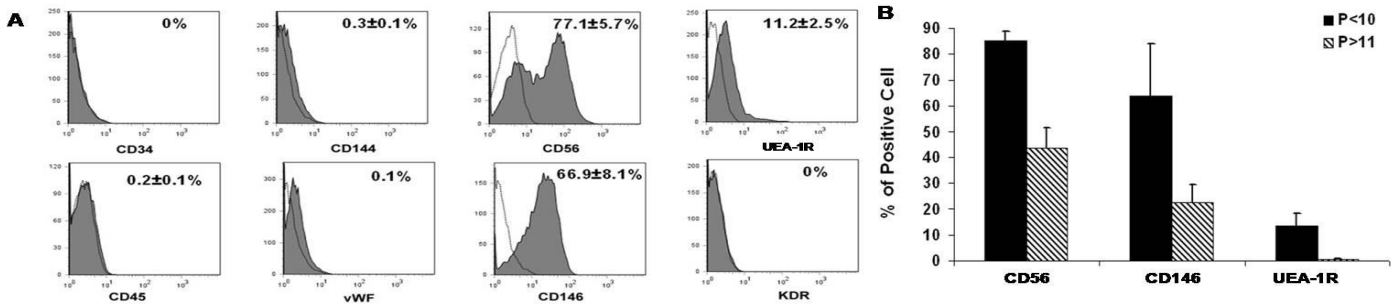

Figure 2. Differential expressions of myogenic and endothelial markers by cryopreserved human skeletal muscle cells. (A) Flow cytometry analysis quantitatively confirmed the diverse cell composition of cryopreserved skeletal muscle cells (B) The number of cryopreserved skeletal muscle cells positive for CD56, CD146, or UEA-1R decreased dramatically when cells were cultured beyond passage 10 (passage>10).

Isolation of myogenic stem/progenitor cells: Using a collection of cell lineage markers, we analyzed cryopreserved cells by flow cytometry for their expression of hematopoietic (CD45), myogenic (CD56), endothelial (UEA-1R), and perivascular (CD146) cell markers. After the exclusion of $CD45^+$ cells, four distinct cell fractions were identified, including myoblasts (Myo) ($CD56^+/CD45^-CD146^-UEA\text{-}1R^-$), endothelial cells (ECs) ($UEA\text{-}1R^+/CD45^-CD56^-CD146^-$), perivascular stem cells (PSCs) ($CD146^+/CD45^-CD56^-UEA\text{-}1R^-$), and myogenic endothelial cells (MECs) which expressed all three cell lineage markers ($CD56^+UEA\text{-}$

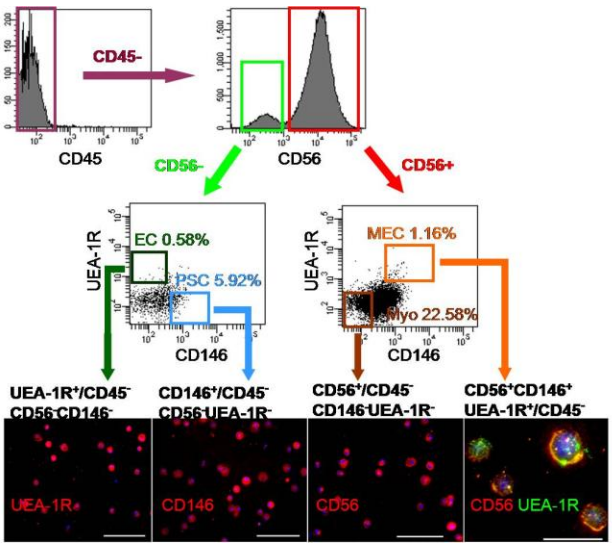

Figure 3. Identification and purification of myogenic stem cells within cryopreserved muscle cell populations. $CD45^-$ cells were separated based on CD56 expression. $CD56^+$ and $CD56^-$ populations were further gated on UEA-1R by CD146 to identify and/or sort four distinct cell populations: myogenic endothelial cells (MEC) ($CD56^+UEA\text{-}1R^+CD146^+/CD45^-$), myoblasts (Myo) ($CD56^+/CD45^-CD146^-UEA\text{-}1R^-$), perivascular stem cells (PSC) ($CD146^+/CD45^-CD56^-UEA\text{-}1R^-$), and endothelial cells (EC) ($UEA\text{-}1R^+/CD45^-CD56^-CD146^-$). The purities of the sorted populations were 90.73±4.82%, 92.94±1.23%, 93.86±1.72, and 94.9±0.64, respectively. Immunocytochemistry confirmed the expression of key cell lineage makers by freshly sorted cells: UEA-1R, CD146, and/or CD56. (Scale bars = 100μm except in CD56/UEA-1R double staining = 20μm)

$1R^+CD146^+/CD45^-$). The composition of long-term cultured cryopreserved muscle cells included 22.58±6.32% Myo, 0.58±0.23 % ECs, 5.92±4.66% PSCs, and 1.16±0.19% MECs (Figure 3). These four cell subsets were subsequently fractionated by FACS (Figure 3).

Next, we examined the in vitro differentiation capacity of myoendothelial cells and pericytes. Cells were stimulated for 1 week under conditions of low serum and high density and we observed a marked difference in the ability to undergo myogenic differentiation, as noted by the presence of multinucleated myotubes and positive immunostaining for myosin heavy chain (MHC) and desmin (Figure 4).

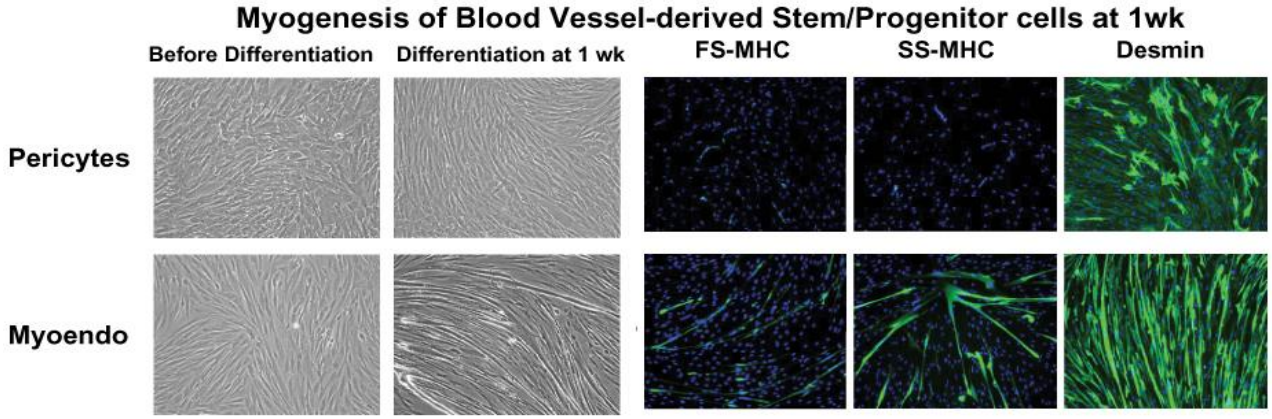

Figure 4. Myoendothelial cells displayed a higher myogenic potential as compared to pericytes. After 1 week in myogenic conditions, we find more myotubes, and greater expression of myosin heavy chain (MHC, green) and desmin (green) in the myoendothelial cell populations as compared to pericytes populations. Nuclei are DAPI stained.

Finally, to evaluate the myogenic capacities of these purified cell fractions, all freshly sorted cells were immediately transplanted into cardiotoxin-injured skeletal muscles of SCID mice (n=7 per cell fraction). Unpurified muscle cell- and saline-injected muscles were employed as controls. Mouse muscles were harvested 2 weeks post-injection, cryosectioned, and examined by immunohistochemistry to detect muscle fiber regeneration *in vivo*. An antibody against human spectrin, a myofiber cytoskeletal protein, was used to identify human cell-derived skeletal myofibers in the tissue sections. Quantitative analyses revealed that the myogenic regeneration index, indicated by human spectrin-positive skeletal myofibers per 1×10^3 injected cells, was 71.23±27.15 for MECs, 31.26±11.57 for endothelial cells (ECs), 11.44±3.79 for PSCs, 4.23±1.16 for myoblasts (Myo), and 0.55±0.36 for unsorted muscle cells (Unsort) (Figure 4). MECs exhibited the highest regeneration of human skeletal myofibers among all five cell fractions tested ($p<0.05$) (Figure 4). PSCs regenerated more myofibers than the Myo ($p>0.05$) and the Unsort ($p<0.05$) (Figure 5). Purified myoblasts displayed a higher myogenic capacity than the unsorted cells ($p<0.05$) (Figure 5).

Similar experiments are currently under way where the cell populations have been transplanted into the gastrocnemius muscles of mdx/SCID mice – a mouse model of Duchenne muscular dystrophy that is dystrophin deficient and also is immune deficient to inhibit the rejection of the injected human cell populations. These in vivo experiments will allow us to compare the myogenic potential of the cells in a DMD model verse the acute muscle injury model used above (i.e., the cardiotoxin injured mice).

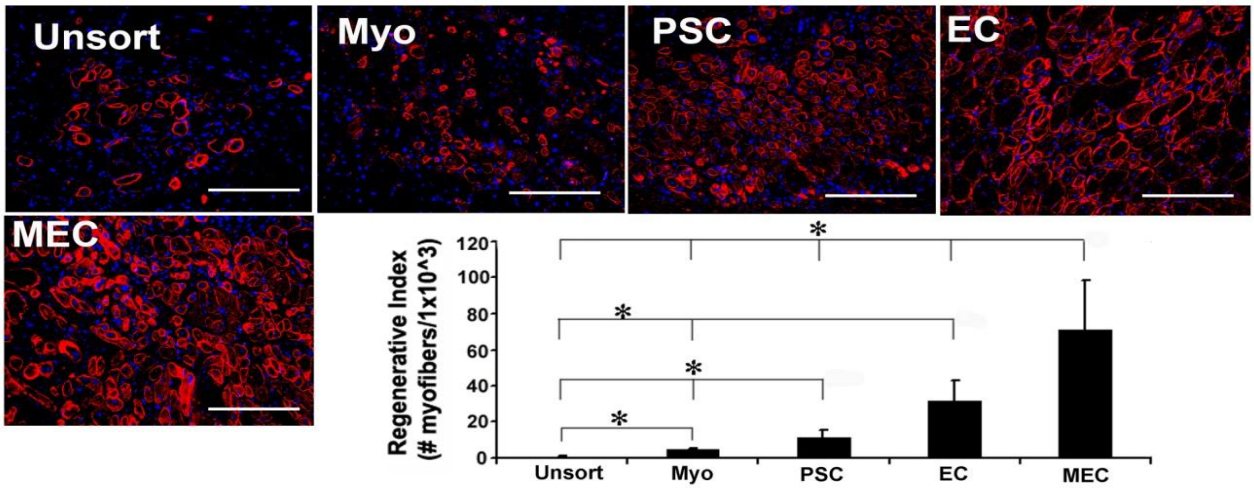

Figure 5. Comparison of myogenic regenerative capacities *in vivo*. Freshly sorted cells were transplanted into the cardiotoxin-injured skeletal muscles of SCID mice. Quantitative analyses of human spectrin-positive skeletal myofibers on tissue sections revealed that myogenic endothelial cells (MEC) mediated the highest myogenic regeneration among all five cell fractions tested (* $p<0.05$). Injection of perivascular stem cells (PSC) regenerated more human myofibers than injections of myoblasts (Myo) ($p>0.05$) and unpurified muscle cells (Unsort) (* $p<0.05$). Finally, myoblasts (Myo) displayed a higher myogenic capacity than unpurified muscle cells (Unsort) (* $p<0.05$). (Red immunostaining is spectrin, Blue nuclei are DAPI stained)

KEY RESEARCH ACCOMPLISHMENTS:

- Demonstration of prospective isolation of myoblasts, pericytes and myo-endothelial cells derived from human skeletal muscle biopsy, and from both expanded and cryopreserved populations.
- Demonstration that the myo-endothelial cells show a higher level of myogenic potential in vitro as compared to myoblasts and pericytes.
- Demonstration that both expanded and cryopreserved cells continue to show some myogenic potential in vitro.
- Demonstration that the myo-endothelial cells show a significantly higher level of skeletal muscle regeneration in vivo as compared to myoblasts and pericytes.
- Obtained preliminary evidence that PP3 cells isolated from young female skeletal muscle has a higher myogenic capacity than PP3 cells isolated from old skeletal muscle.
- Obtained preliminary evidence that myoendothelial cells isolated from young skeletal muscle is more resistant to the effects of oxidative stress than those isolated from old skeletal muscle.
- Preliminary evidence that young and old myondothelial cells possess a similar proliferation capacity.
- Optimized the growth medium for human myoendothelial cells in order to increase their proliferation rates and reduce their differentiation rates by maintaining their stem-like state in culture.
- Identified an antibody that could be used without significant background staining in our mdx/SCID model of DMD.
- Initiated studies comparing male and female myoendothelial regeneration efficiencies in vitro.
- Identified a physiological testing system (DigiGait system) that could give us excellent physiologic readouts of our transplanted animals.
- Immunomodulatory properties of muscle-derived stem cells are associated with reduced NF-κB/p65 signaling.
- p65 +/- MDSC transplantation can improve muscle histology in dKO mice (mice deficient for both utrophin and dystrophin) after IP transplantation.

- Further preliminary studies have demonstrated human muscle-derived cell engraftment in the mdx/SCID model; however, there is poor to no dystrophin expression in the transplanted muscles of these mice with any of the human population utilized.
- Engraftment has been confirmed with GFP and human MHC-1 antibodies.
- Identification of another potential model of DMD to complete the aims of this grant has led to studies using a dystrophin/utrophin-/- (double knock-out, dKO) model of DMD which has been shown to demonstrate an association between rapid muscle progenitor cell pool exhaustion with the progression of the DMD pathology.
- Further study of the dKO model led us to discover that the MDCs responsible for myogenesis differ from MDCs involved in adipogenesis in the dKO mice.
- We have also demonstrated the role of RhoA signaling in regulating the process *of* heterotopic ossification in the dystrophic muscle of dKO mice which indicates that RhoA may serve as a potential target for repressing injury-induced and congenital heterotopic ossification in humans.
- Found that NF-kB has a broader role in muscle stem and progenitor cells than previously thought, and that the anti-inflammatory molecules secreted by stem cells, such as HGF, could potentially be harnessed to control secondary pathologies of muscle diseases such as DMD.
- Found that the defect in the MDCs might be related to the dystrophic microenvironment or circulating factors which could indicate that changing the dystrophic microenvironment could be a new approach to improve muscle weakness in DMD patients, despite their continued lack of dystrophin expression.

REPORTABLE OUTCOMES:

1. Chen C, Okada M, Tobita K, Crisan M, Péault B, Huard J; **Transplantation of Purified Human Skeletal Muscle-Derived Pericytes Reduce Fibrosis in Injured Ischemic Muscle Tissues**. Orthopaedic Research Society; March 6-9, 2010; New Orleans, La **(Appendix 1)**

2. Aiping Lu, Qing Yang, Minakshi Poddar, Bing Wang, Denis C. Guttridge, Paul D. Robbins, Johnny Huard; **Transplantation of p65 Deficient Stem Cells Improved the Histopathology of Skeletal Muscle in Dystrophic Mice.** Orthopaedic Research Society; 2011 ORS Annual Meeting; January 13-16, 2011; Long Beach, CA. **(Appendix 2)**

3. Proto, J., Lu, A., Robbins, P.D., Huard, J; **Immunomodulatory properties of muscle-derived stem cells associated with reduced NF-κB/p65 signaling.** Orthopaedic Research Society; 2011 ORS Annual Meeting; January 13-16, 2011; Long Beach, CA. **(Appendix 3)**

4. Aiping Lu, Jonathan Proto, Lulin Guo, Ying Tang, Mitra Lavasani, Jeremy S. Tilstra, Laura J. Niedernhofer, Bing Wang, Denis C. Guttridge, Paul D. Robbins, Johnny Huard J.H. **NF-κB negatively impacts the myogenic potential of muscle-derived stem cells.** Molecular Therapy 2012; 20(3): 661-8. PMID: 22158056 **(Appendix 4)**

5. Zheng B, Chen C, Li G, Thompson S, Poddar M, Peault B, Huard J. **Isolation of myogenic stem cells from cultures of cryopreserved human skeletal muscle.** Cell Transplantation 2012 Apr, Epub ahead of print. PMID: 22472558 **(Appendix 5)**

6. Bo Zheng, Guangheng Li, William Chen, Bridget M Deasy, Jonathan B Pollett, Bin Sun, Lauren Drowley, Burhan Gharaibeh, Arvydas Usas, Alison Logar, Bruno Peault , Johnny Huard; **Human Myogenic Endothelial Cells Exhibit Chondrogenic and Osteogenic Potentials at the Clonal Level.** Journal of Orthopaedic Research (Under review) (**Appendix 6)**

7. Aiping Lu; Jonathan Proto; Xiaodong Mu; Ying Tang; Minakshi Poddar; Bing Wang; Johnny Huard**. Progression of muscular dystrophy in dystrophin/utrophin-/- mice is associated with rapid muscle progenitor cell exhaustion.** Orthopaedic Research Society; 2013 ORS Annual Meeting; January 26-30, 2013; San Antonio, TX **(Appendix 7)**

8. Jihee Sohn, Ying Tang, Bing Wang, Aiping Lu, Johnny Huard. **Muscle-derived cells (MDCs) responsible for myogenesis differ from MDCs involved in adipogenesis in dystrophin/utrophin-/- mice.** Orthopaedic Research Society; 2013 ORS Annual Meeting; January 26-30, 2013; San Antonio, TX **(Appendix 8)**

9. Xiaodong Mu, Arvydas Usas, Ying Tang, Aiping Lu, Jihee Sohn, Bing Wang, Kurt Weiss, and Johnny Huard. **RhoA signaling regulates heterotopic ossification and *fatty infiltration* in dystrophic skeletal muscle.** Orthopaedic Research Society; 2013 ORS Annual Meeting; January 26-30, 2013; San Antonio, TX **(Appendix 9)**

10. Proto, J., Tang, Y; Lu, A., Robbins, P.D., Wang, B. Huard, J. **Suppression of skeletal muscle inflammation by muscle stem cells is associated with hepatocyte growth factor in wild type and *mdx*;p65$^{+/-}$ mice.** Orthopaedic Research Society; 2013 ORS Annual Meeting; January 26-30, 2013; San Antonio, TX **(Appendix 10)**

11. Aiping Lu, Hongshuai Li, ying Tang, Xiaodong Mu, Minakshi Poddar, Bing Wang, Johnny Huard. **Improved muscle histology in old dystrophic mice exposed to young dystrophic peripheral circulation: a parabiotic paring study.** Orthopaedic Research Society; 2013 ORS Annual Meeting; January 26-30, 2013; San Antonio, TX **(Appendix 11)**

CONCLUSION:

Year 1: Our results to date show that even after *in vitro* expansion and cryopreservation, primary human muscle cells harbored various subpopulations of cells. We have identified and purified to homogeneity four distinct cell populations from cryopreserved primary human muscle cells including two stem cell subpopulations: Pericytes (PSCs) (CD146^{+}/CD45^{-}CD56^{-}UEA-1R^{-}) and myoendothelial cells (MECs) (CD56^{+}CD146^{+}UEA-1R^{+}/CD45^{-}). Freshly sorted MECs, PSCs, endothelial, and myogenic cells were transplanted into the injured skeletal muscles of SCID mice to examine their myogenic efficacy. MECs displayed the highest muscle regenerative capacity among all cell subsets tested, and PSCs were superior to myoblasts and unpurified cryopreserved primary human muscle cells. These results were consistent with previous observations from the injection of cells isolated from fresh muscle biopsies. Taken together, our results suggest the presence of distinct subpopulations of highly myogenic stem/progenitor cells within expanded cryopreserved primary human muscle cells and support the feasibility of further purifying stem cell fractions from cryopreserved human cells. Most importantly, these findings infer the practicability of prospective isolation of myogenic stem/progenitor cell populations from banked human skeletal muscle cells, highlighting a new technology to further enhance the availability and efficacy of cell-mediated therapies.

Year 2: We have preliminary evidence that there are no differences in the proliferative abilities between old and young human muscle derived cells; however, there appears to be a difference in the MDCs myogenic differentiation capacity and resistance to oxidative stress. We also formulated a medium that optimizes the proliferative capacity of our human MDCs while reducing their premature myogenic differentiation and identified a non-invasive behavioral testing system to detect the functional physiological improvements of the muscles that have been transplanted with our muscle derived stem cells. Moreover, we have demonstrated that NF-κB inhibition stimulates MDSC-mediated muscle regeneration through multiple mechanisms, including

through the expression of anti-inflammatory factors that attenuate inflammation and necrosis. These experiments have identified the NF-κB signaling pathway as a potential therapeutic target to enhance muscle regeneration following injury or disease. Our results have demonstrated less inflammation within the regenerating areas of muscles of mice injected with $p65^{+/-}$ MDSCs (MDSCs with ½ the expression of the NF-κB sub unit p65) compared to the untreated muscles; hence the use of NF-kappa blockade may be useful to improve the regeneration index of human muscle-derived stem cells in the skeletal muscle of MDX/SCID mice and potentially in the skeletal muscle to DMD patients.

Year 3: Mdx/SCID mice skeletal muscle generates high levels of background when immunostained with an antibody against "human dystrophin", which has been an ongoing problem with this animal model. We have been performing additional tangential experiments on another model of DMD that is deficient for both dystrophin and utrophin known as the double-knock out (dKO) mouse. This model was being used because its pathophysiology more accurately resembles that of DMD patients and we felt might better accommodate the experiments outline in this grant, since we were experiencing the technical problems with the mdx/SCID model. In a set of experiments performed on the dKO mice, we demonstrated that MPCs isolated from the skeletal muscle of old dKO mice have a reduced ability to proliferate and differentiate compared to MPCs isolated from young mice. Moreover, the numbers of Pax7 positive cells *in vivo* undergo a rapid decline in the skeletal muscle of dKO mice during aging and disease progression. This study suggested that the exhaustion of stem cells contributes to the histopathology associated with DMD and that blocking the exhaustion of muscle progenitor cells and stem cell-mediated therapy could be used as a potential clinical strategy to treat muscle disease. In another set of experiments we found that dKO-RACs, mesenchymal progenitor cells in skeletal muscle, may contribute to adipogenesis and are responsible for ectopic fat cell formation within skeletal muscle in pathological conditions such as DMD. Therefore, targeting RACs to block adipogenesis in skeletal muscle may open new opportunities to treat muscle diseases. We also found that DMD mouse models featuring different severities of muscular dystrophy may have varied potentials for developing HO or fatty infiltration in the dystrophic muscle, and RhoA signaling might be a critical mediator of the determining these differential fates, including the progression towards HO, fatty infiltration, or normal muscle regeneration. In another set of experiments we found that NF-kB has a broader role in muscle stem and progenitor cells than previously thought, and that the anti-inflammatory molecules secreted by stem cells, such as HGF, could potentially be harnessed to control secondary pathologies of muscle diseases such as DMD. In a final set of experiments we demonstrated that changes to the dystrophic microenvironment could be a new approach to improving muscle weakness in DMD patients, despite their continued lack of dystrophin expression. We believe that the information gained from these experiments highlight potential treatment regimes that could rescue the stem cell defect in muscular dystrophy and could prove to be highly successful in delaying the disease progression in DMD.

REFERENCES:
N/A

APPENDICES:

Refer to Manuscripts/Reprints, Abstracts Section

MANUSCRIPTS/REPRINTS, ABSTRACTS:

1. Chen C, Okada M, Tobita K, Crisan M, Péault B, Huard J; **Transplantation of Purified Human Skeletal Muscle-Derived Pericytes Reduce Fibrosis in Injured Ischemic Muscle Tissues**. Orthopaedic Research Society; March 6-9, 2010; New Orleans, La **(Appendix 1)**
2. Aiping Lu, Qing Yang, Minakshi Poddar, Bing Wang, Denis C. Guttridge, Paul D. Robbins, Johnny Huard; **Transplantation of p65 Deficient Stem Cells Improved the Histopathology of Skeletal**

Muscle in Dystrophic Mice. Orthopaedic Research Society; 2011 ORS Annual Meeting; January 13-16, 2011; Long Beach, CA. **(Appendix 2)**

3. Proto, J., Lu, A., Robbins, P.D., Huard, J; **Immunomodulatory properties of muscle-derived stem cells associated with reduced NF-κB/p65 signaling.** Orthopaedic Research Society; 2011 ORS Annual Meeting; January 13-16, 2011; Long Beach, CA. **(Appendix 3)**
4. Aiping Lu, Jonathan Proto, Lulin Guo, Ying Tang, Mitra Lavasani, Jeremy S. Tilstra, Laura J. Niedernhofer, Bing Wang, Denis C. Guttridge, Paul D. Robbins, Johnny Huard J.H. **NF-κB negatively impacts the myogenic potential of muscle-derived stem cells.** Molecular Therapy 2012; 20(3): 661-8. PMID: 22158056 **(Appendix 4)**
5. Zheng B, Chen C, Li G, Thompson S, Poddar M, Peault B, Huard J. **Isolation of myogenic stem cells from cultures of cryopreserved human skeletal muscle.** Cell Transplantation 2012 Apr, Epub ahead of print. PMID: 22472558 **(Appendix 5)**
6. Bo Zheng, Guangheng Li, William Chen, Bridget M Deasy, Jonathan B Pollett, Bin Sun, Lauren Drowley, Burhan Gharaibeh, Arvydas Usas, Alison Logar, Bruno Peault , Johnny Huard; **Human Myogenic Endothelial Cells Exhibit Chondrogenic and Osteogenic Potentials at the Clonal Level.** Journal of Orthopaedic Research (Under review) (**Appendix 6)**
7. Aiping Lu; Jonathan Proto; Xiaodong Mu; Ying Tang; Minakshi Poddar; Bing Wang; Johnny Huard**. Progression of muscular dystrophy in dystrophin/utrophin-/- mice is associated with rapid muscle progenitor cell exhaustion.** Orthopaedic Research Society; 2013 ORS Annual Meeting; January 26-30, 2013; San Antonio, TX **(Appendix 7)**
8. Jihee Sohn, Ying Tang, Bing Wang, Aiping Lu, Johnny Huard. **Muscle-derived cells (MDCs) responsible for myogenesis differ from MDCs involved in adipogenesis in dystrophin/utrophin-/- mice.** Orthopaedic Research Society; 2013 ORS Annual Meeting; January 26-30, 2013; San Antonio, TX **(Appendix 8)**
9. Xiaodong Mu, Arvydas Usas, Ying Tang, Aiping Lu, Jihee Sohn, Bing Wang, Kurt Weiss, and Johnny Huard. **RhoA signaling regulates heterotopic ossification and *fatty infiltration* in dystrophic skeletal muscle.** Orthopaedic Research Society; 2013 ORS Annual Meeting; January 26-30, 2013; San Antonio, TX **(Appendix 9)**
10. Proto, J., Tang, Y; Lu, A., Robbins, P.D., Wang, B. Huard, J. **Suppression of skeletal muscle inflammation by muscle stem cells is associated with hepatocyte growth factor in wild type and *mdx*;p65$^{+/-}$ mice.** Orthopaedic Research Society; 2013 ORS Annual Meeting; January 26-30, 2013; San Antonio, TX **(Appendix 10)**
11. Aiping Lu, Hongshuai Li, ying Tang, Xiaodong Mu, Minakshi Poddar, Bing Wang, Johnny Huard. **Improved muscle histology in old dystrophic mice exposed to young dystrophic peripheral circulation: a parabiotic paring study.** Orthopaedic Research Society; 2013 ORS Annual Meeting; January 26-30, 2013; San Antonio, TX **(Appendix 11)**

Sub-Project 2: Generation of human hepatocytes from patient-specific stem cells for treatment of life-threatening liver injury

PIs: David Perlmutter and Ira J. Fox

INTRODUCTION:

These studies are focused on generating human hepatocytes from patient-specific stem cells for the treatment of life-threatening liver injury. Two technical objectives were proposed: 1) Determine the extent to which human patient-specific, induced pluripotent stem (iPS) cells can be differentiated into primary human hepatocytes, and 2) Determine the extent to which the PiZ mouse model of alpha-1-antitrypsin (AT) deficiency can be developed as a platform for pre-clinical testing of hepatic stem cell transplantation as a treatment for severe liver injury and disease. In order to accomplish these objectives, we have generated 3 human iPS cell lines from normal patients and 11 iPS cell lines from patients with alpha-1-antitrypsin deficiency (ATD). These cell lines have now been characterized and 3 of which have been differentiated into hepatocytes. We have demonstrated that iPS cell-derived hepatocytes from ATD patients recapitulate the pathobiological defects observed in ATD hepatocytes. We show that there is decreased AT secretion in differentiated ATD iPS cells compared to differentiated normal iPS cells. We show that there is a decreased rate of disappearance of intracellular AT in ATD iPS cell-derived hepatocytes compared to normal iPS cell-derived hepatocytes. We have demonstrated that iPS derived cells can be transplanted in rodents that are models of human disease and that engraftment and expansion of the derived hepatocytes corrects the disease. Finally, we have further determined the ability of donor hepatocytes to expand in the PiZ mouse, and we have generated PiZ mice on an immune-deficient background and have begun studies showing engraftment and expansion of pluripotent stem cell-derived hepatocytes in these mice.

BODY:

1.1. Generation of human induced pluripotent stem cells (iPS cells).

We hypothesized that patient specific iPS cells could be generated from primary human cells, including hepatocytes, and that under appropriate conditions, the iPS cells could be induced to differentiate back to hepatocytes that could be used as cellular therapy to treat the liver defect. Here, we report the generation of multiple human iPS cell lines from primary human cells following exposure to either lentiviral, excisable lentiviral stem cell cassette or plasmid constructs carrying reprogramming factors. In **Table 1** and **2**, we characterize lines derived from normal controls, and patients with ATD. We have characterized the lines for markers of pluripotency, including alkaline phosphatase activity, nuclear NANOG, OCT3/4 and SOX2 staining, and reactivity to antibodies to the surface markers SSEA-4 and TRA1-60, and confirmed these results by qPCR. In addition, genotyping has been completed on most of the ATD and control iPS cell lines.

Table 1. List of normal iPS cell lines

Source of iPS cell line	Normal human hepatocyte (biopsy)	Normal dermal fibroblast	Normal dermal fibroblast
Vector used for iPS induction	Lentivirus	Excisable Lentiviral Stem Cell Cassette	Non-integrating plasmids
Characterization of Pluripotency			
qPCR	✔	ongoing	ongoing
Immunostaining	✔	ongoing	ongoing
Teratoma formation	✔	ongoing	ongoing

Genotype*	ongoing	G/G	G/G
Name of iPS cell line	**HH1591** iPS cells (Control)	**BMC-1** iPS cells (Control)	**NF-IF** iPS cells (Control)

*** G/G: Homozygous for the wild type allele**

Table 2. List of ATD iPS cell lines

Source of iPS cell line	AT deficient human hepatocyte (Biopsy, CHP HH1764 (7/21/2010), 10(Y) M	AT deficient lung fibroblast (Biopsy)	AT deficient lung fibroblast (Biopsy)	AT deficient lung fibroblast (Biopsy)	AT deficient lung fibroblast (Biopsy)
Vector used for iPS induction	Lentivirus	Lentivirus	Excisable Lentiviral Stem Cell Cassette	Excisable Lentiviral Stem Cell Cassette	Excisable Lentiviral Stem Cell Cassette
Characterization of Pluripotency					
qPCR	✔	✔	ongoing	ongoing	ongoing
Immunostaining	✔	✔	ongoing	ongoing	ongoing
Teratoma formation	✔	✔	ongoing	ongoing	ongoing
Genotype	A/A	A/A	A/A	A/A	A/A
Name of iPS cell line	**ATH-1** iPS cells (AT deficient)	**AT-10 c1-6** iPS cells (AT deficient) 6 other clones	**100-3-Cr-1** iPS cells (AT deficient)	**102-37B-Cr-2** iPS cells (AT deficient)	**103-3-Cr-1** iPS cells (AT deficient)

*** A/A: Homozygous for the Z allele**

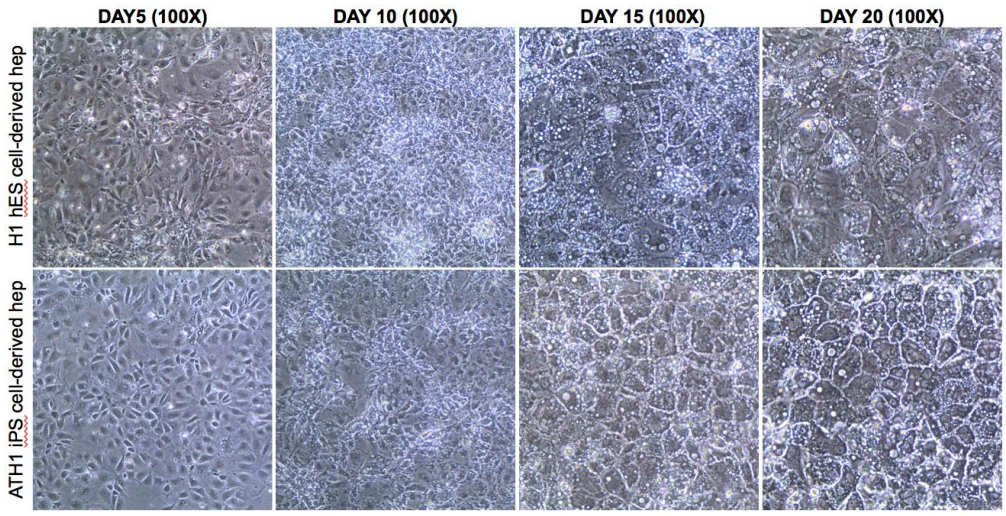

Figure 1. Morphologic changes during hepatocyte differentiation of H1 hES cell and ATD iPS cell after days 5 to 20. Morphology of iPS cells after the phase of definitive endoderm (day 5), hepatic specification (day 10), hepatic induction (day 15), and hepatic maturation (day 20).

1.2. Differentiation of human iPS cells into hepatocytes.

We have now generated iPS cell-derived hepatocytes in a manner similar to what we have published[1], and using a variation on the technique described by Si-Tayeb [2]. **Figure 1** illustrates the morphologic changes that occur

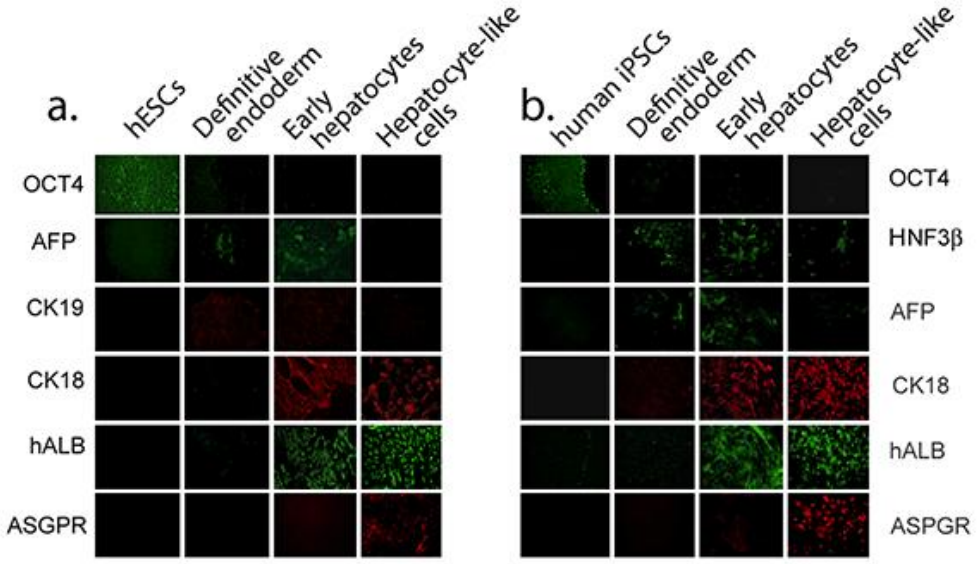

Figure 2. Expression of cellular marker proteins during differentiation of human ES (a) and iPS (b) cells. The ES and iPS cells were differentiated sequentially to definitive endoderm, early hepatocytes and hepatocyte-like cells. Immunofluorescence staining for human OCT4, alpha-fetoprotein (AFP), cytokeratin 19 (CK19), cytokeratin 18 (CK18), hepatic nuclear factor 3β (HNF3β), human serum albumin (hALB) and asialoglycoprotein receptor (ASGPR) are shown.

during differentiation, and **Figure 2** demonstrates changes in the expression profile during various stages of the later differentiation process. Not shown is that after completion of the differentiation protocol, UGT1A1 activity in the cells was 15-20% of that in human liver homogenates. **Figure 3** shows that the differentiated H1 hES cells and ATD iPS cells exhibit several ultrastructural features seen in primary human hepatocytes.

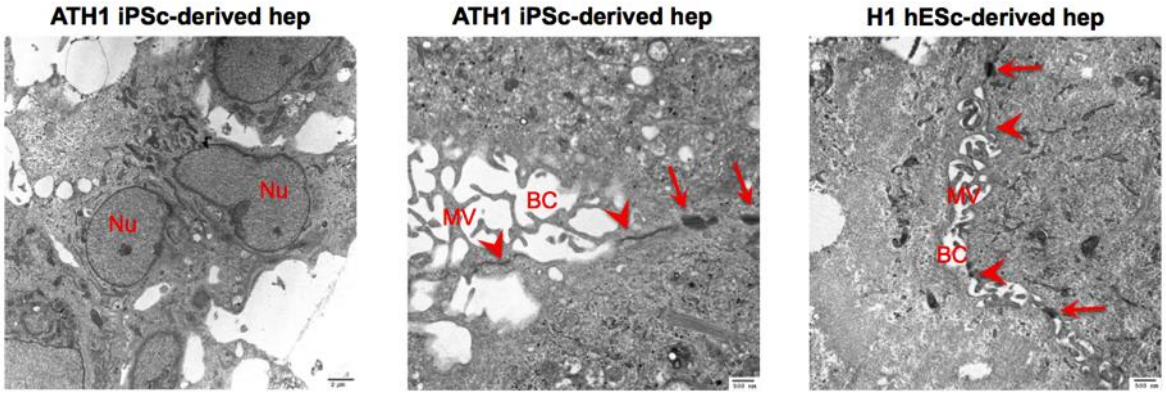

Figure 3. Electron micrograph of H1 hES cells and ATD iPS cells following hepatocyte-specific differentiation. Shown are the nuclei (Nu), bile canaliculi (BC), microvilli (MV), tight junctions (arrowhead), and desmosomes (arrow).

1.3. Analysis of differentiated ATD iPS cells.

We performed several experiments to determine whether ATD iPS cell-derived hepatocytes recapitulate the defect observed in ATD hepatocytes. In **Figure 4**, we show that differentiated cells secreted 50-65% of the albumin levels secreted by 1° human hepatocytes but ATD iPS cell-derived hepatocytes secreted only 50% of the level of AT secreted by WT iPS cell-derived or 1° human hepatocytes. In **Figure 5**, we show that similar to an ATD patient liver biopsy, electron micrograph of ATD iPS cell-derived hepatocytes showed poorly organized and markedly dilated rER. In **Figure 6**, we show using a pulse-chase analysis that there is a slower rate of disappearance of intracellular AT in differentiated ATD iPS cells (t½=2.1 to 4 hr) compared to control cells (t½=1.3 hr). More importantly, ATD iPS cell-derived hepatocytes from a patient with severe liver disease showed a more prominent delay in the disappearance of intracellular AT (ATH-1 iPS t½=4 hr) compared to those from a patient with no liver disease (AT-10 iPS t½=2.1 hr).

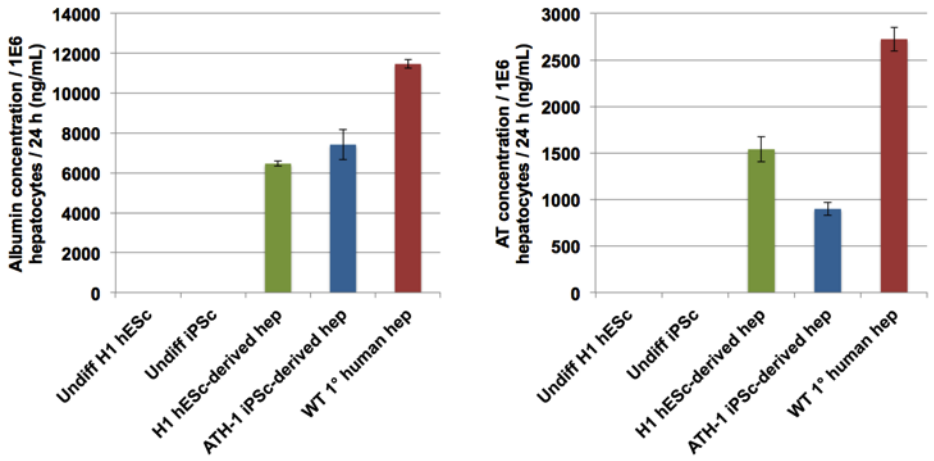

Figure 4. ELISA results following hepatocyte-specific differentiation of H1 hES cells and ATD iPS cells. Shown are the albumin and AT-specific ELISA measurements derived from the supernatant of differentiated cells over a period of 24 hours after the hepatic maturation step of differentiation compared to the results from control fresh primary human hepatocytes.

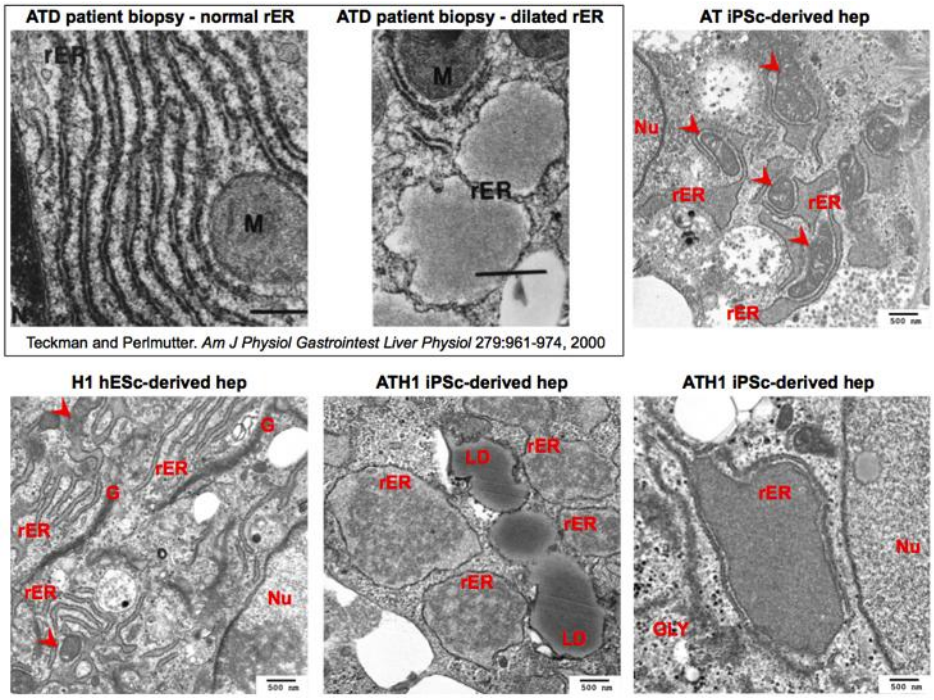

Figure 5. Electron micrograph of differentiated H1 hES cells and ATD iPS cells following hepatocyte-specific differentiation show markedly dilated rER in differentiated ATD iPS cells. Shown are the nuclei (Nu), rough endoplasmic reticulum (rER), Golgi bodies (G), lipid droplets (LD), glycogen rosettes (GLY), microvilli (MV), and mitochondria (arrowhead. For comparison, micrographs of normal and dilated rER obtained from a liver biopsy of an ATD patient are also shown (inset).

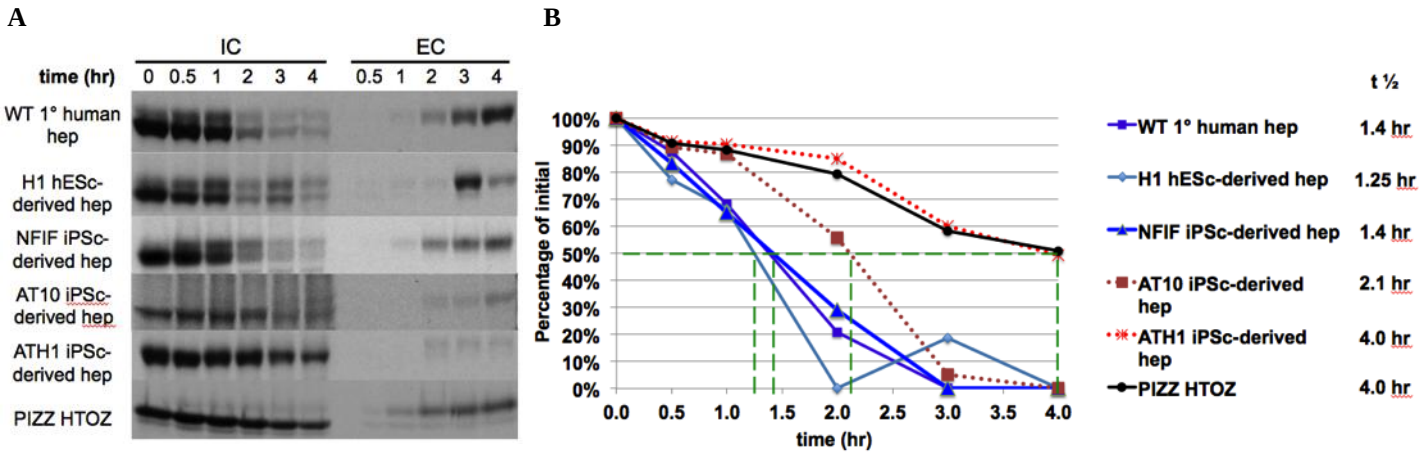

Figure 6. Pulse chase analysis of differentiated stem cells and control cells. After cells were pulsed for 1 hour with 35S-methionine-containing medium, intracellular (IC) and extracellular (EC) fractions were collected at each of the indicated chase time points (0 to 4 hours). Samples were run on an SDS-PAGE gel and an autoradiograph was obtained (A). Densitometric analysis was performed in order to calculate the half-life (t½) of the rate of disappearance of intracellular AT (B).

1.4. Transplantation of human iPS cell-derived hepatocytes with correction of hyperbilirubinemia in the Gunn rat model of Crigler-Najjar syndrome type 1.

To determine the extent to which stem cell-derived human hepatocytes could be engrafted in immune suppressed rat hosts, we transplanted iPS cell-derived hepatocytes into Gunn rat livers by intrasplenic injection [3]. To provide a proliferative advantage to the transplanted cells,

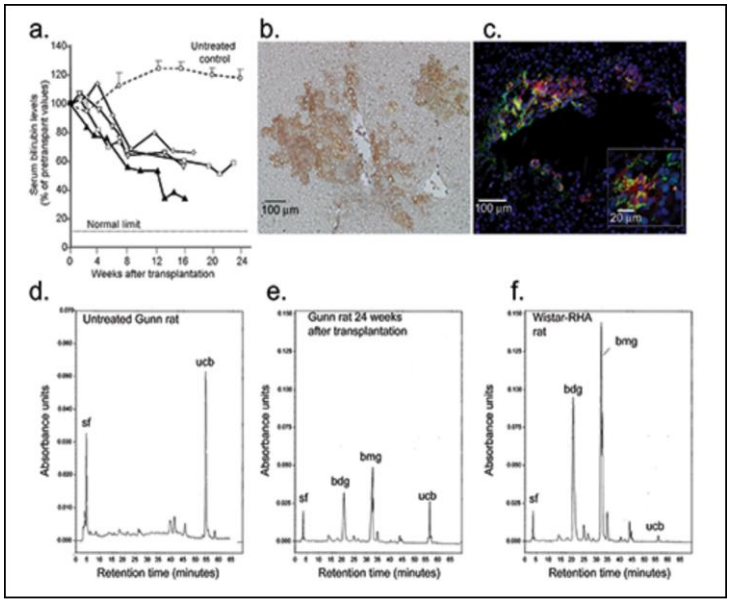

Figure 7. Effect of repopulation of the Gunn rat liver by iPS cell-derived hepatocytes. a, Serum bilirubin levels in the four recipient Gunn rats (diamond, square, open and closed triangles) at the indicated time points after transplantation of human iPS cell-derived hepatocytes are shown as percentage of pre-transplantation levels. Bilirubin levels of untreated age-matched controls are also shown (open circles, mean+SEM of 6 rats). The upper limit of serum bilirubin levels in congenic normal Wistar-RHA rats is shown as a dotted line. b and c, Representative liver sections from a recipient Gunn rat 4-6 months after transplantation of human iPS-derived hepatocytes. b, Immunohistochemical staining for human UGT1A1 showing cell clusters derived from the transplanted cells. c, Dual immunofluorescence staining showed that a majority of cells positive for human serum albumin (green) were also positive for human UGT1A1 (red). The nuclei are stained blue (DAPI). A magnified view is shown in the insert. d-f, HPLC analysis of bilirubin species excreted in the bile of a control Gunn rat, a rat receiving iPS-derived hepatocytes and a congeneic normal Wistar RHA rat is shown. sf, solvent front; ucb, unconjugated bilirubin; bdg, bilirubin diglucuronide; bmg, bilirubin monoglucuronide. Note the difference in the absorbance unit scale in panel c from that in panels d and e.

part of the host liver was irradiated (50Gy) and an adenovirus vector expressing hepatocyte growth factor was injected. For immune suppression, Tacrolimus (2mg/kg) was injected daily beginning 7 days before transplantation. After transplantation, serum bilirubin levels declined, as shown in **Figure 7**, and immuno-histochemistry of liver sections showed clusters of human albumin and UGT1A1-positive cells, and bilirubin conjugates appeared in the bile, indicating function by engrafted, UGT1A1-expressing iPS-derived hepatocytes.

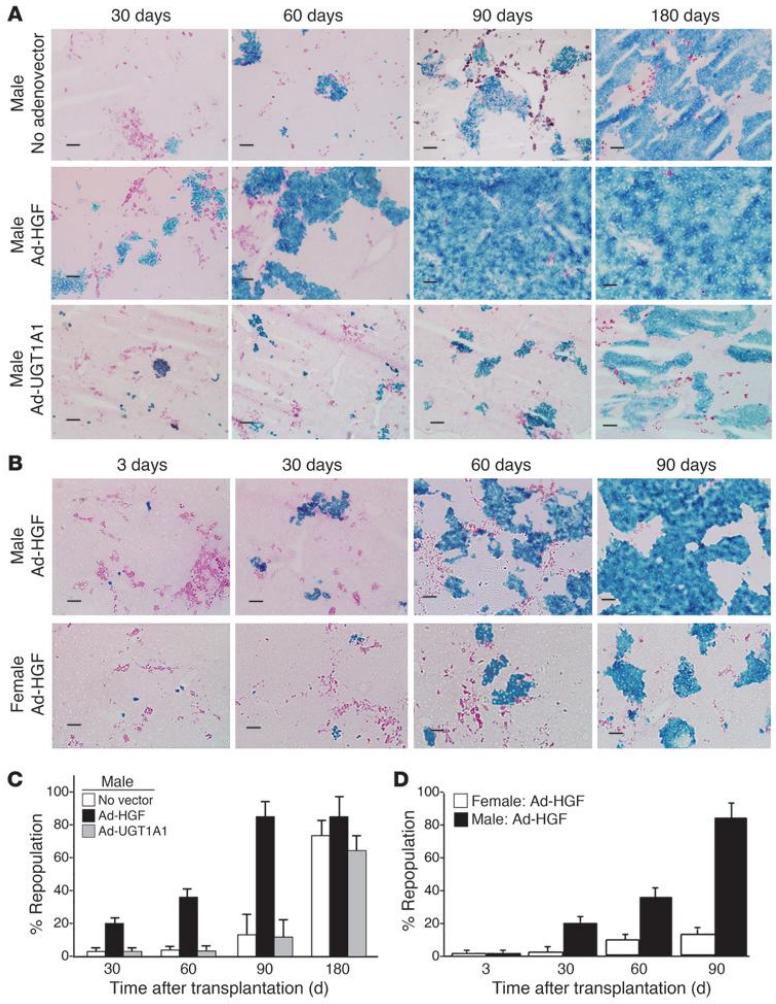

Figure 8. Kinetics of hepatic repopulation in PiZ mice. (A) Ad-HGF administration accelerated repopulation. ROSA26 mouse hepatocytes (1 × 106) were transplanted into male PiZ mice without (upper row) or with (lower row) Ad- HGF (1 × 1011 particles, i.v.). Liver sections were stained for *E. coli* β-gal (blue), and diastase plus PAS (magenta) to visualize AAT-Z globules. Scale bars: 100 μm. Data are from representative mice from each group (*n* = 6). (B) Repopulation was greater in male recipients. Male and female PiZ mice received Ad-HGF (*n* = 6). Hepatocyte transplantation and staining of liver sections were as in A. (C and D) Quantitative DNA PCR. Quantitative PCR for the *E. coli lacZ* gene was performed on DNA extracted from livers of recipient mice. Percentage of repopulation was calculated as described in the text. (C) Graphic presentation of data from experimental groups shown in A (mean ± SEM; *n* = 6 in each group), showing significantly higher repopulation in the Ad-HGF group at all time points (*P* < 0.05). (D) Data are from the experimental groups shown in B (mean ± SEM; *n* = 6 in each group), showing significantly higher repopulation in males 30, 60, and 90 days after transplantation (*P* < 0.05).

1.5. Hepatocyte engraftment and proliferation in AT (PiZ) transgenic mice.

In several animal models, transplanted hepatocytes have a proliferation advantage over the host liver cells, and nearly 100% of the native liver can be replaced by the donor cells [4, 5]. In AT deficiency, the abnormal Z protein can aggregate in hepatocytes and these aggregates may damage cells. Through this mechanism, AT deficiency patients may develop liver disease. Since Z protein aggregation leads to hepatocyte apoptosis, it has been hypothesized that PiM hepatocytes transplanted into PiZ livers would have a similar selective advantage and may progressively increase their relative contribution to liver mass. To examine this possibility, hepatocytes isolated from ROSA26 (beta-galactosidase transgenic mice) were transplanted into 6-8 week old human AT (hAT) transgenic mice. Three months after transplantation approximately 20% of the native liver was replaced by ROSA26 hepatocytes, as assessed histologically by lacZ staining **(Figure 8)**. These data provide direct evidence, in an animal model, that PiM hepatocytes have the capacity to progressively replace PiZ-expressing hepatocytes following transplantation. In addition, we have accumulated direct evidence that expansion of donor hepatocytes occurs in association with specific areas in the native liver where high levels of the mutant AT protein can be found as aggregates in the host hepatocytes, presumably leading to apoptosis [6].

We then hypothesized that expression of the mutant AT-Z should reduce the capacity of the host hepatocytes to proliferate in response to mitotic stimuli, which should accelerate repopulation by transplanted wildtype cells. To test this, we examined the extent of hepatic repopulation after hepatocyte transplantation in groups of recipient PiZ mice with administration of Ad-HGF. The extent of repopulation was significantly greater at all time points in the group that received Ad-HGF. A control group that received an adenovector that expressed an irrelevant gene did not exhibit accelerated repopulation. Ninety days after transplantation 40-60% of the hepatocytes were replaced by donor cells, and in occasional PiZ recipients, the repopulation was nearly complete, so that only the bile duct epithelial cells and the non-parenchymal cells remained from the host liver **(Figure 8)**. The increased death rate of host hepatocytes, combined with a greater mitotic activity of the donor cells resulted in progressive repopulation of the host liver by the donor cells, while the liver size remained unaltered.

1.6. iPS cell-derived human hepatocyte engraftment and proliferation in immune-deficient AT transgenic mice.

In last year's report we examined whether human hES cell-derived hepatocytes could engraft and proliferate spontaneously in the livers of immune deficient PiZ mice. We have now examined whether iPS-derived hepatocytes can engraft in such animals. We generated SCID/PiZ mice, and the PiZ genotype in the offspring and zygosity for the SCID mutation were determined by PCR and pyrosequencing, respectively. Human iPS cells were then differentiated to hepatocytes as described, and one million cells were transplanted into the livers of SCID/PiZ mice by intrasplenic injection. To stimulate mitosis of hepatocytes, $1x10^{11}$ adenovirus vector particles expressing hepatocyte growth factor (Ad-HGF) were injected IV into recipients one day after transplantation. Engrafted hepatocytes were identified by immunofluorescence staining for human serum albumin (HSA). The engrafted human cells had hepatocyte-like morphology and,
by three months after transplantation, engrafted iPS-derived hepatocytes were present as large colonies within the host liver **(Figure 9)**. Host cells exhibited diastase/PAS-positive AT-Z globules, but the HSA-positive human hepatocytes did not. These studies indicate that immune deficient PiZ mice are an excellent model for evaluating stem cell-derived human hepatocytes in terms of engraftment, proliferation and function [7].

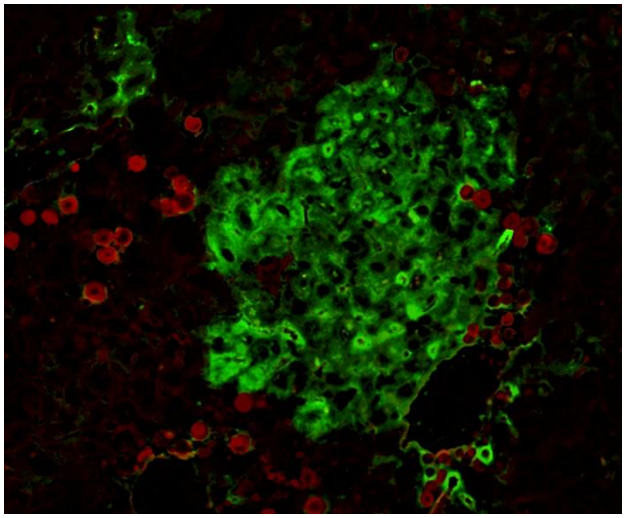

Fig 9. Transplantation of ES-derived human hepatocytes in SCID-PiZ mice. Three-months following transplantation of iPS-derived hepatocytes into immune deficient PiZ mice, immunofluorescence shows large clusters of engrafted iPS-derived hepatocytes stained green for human albumin. Red staining represents hAT globules in host hepatocytes. Nuclei are stained with Dapi (blue).

KEY RESEARCH ACCOMPLISHMENTS:

1. Generation and characterization of iPS cell lines from control patients and patients with AT-deficiency
2. Further characterization of iPS cells during differentiation into hepatocyte-like cells
3. Determination of AT secretion by ELISA, ultrastructure by electron microscopy and rate of disappearance of intracellular AT by pulse chase analysis in ATD iPS cell-derived hepatocytes compared to controls.
4. Transplantation and expansion of human iPS-derived hepatocytes in rats, with correction of hyperbilirubinemia in the Gunn rat model of Crigler-Najjar syndrome type 1.
5. Complete repopulation of PiZ mouse livers with allogeneic hepatocytes facilitated by the use of hepatocyte growth factor administration after transplantation
6. Engraftment and proliferation of human pluripotent stem cell-derived hepatocytes in immune-deficient alpha-1-antitrypsin-deficient transgenic mice

REPORTABLE OUTCOMES:

1. Tafaleng E, Han B, Hale P, Soto-Gutierrez A, Nagaya M, Duncan S, Stolz D, Strom S, Roy-Chowdhury J, Perlmutter D, Fox I. In vitro modeling of alpha-1-antitrypsin deficiency using induced pluripotent stem cell-derived hepatocytes from alpha-1-antitrypsin deficient patients. AASLD 2012.
2. Ding J, Yannam GR, Roy-Chowdhury N, Hidvegi T, Basma H, Rennard SI, Wong RJ, Avsar Y, Guha C, Perlmutter DH, Fox IJ, Roy-Chowdhury J. Spontaneous repopulation of the liver of transgenic mice expressing mutant human alpha 1-anti-trypsin by wildtype donor hepatocytes. J Clin Invest 2011;121(5):1930-1934.
3. Roy-Chowdhury N, Chen Y, Atienza K, Chang C, Wang X, Guha C, Fox IJ, Bouhassira EE, Roy-Chowdhury J. Amelioration of hyperbilirubinemia in Gunn rats after transplantation of human hepatocytes derived from induced pluripotent stem cells. Science Trans Med (submitted).
4. Atienza K, Ding J, Chang C-J, Bouhassira E, Chen Y, Wang X, Avsar Y, Liu L, Guha C, Fox IJ, Salido E, Roy-Chowdhury J, Roy-Chowdhury N. Reduction of urinary oxalate excretion after transplantation of human induced pluripotent stem cell-derived hepatocytes in a mouse model of primary hyperoxaluria-1. AASLD 2011.
5. Ding J, Wang X, Neufeld D, Hansel M, Strom S, Fox IJ, Guha C, Roy-Chowdhury N, Roy-Chowdhury J. SCID/PiZ mice: a novel animal model for evaluating engraftment and proliferation of human stem cell-derived hepatocytes. AASLD 2011.
6. Avsar Y, Zhou H, Wang X, Ding J, Guha C, Fox IJ, Roy-Chowdhury N, Roy-Chowdhury J. Pharmacological enhancement of hepatocyte engraftment augments the hypobilirubinemic effect of hepatocyte transplantation in the Gunn rat model of Crigler-Najjar syndrome type 1. AASLD 2011.
7. Ito R, Fong J, Setoyama K, Gramignoli R, Tahan V, Nagaya M, Soto-Gutierrez A, Strom S, Fox IJ. Hepatocyte Xenografts Undergo Stable Long-Term Engraftment in Rats Treated with FK506 but Discordant Xenograft Albumin Secretion is 100-Fold Lower than Allograft Albumin Secretion. AST 2011.
8. Invited Speaker, iPS cell Banking Workshop, California Institute for Regenerative Medicine, San Francisco, CA, November 17-18, 2010.
9. Invited Speaker, Oregon Health and Science University Stem Cell Center, "Use of stem cells to study and treat liver disease" Portland, Oregon, February 7-8, 2011
10. Invited Speaker, AASLD Basic Research Single Topic Conference – Stem Cell in Liver Diseases and Cancer: Discovery and Promise, "Stem cells and the treatment of liver disease: understanding liver failure and cirrhosis, Atlanta, Georgia, March 19-20, 2011.
11. Invited Speaker, Yale University Stem Cell Center Seminar Series, "Stem cells and the liver" New Haven, Connecticut, March 28-29, 2011.
12. Invited Speaker, Medical College of Wisconsin, "Use of hepatocytes and stem cells to study and treat liver disease", Milwaukee, Wisconsin, May 10-11, 2011.

13. Invited Speaker, The 66th General Meeting of the Japanese Society of Gastroenterological Surgery, "Overcoming barriers to the use of hepatocytes and stem cells in treating patients with liver diseases", Nagoya, Japan, July 13-15, 2011.
14. Invited Speaker, Research Seminar Series in Developmental and Regenerative Biology, University of Kansas Medical Center, "Use of hepatocytes and stem cells to study and treat liver disease", Kansas City, Kansas, November 9-10, 2011.
15. Keynote Speaker, ISMRM Workshop on MRI-based cell tracking "Hepatocyte transplantation and the need to track engrafted cells", Miami Beach, Florida, January 29 – February 1, 2012.
16. Invited Speaker, Challenging the Paradigms: Liver Transplantation for Metabolic Disease, Children's Hospital of Pittsburgh, "Hepatocyte transplantation", Pittsburgh, PA, May 4-5, 2012.
17. Invited Speaker, American Society of Gene & Cell Therapy 15th Annual Meeting, "Overcoming barriers to successful cell therapy to treat liver disease", Philadelphia, PA May 16-19, 2012
18. Invited Speaker, 16th Maple Syrup Urine Disease Symposium, "Clinical hepatocyte transplantation for the treatment of metabolic liver diseases", Philadelphia, PA, June 28-30, 2012
19. Moderator, Mid-day Symposium: "Allotransplants, Cellular Transplants, Organ Repair, and Xenotransplants? A Debate about the Future of Organ Transplantation", American Transplant Congress, Boston, MA, June 2-6, 2012.
20. Invited Speaker, Liver Biology: Fundamental Mechanisms & Translational Application, FASEB Summer Research Conference, "Hepatocyte, stem cell transplantation, tissue engineering", Snowmass Village, Colorado, July 29 – August 3, 2012.
21. Invited Speaker, 8th Royan International Congress on Stem Cell Biology and Technology, "Overcoming barriers to the use of hepatocytes and stem cells in treating patients with liver diseases" and "Use of hepatocytes and stem cells in understanding and treating liver failure and cirrhosis", Tehran, Iran, September 5-7, 2012.

CONCLUSIONS:

The outcomes of our studies are being accomplished as expected, and there is no change anticipated in the research plan. The intention for future studies is to attain better engraftment and more complete characterization of differentiated cells following transplantation.

REFERENCES

1. Basma H, Soto-Gutierrez A, Yannam GR, et al. Differentiation and transplantation of human embryonic stem cell-derived hepatocytes. Gastroenterology 2009;136:990-9.
2. Si-Tayeb K, Noto FK, Nagaoka M, et al. Highly efficient generation of human hepatocyte-like cells from induced pluripotent stem cells. Hepatology;51:297-305.
3. Roy-Chowdhury N, Chen Y, Atienza K, et al. Amelioration of hyperbilirubinemia in Gunn rats after transplantation of human hepatocytes derived from induced pluripotent stem cells. . AASLD 2010.
4. Overturf K, Al-Dhalimy M, Tanguay R, et al. Hepatocytes corrected by gene therapy are selected in vivo in a murine model of hereditary tyrosinaemia type I. Nat Genet 1996;12:266-73.
5. Rhim JA, Sandgren EP, Degen JL, Palmiter RD, Brinster RL. Replacement of diseased mouse liver by hepatic cell transplantation. Science 1994;263:1149-52.
6. Ding J, Yannam GR, Roy-Chowdhury N, et al. Spontaneous hepatic repopulation in transgenic mice expressing mutant human alpha1-antitrypsin by wild-type donor hepatocytes. The Journal of Clinical Investigation 2011;121:1930-4.
7. Ding J, Wang X, Neufeld DS, et al. SCID/PiZ mice: a novel animal model for evaluating engraftment and proliferation of human stem cell-derived hepatocytes. AASLD 2011.

TRANSPLANTATION OF PURIFIED HUMAN SKELETAL MUSCLE-DERIVED PERICYTES REDUCE FIBROSIS IN INJURED ISCHEMIC MUSCLE TISSUES

[1,2,4]Chien-Wen Chen, [2,4]Masaho Okada, [1,3,4,5]Kimimasa Tobita, [4]Mihaela Crisan, [3,4,5,6]Bruno Péault, [2,4,5]Johnny Huard
Department of Bioengineering[1], Orthopedic Surgery[2], Pediatrics[3], Stem Cell Research Center, Children's Hospital of Pittsburgh[4], and McGowan Institute for Regenerative Medicine[5], University of Pittsburgh and UPMC and [6]David Geffen School of Medicine, University of California at Los Angeles;
jhuard@pitt.edu

INTRODUCTION

Vascular pericytes are the mural cells that tightly encircle capillaries and microvessels throughout the body. In general, pericytes control blood vessel maturation, stability and contractility.

Multi-lineage stem/progenitor cells have been identified within virtually all organs in both human and mouse and are named diversely [1]. However, due to the retrospective discovery of these multi-lineage stem/progenitor cells in culture, the true identity of these cells *in situ* remained obscure. It has been hypothesized that vascular pericytes are indeed, or at least contain, stem/progenitor cells that are able to differentiate into bone, cartilage, fat tissue and odontoblasts [2]. Recently, we and others laboratories have shown that vascular pericytes purified from multiple human organs not only express classic MSC markers but harbor stem cell properties such as myo-, osteo-, chondro- and adipogenic potentials [2]. Consequently, pericytes are assumed to be one of the developmental origins of MSC. Human skeletal muscle-derived pericytes were not only shown to regenerate skeletal muscle fibers in dystrophic as well as cardiotoxin-injured mouse muscle but also sustain impaired cardiac function after myocardial infarction *in vivo* [2]. Nevertheless, whether transplanted vascular pericytes contribute to the reduction of fibrosis at the site of injury remains to be elucidated. Matrix metalloproteinases (MMPs) are proteolytic enzymes responsible for extracellular matrix protein degradation with an important role in tissue remodeling processes. MMP-2 and MMP-9 activities are often implicated in fibrosis [3]. Using the animal model that has been established previously, we commenced to explore whether or not pericytes influences scar tissue formation within the damaged ischemic myocardium and attempt to elucidate the mechanism(s) of action [4].

METHODS

Cell Isolation and Cell Sorting: Fresh specimens of human fetal skeletal muscle were mechanically dissociated and digested with collagenases. After lysis of erythrocytes, single cell suspension was obtained by filtering with 70-μm cell strainer. For cell sorting, cells were incubated with the following directly-conjugated antibodies: anti-CD34-PE, anti-CD45-APC, anti-CD56-PE-Cy7, and anti-CD146-FITC. For dead cell exclusion, 7-amino-actinomycin D (7-AAD) was added to stained cells before running on a FACSAria flow cytometer. Flow cytometry with an identical gating strategy was used to verify the purity of long-term cultured muscle-derived pericytes.

Animal Model of Fibrosis: Permanent ligation of the left coronary artery was performed on NOD/SCID mice under open-chest surgery. Immediately after the ligation, skeletal muscle-derived pericytes from cultures were injected into the ischemic myocardium (3×10^5 cells/heart), while the control groups received saline injections (PBS).

Histology: Masson's trichrome staining was employed to reveal myocardial fibrosis. The ratio of fibrotic area was estimated by total collagen deposition versus total sectional area using Image J software.

Hypoxic Culture: Pericytes were cultured *in vitro* under hypoxic conditions (2.5% oxygen) for 24 hours. Supernatants and cell pellets were subsequently collected for analysis.

Real-time Quantitative PCR: Real-time Quantitative PCR analysis was performed to detect gene expressions of matrix metalloproteinase-2 (MMP-2) and -9 (MMP-9) in total muscle lysates and muscle-derived pericytes cultured under normal and hypoxic conditions.

RESULTS

Purification of Human Muscle-derived Pericytes: $CD34^-45^-56^-146^{high}$ muscle-derived pericytes were sorted and cultured as previously described [2]. To ensure long-term cultured muscle-derived pericytes remain homogeneous and retain their native properties, flow cytometry was employed to examine the expression of cell surface markers used to select these cells plus alkaline phosphatase (ALP), another pericyte marker. The result shows that after long-term culturing (>10 passages), all cells remain negative for CD34, CD45 and CD56, and virtually all pericytes are positive for CD146 and ALP (Figure 1a).

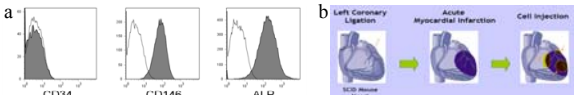

Figure 1. (a) Flow cytometry analysis of long-term cultured $CD34^-CD45^-CD56^-CD146^{high}$ pericytes . (b) Schematic depiction of transplantation of muscle-derived pericytes.

Transplantation of Muscle-derived Pericytes: Immediately after permanent ligation of the left coronary artery, muscle-derived pericytes from cultures were injected into the ischemic myocardium at a density of 3×10^5 cells/heart (Figure 1b) [4].

Scar Tissue Formation: Masson's trichrome staining revealed myocardial fibrosis after infarction with collagen deposition stained in blue (Figure 2a). Quantification at 2 weeks post injection demonstrated a 38% reduction of the fibrotic area in pericyte-injected left ventricles, compared to saline-injection (Figure 2b).

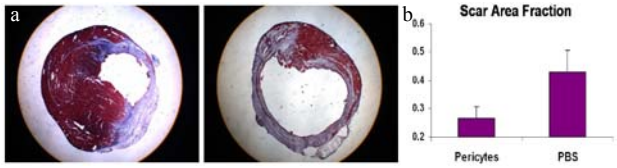

Figure 2. (a) Collagen deposition was stained blue to show the extent of myocardial fibrosis. (b) Pericyte-injected hearts had an average 38% reduction of the scar area.

Expression of MMP-2 by Muscle-derived Pericytes: Real-time quantitative PCR results revealed that cultured muscle pericytes have higher expression of MMP-2 gene than total muscle lysates, but not MMP-9. Under hypoxic culture conditions, muscle pericytes retain high expression of MMP-2 gene, while MMP-9 remained very low (Figure 3).

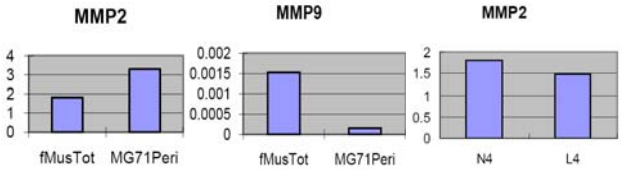

Figure 3. Real-time qPCR results of (a) MMP-2 gene (b) MMP-9 gene expression level of total muscle lysates and long-term cultured muscle pericytes. MMP-2 gene expression level was compared between muscle pericytes cultured under normoxia (N4) and hypoxia (L4).

DISCUSSION

We demonstrated that transplantation of purified skeletal muscle-derived pericytes ameliorate fibrosis in injured ischemic cardiac muscle, possibly exerting a preventative effect. Reduced MMP-2 activity has been shown to contribute to cardiac fibrosis in pathological conditions [5]. We consequently hypothesized that the high expression level of MMP-2 by muscle-derived pericytes, even under hypoxic conditions, may play a key role in pericyte-mediated reduction of fibrosis. We are currently conducting experiments to demonstrate the efficacy of muscle pericyte transplantation in diminishing chronic fibrosis. We are also investigating the influence of increased angiogenesis, a beneficial effect displayed by muscle pericytes, on reduction of fibrosis. Overall, this study will shed light on the therapeutic value of muscle-derived pericytes for the treatment of fibrosis in the injured tissues including musculoskeletal tissues.

ACKNOWLEDGMENTS

This work was partly supported by funding from the National Institutes of Health (1R21 HL083057-01A2 awarded to B.P.) and by the Henry J. Mankin Endowed Chair for Orthopaedic Research at the University of Pittsburgh (held by J.H.).

REFERENCES

1. Péault et al. Mol Ther. 2007 May;15(5):867-77.; **2.** Crisan et al. Cell Stem Cell 2008; 3(3):301-13**.;** 3. Tanriverdi-Akhisaroglu et al. Cell Biochem Funct. 2009 Mar;27(2):81-7.; 4. Okada et al. J Am Coll Cardiol. 2008; 52(23):1869-80.; 5. Van Linthout et al. Basic Res Cardiol. 2008 Jul;103(4):319-27.

Transplantation of p65 Deficient Stem Cells Improved the Histopathology of Skeletal Muscle in Dystrophic Mice

[1]Aiping Lu; [2] Qing Yang; [1]Minakshi Poddar; [1]Bing Wang; [3]Denis C. Guttridge; [4]Paul D. Robbins; [1]+ Johnny Huard
[1]+Stem Cell Research Center and Department of Orthopaedic Surgery, University of Pittsburgh, Pittsburgh, PA
[2]Department of Orthopaedic Surgery, Tongji Hospital, Huazhong University of Science and Technology, Wuhan, China
[3]Department of Molecular Virology, Immunology and Medical Genetics, Ohio State University, Columbus, OH
[4]Department of Microbiogy and Molecular Genetics. University of Pittsburgh, Pittsburgh, PA
jhuard@pitt.edu

INTRODUCTION

Duchenne muscular dystrophy (DMD) is a deadly genetic disease mainly characterized by progressive weakening of the skeletal, cardiac and diaphragmatic muscles. It is critical to find a successful therapy that will improve the histopathology of the muscles of DMD patients and restore their normal function. Recent studies have demonstrated that blocking p65, a subunit of NF-κB, enhances muscle regeneration in injured and diseased skeletal muscle [1, 2], which suggests that the NF-kB signaling pathway is a contributing factor to the dystrophic pathology in DMD patients. Previously we demonstrated that muscle derived stem cells (MDSCs) isolated from the skeletal muscles of heterozygote P65 knock-out (*P65*$^{+/-}$) mice showed better muscle regeneration *in vitro* and *in vivo* compared to the MDSCs isolated from wild-type (WT) mice. We also demonstrated that the transplantation of P65$^{+/-}$ MDSCs could reduce inflammation. Based on these results we performed a set of experiments to determine if these P65$^{+/-}$ MDSCs could alleviate the pathology associated with DMD more efficiently than wild-type MDSCs. When we injected p65$^{+/-}$ MDSCs intraperitoneally into dystrophin/utrophin deficient (dys-/-:utro-/-, dKO) mice, a reliable mouse model of DMD, we found that the histopathology of various skeletal muscles improved and observed a reduction in inflammation, necrosis and pathological muscle regeneration.

MATERIALS AND METHODS

Cell Isolation: MDSCs were isolated from 5 month old P65$^{+/-}$ and WT mice as previously described via a modified preplate technique [3]. The cell suspensions from both P65$^{+/-}$ and WT muscle were plated on collagen coated flasks and cultured in proliferation medium (DMEM supplemented with 10% fetal bovine serum, 10% horse serum, 0.5% chicken embryo extract and 1% Penicillin-streptomycin) until the cell number was sufficient for injection.

***Intraperitoneal injection* (IP):** A total of 5-9 x10^5 viable cells were suspended in 50 µl of PBS and injected IP into 5-7 days old of dKO mice. Four to six weeks after transplantation, the mice were sacrificed and their muscles were harvested and flash frozen in liquid nitrogen-cooled 2-methylbutane. 10µm serial cryosections were prepared from the frozen muscle.

Immunohistocytochemistry

Cryosections were fixed with 5% formalin, blocked with 5% Donkey serum, and then incubated with an antibody against mouse IgG (Biotinlated) to determine the extent of muscle fiber necrosis. An antibody against embryonic muscle heavy chain (E-MyHC) was used to evaluate myogenic regeneration and an antibody against F4/80 (macrophage marker) was used to analyze the extent of inflammation in the muscle tissues. Streptavidin Cy3 conjugate and Alexafluor 488 conjugated anti-mouse IgG were used as secondary antibodies. H&E staining was performed to assess myofiber morphology and fibrosis.

RESULTS

Transplantation of P65+/- MDSCs improved muscle histology

H&E showed histology improvement in various skeletal muscles including the gastrocnemius, diaphragm, thigh and tibialis anterior muscles. We observed many centrally nucleated muscle fibers (new regenerated fibers) and decreased fibrosis in the p65$^{+/-}$ MDSC injection group (**Figure 1,** thigh muscle**)**.

Transplantation of P65+/- MDSCs reduced muscle necrosis

Mouse IgG staining showed that there were less necrotic muscle fibers in the mice injected with p65$^{+/-}$ MDSCs compared to the un-treated muscle **(Figure2)**

Transplantation of P65$^{+/-}$ MDSCs reduced inflammation and pathological muscle regeneration

Less inflammation and E-MyHC positive myofibers were found in the muscles of mice injected with p65$^{+/-}$ MDSCs compared to non-treated muscle **(Figure3).**

Figure1

DKO untreated muscle **DKO muscle treated with MDSCs**

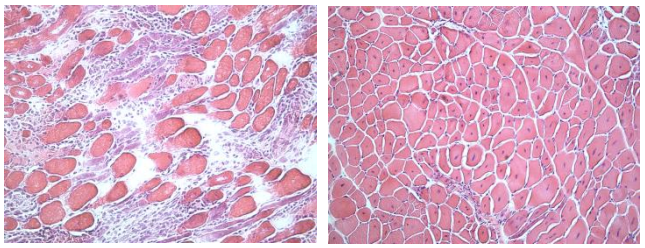

Figure2

DKO untreated muscle **DKO muscle treated with MDSCs**

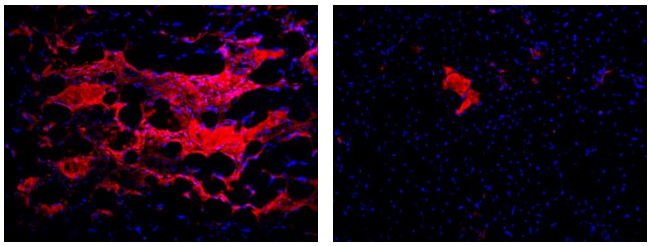

Figure3

DKO muscle nontreated **DKO muscle treated with MDSCs**

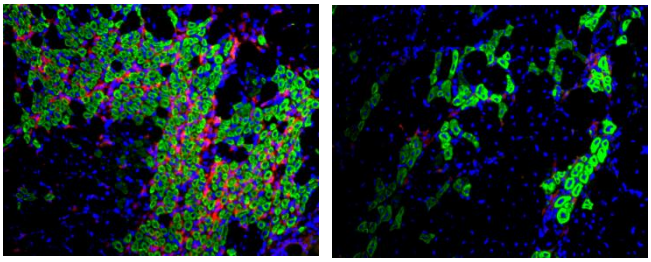

DISCUSSION

In this study we used MDSCs isolated from p65+/- mice to treat dystrophin-/-utrophin-/- mice. The up-regulation of the NF-κB pathway in these mice is associated with chronic inflammation which results in pathologies such as muscle fibrosis, necrosis, and muscle wasting. Our findings indicated that blocking p65, a subunit of NF-κB, can decrease macrophage infiltration, fibrosis formation, necrosis, and diminishes pathologic regeneration in 4 to 6 week dKO mice. We also attempted to inject the WT MDSCs isolated from normal animals; however, the results did not show an improvement in the histopathology of the mice. These results suggest that reducing the activity of the IKK/NF-κB pathway is a potential therapeutic target for the treatment of DMD. These are only preliminary data; however they are very exciting and we are planning to test additional animals in order to further confirm these results.

REFERENCES:

[1] Thaloor, D, et al Am. J.Physiol 1999; 277:C320–C329. [2] Acharyya S et al, J. Clin. Invest 2007 ; 117 :889-901. [3] Gharaibeh, et al. Nat Protoc. 2008; 3:1501-9

Immunomodulatory properties of muscle-derived stem cells associated with reduced NF-κB/p65 signaling

[1]Proto, J.; [1]Lu, A.; [2]Robbins, P.D.; [1]+Huard, J.
[1]+ Stem Cell Research Center, Children's Hospital of Pittsburgh, and Department of Orthopedic Surgery;
[2]Departments of Microbiology and Molecular Genetics, University of Pittsburgh School of Medicine, Pittsburgh, PA
jhuard@pitt.edu

INTRODUCTION

The nuclear factor kappa B (NF-kB) signal pathway has been implicated in both the normal and disease states of many different tissues. In skeletal muscle, for example, constitutive activation of inhibitor of kappa B kinase (IKKβ), a potent activator of NF-kB, leads to muscle wasting[1]. Inversely, muscle specific deletion of IKKβ in a murine model of muscular dystrophy improves dystrophic pathology and is accompanied by an increase in the number of cells fitting a muscle progenitor marker profile ($CD34^+/Sca1^-$), suggesting that NF-kB has a direct effect on muscle stem cells[2]. The NF-kB protein family includes five subunits, two of which, a p65-p50 heterodimer, are thought to play a role in blocking early myogenesis[3]. In this study, we examined the role of NF-kB signaling in the regenerative phenotype of muscle-derived stem cells (MDSCs) isolated from the gastrocnemius of p65 deficient mice (heterozygous, $p65^{+/-}$) and wild type littermates ($p65^{+/+}$). We previously found that $p65^{+/-}$ MDSCs have enhanced cell proliferation, survival under oxidative stress, differentiation, and muscle regeneration capacity. Furthermore, we have found that $p65^{+/-}$ engraftments in wild type skeletal muscle are associated with reduced inflammation and fiber necrosis compared to $p65^{+/+}$ MDSC engraftments. *In vitro* and *in vivo* experiments suggest that reduction of p65 signaling enhances the regenerative phenotype of MDSCs, suggesting this pathway as a candidate target to improve stem cell-based therapies for muscle disease and injury.

MATERIALS AND METHOD

Cell Isolation: MDSCs were isolated from five month old (n=3) $p65^{+/+}$ or $p65^{+/-}$ mice via a preplate technique [4]. A population of slowly adhering cells was obtained and expanded in DMEM containing 10% fetal bovine serum (FBS), 10% horse serum, 1% penicillin-streptomycin, and 0.5% chick embryo extract. Cells were used between passages 15 and 30.

In vivo regeneration assay: Muscle injury was induced in C57Bl/6J mice by cardiotoxin injected into gastrocnemius. One day later, MDSCs were injected into the injured muscles. Six days following transplantation, mice were sacrificed and injected muscles were harvested and snap-frozen. Serial cryosections were prepared and immunohistochemistry was performed to assess inflammation (CD14) and necrosis (IgG). The number of CD14 (+) cells was counted to assess infiltration of macrophages/monocytes. Necrosis was determined by mouse IgG staining and quantified by assessing the percentage of positively stained area.

In vitro Inflammation Model: MDSCs were grown for 24 hours in proliferation medium, after which the medium was collected and sterile filtered. RAW264.7 cells, immortal murine macrophage-like cells, were activated by exposure to 100 ng/mL LPS in either $p65^{+/+}$-, $p65^{+/-}$-, or muscle-derived fibroblast conditioned medium for 24 hours.

***Gene Expression Analysis*:** Cells were washed and RNA collected by Trizol extraction. Total RNA was reverse transcribed with Superscript III reverse transcriptase (Invitrogen) according to manufacturer's protocols. The PCR reaction was carried out with Taq Polymerase (Promega), according to manufacturer's protocols. PCR products were analyzed by electrophoresis on a 1.5% agarose gel

RESULTS

Wild type mice were injected with either $p65^{+/+}$ (Fig 1A) or $p65^{+/-}$ (Fig 1B) MDSCs in the gastrocnemius muscle and sacrificed six days later. Tissues were cryosectioned and immunostained with antibodies against CD14 to identify a monocyte/macrophage infiltrate, indicating inflammation, as well as with antibodies against mouse immunoglobulin G, a marker of necrosis. Injections of $p65^{+/-}$ cells were associated with a decrease in both necrosis and inflammation (Fig 1B-D), compared to $p65^{+/+}$ injections (Fig1A, C-D).

Figure 1.

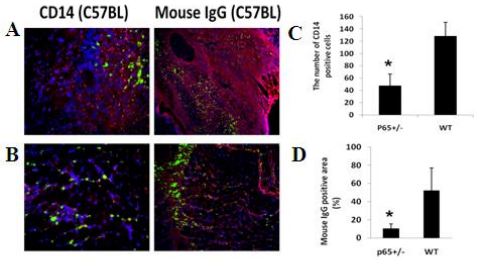

To investigate anti-inflammatory properties of MDSCs, we utilized an *in vitro* inflammation model in which RAW264.7 cells, immortal murine macrophage-like cells, are activated by LPS exposure. We found that RAW264.7 cells exposed to LPS in $p65^{+/-}$ CM expressed less IL-1 compared to controls, suggesting that p65+/- MDSCs secrete immunomodulatory factors that hinder pro-inflammatory macrophage activation.

Figure 2.

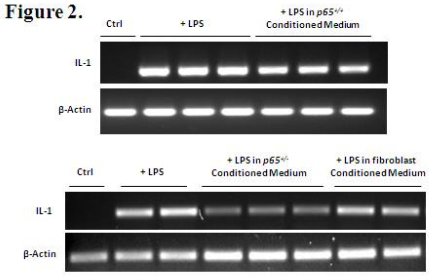

DISCUSSION

The data presented here provides evidence supporting that NF-kB inhibition stimulates MDSC-mediated muscle regeneration through multiple mechanisms, including through the expression of anti-inflammatory factors that attenuate inflammation and necrosis. These experiments identify the NF-κB signaling pathway as a potential therapeutic target to enhance muscle regeneration following injury or disease. Future directions for this project include investigating modulation of the IKK/NF-kB pathway as a means to rejuvenate the phenotype of aged muscle stem and progenitor cells. Clinical research should be conducted to test the efficacy of p65 inhibition therapy in patients suffering from muscle disorders.

REFERENCES

[1]Cai, D., et al. Cell 2004, 119:285-298. [2]Acharyya, S., et al., J Clin Invest 2007, 117:889-901. [3]Bakkar, N., et al. JCB 2008, 180(25): 787-802. [4] Gharaibeh, et al. Nat Protoc. 2008; 3:1501-9

Appendix 4

NF-κB Negatively Impacts the Myogenic Potential of Muscle-derived Stem Cells

Aiping Lu[1], Jonathan D Proto[1], Lulin Guo[1], Ying Tang[1], Mitra Lavasani[1], Jeremy S Tilstra[2], Laura J Niedernhofer[2], Bing Wang[1], Denis C Guttridge[3], Paul D Robbins[2] and Johnny Huard[1]

[1]Stem Cell Research Center, School of Medicine and Department of Orthopedic Surgery, University of Pittsburgh, Pittsburgh, Pennsylvania, USA; [2]Department of Microbiology and Molecular Genetics, University of Pittsburgh, Pittsburgh, Pennsylvania, USA; [3]Department of Molecular Virology, Immunology and Medical Genetics, The Ohio State University, Columbus, Ohio, USA

Inhibition of the inhibitor of kappa B kinase (IKK)/nuclear factor-kappa B (NF-κB) pathway enhances muscle regeneration in injured and diseased skeletal muscle, but it is unclear exactly how this pathway contributes to the regeneration process. In this study, we examined the role of NF-κB in regulating the proliferation and differentiation of muscle-derived stem cells (MDSCs). MDSCs isolated from the skeletal muscles of $p65^{+/-}$ mice (haploinsufficient for the p65 subunit of NF-κB) had enhanced proliferation and myogenic differentiation compared to MDSCs isolated from wild-type (wt) littermates. In addition, selective pharmacological inhibition of IKKβ, an upstream activator of NF-κB, enhanced wt MDSC differentiation into myotubes *in vitro*. The $p65^{+/-}$ MDSCs also displayed a higher muscle regeneration index than wt MDSCs following implantation into adult mice with muscular dystrophy. Additionally, using a muscle injury model, we observed that $p65^{+/-}$ MDSC engraftments were associated with reduced inflammation and necrosis. These results suggest that inhibition of the IKK/NF-κB pathway represents an effective approach to improve the myogenic regenerative potential of MDSCs and possibly other adult stem cell populations. Moreover, our results suggest that the improved muscle regeneration observed following inhibition of IKK/NF-κB, is mediated, at least in part, through enhanced stem cell proliferation and myogenic potential.

Received 15 April 2011; accepted 5 November 2011; published online 13 December 2011. doi:10.1038/mt.2011.261

INTRODUCTION

Nuclear factor-kappa B (NF-κB) is a ubiquitously expressed nuclear transcription factor that is evolutionarily conserved. In mammals, the NF-κB family consists of five subunits, p65 (RelA), c-Rel, RelB, p50, and p52.[1] Transcriptionally active NF-κB exists as a dimer, with the most common form being a p50–p65 heterodimer. Under nonstress conditions, the heterodimer is maintained in an inactive state in the cytoplasm via its interaction with inhibitor of kappa B (IkB) proteins. Classic NF-κB activation is mediated by IkB kinase (IKK), a large, 700–900 kDa complex consisting of two catalytic subunits, IKKα and IKKβ, and a regulatory subunit named IKKγ or NEMO (NF-κB essential modulator). In response to a variety of stimuli, including proinflammatory cytokines, bacterial products, viruses, growth factors, and oxidative stress, the complex is activated. Activated IKKβ phosphorylates IkB, leading to its polyubiquitylation and subsequent degradation by the 26S proteasome. IkB degradation allows NF-κB to translocate to the nucleus where it binds to its cognate DNA site, as well as coactivators such as CBP/p300, to induce gene expression.[2–5] Dysregulation of this pathway can result in chronic activation of IKK or NF-κB, and is seen in several pathophysiological states including cancer, rheumatoid arthritis, sepsis, muscular dystrophy, heart disease, inflammatory bowel disease, bone resorption, and both type I and II diabetes.[6,7]

The NF-κB pathway, long recognized as an important component of innate and adaptive immunity, has also more recently emerged as a key player in the regulation of skeletal muscle homeostasis.[8] Furthermore, activation of NF-κB in skeletal muscle has been linked to cachexia, muscular dystrophies, and inflammatory myopathies.[9–13] Conversely, knockout of p65, but not other subunits of NF-κB, enhances myogenic activity in MyoD-expressing mouse embryonic fibroblasts.[14] Although it is known that genetic depletion of p65 enhances muscle regeneration in both mdx and wild-type (wt) murine skeletal muscle,[13] the mechanism through which reduced of NF-κB activity positively impacts skeletal muscle remains unclear.

Given that the repair of damaged tissues is mediated by adult stem cell populations, we hypothesized that NF-κB activity negatively regulates muscle stem cell function. In this study, we specifically focus on the role of p65 in regulating muscle-derived stem cell (MDSC) growth and differentiation. This population of adult stem cells is capable of restoring muscle function.[15,16] As complete knockout of p65 ($p65^{-/-}$) results in embryonic lethality, we isolated MDSCs from the skeletal muscles (SKM) of $p65^{+/-}$ mice and wt littermates.[17] We observed that, *in vitro*, p65 haploinsuffiency was associated with increased cell proliferation and myogenic differentiation. Pharmacologic inhibition of IKK/NF-κB also enhanced myogenic

The first two authors contributed equally to the work.

Correspondence: *Johnny Huard, Stem Cell Research Center, 2 Bridgeside Point, 450 Technology Drive, Pittsburgh, Pennsylvania 15219, USA. E-mail: jhuard@pitt.edu*

differentiation. We also demonstrated that $p65^{+/-}$ MDSCs have a higher capacity for muscle regeneration after implantation into dystrophic, mdx mouse SKM. Furthermore, we show that muscle inflammation and necrosis post-injury is decreased following $p65^{+/-}$ MDSC implantation into cardiotoxin (CTX) injured SKM. These results suggest that reducing the activity of the IKK/NF-κB pathway is an effective approach to improve the myogenic potential of MDSCs and possibly other adult stem cell populations. Our results provide a novel mechanistic insight as to why the inhibition of this pathway promotes SKM healing.

RESULTS

Isolation and phenotypic characterization of MDSCs from $p65^{+/-}$ and wt mice

To examine the effect of NF-κB activity on MDSC function, we purified populations of muscle stem cells from the SKM of mice heterozygous for the p65 subunit of NF-κB ($p65^{+/-}$) and wt littermates. Using a modified preplate technique,[18] we isolated independent populations of MDSCs from three mice of each genotype. To confirm that p65 haploinsufficiency reduced basal levels of NF-κB activity, nuclear p65 was measured via ArrayScan. Nuclear, or active, p65 was found to be 30% lower in $p65^{+/-}$ than the wt MDSCs (**Figure 1a**). Upon activation, NF-κB subunits undergo post-translational modifications, such as phosphorylation, to enhance their activity.[19] Immunoblot analysis revealed that the level of phosphorylated p65 (P-p65) was also reduced; however, stimulation with tumor necrosis factor-α (TNFα) led to an increased level of P-p65 in both wt and $p65^{+/-}$ MDSCs (**Figure 1b**), demonstrating that basal, but not induced, NF-κB activity is affected by knocking-out one allele of *p65*.

To confirm the MDSC phenotype of $p65^{+/-}$ and wt cells, each population was analyzed for the expression of stem (CD34, Sca-1), myogenic (MyoD, desmin), and endothelial (CD144, CD31) cell markers by reverse transcriptase-PCR. For each of the markers, there was variability in expression between cell populations of a single genotype. However upon quantification, no significant differences were found between the different genotypes, with the exception of CD144, which was elevated in $p65^{+/-}$ MDSCs. (**Figure 2a,c,** $P < 0.05$). Such variability in marker expression has been previously reported and interpreted as evidence that these cell populations contain a mixture of stem and committed progenitor cells.[20,21] We next examined the expression of Pax7 and MyoD protein by immmunostaining, and also found no significant difference between $p65^{+/-}$ and wt cells (**Figure 2b,d**). These results suggest that genetic reduction of p65 does not dramatically alter the phenotype of MDSCs.

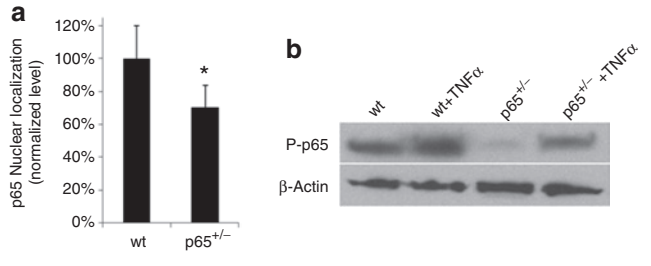

Figure 1 Muscle-derived stem cells (MDSCs) obtained from the skeletal muscles (SKM) of $p65^{+/-}$ mice have a lower level of activated p65 compared to wild-type (wt) MDSCs. (**a**) ArrayScan analysis of nuclear p65 in MDSCs isolated from $p65^{+/-}$ and wt mice. Error bars indicate "mean + SD." (**b**) Immunoblotting for phosphorylated p65 in whole cell lysates of MDSCs before and after tumor necrosis factor-α (TNFα) stimulation for 30 minutes.

$p65^{+/-}$ MDSCs proliferate faster than wt MDSCs

NF-κB is known to regulate cell division, so we investigated whether p65 reduction would alter MDSC proliferation. The three populations of $p65^{+/-}$ and wt MDSCs were plated in collagen-coated flasks and expanded in growth medium for 10–12 passages. Cells were then transferred to 24-well plates and proliferation measured using a previously described Live Cell Imaging system.[22] We observed that $p65^{+/-}$ MDSCs proliferated significantly faster than wt cells (**Figure 3a** and **Supplementary Videos S1–S2**). Equal numbers of cells were also plated on a 96-well plate and grown for three days at which point the differences in cell number were determined using an MTS assay. This assay demonstrated a similar significant increase in cell proliferation in $p65^{+/-}$ MDSCs (**Figure 3b**) suggesting that NF-κB, and in particular p65, limits the proliferation of MDSCs.

$p65^{+/-}$ MDSCs have enhanced myogenic differentiation compared to wt cells

We next measured the ability of the $p65^{+/-}$ and wt MDSCs to undergo myogenic differentiation *in vitro*. Equal numbers of cells were plated in a 24-well plate and switched to differentiation medium once the cells adhered. After 3 days the majority (80%) of the $p65^{+/-}$ cells had differentiated into myotubes, as determined by immunodetection of myosin heavy chain (**Figure 4a**). The differentiation potential of the $p65^{+/-}$ MDSCs was significantly greater than the wt MDSCs (60%; $P < 0.01$; **Figure 4b**). The difference was also demonstrated using the live cell imaging system described above (**Supplementary Videos S3–S4**). These results demonstrate that NF-κB, and in particular p65, represses MDSC differentiation *in vitro*.

Pharmacologic inhibition of IKKβ increases myogenic differentiation *in vitro*

To confirm this finding implicating NF-κB as negatively impacting MDSC differentiation, we tested whether a pharmacologic inhibitor of NF-κB could enhance MDSC myogenic potential *in vitro*. wt MDSCs were exposed to differentiation medium containing various doses of IKK-2 inhibitor IV (IKKi), a specific, reversible inhibitor of IKKβ. Cell lysates were collected at 0, 1, 14, 24, 48, and 72 hours following treatment. Accordingly, myosin heavy chain (MyHC) levels dramatically increased, beginning at 14 hours (**Figure 5a,c**). As expected, we observed a robust time-dependent decrease in P-p65 that was dose-dependent (greater at 3 μmol/l than 1 μmol/l; **Figure 5b**). We next examined NF-κB activity in wt and $p65^{+/-}$ MDSCs at various time points during myogenic differentiation by immunodetection of P-p65 and MyHC. In wt cells, beginning at 48 hours post-transition to differentiation medium, the levels of p-p65 were detectably reduced (**Figure 5d**). This occurred more rapidly (by 24 hours) in $p65^{+/-}$ cells. Similarly, accumulation of MyHC was greater at earlier time points (14 hours) in $p65^{+/-}$ cells than wt. This timeframe for MyHC accumulation is similar

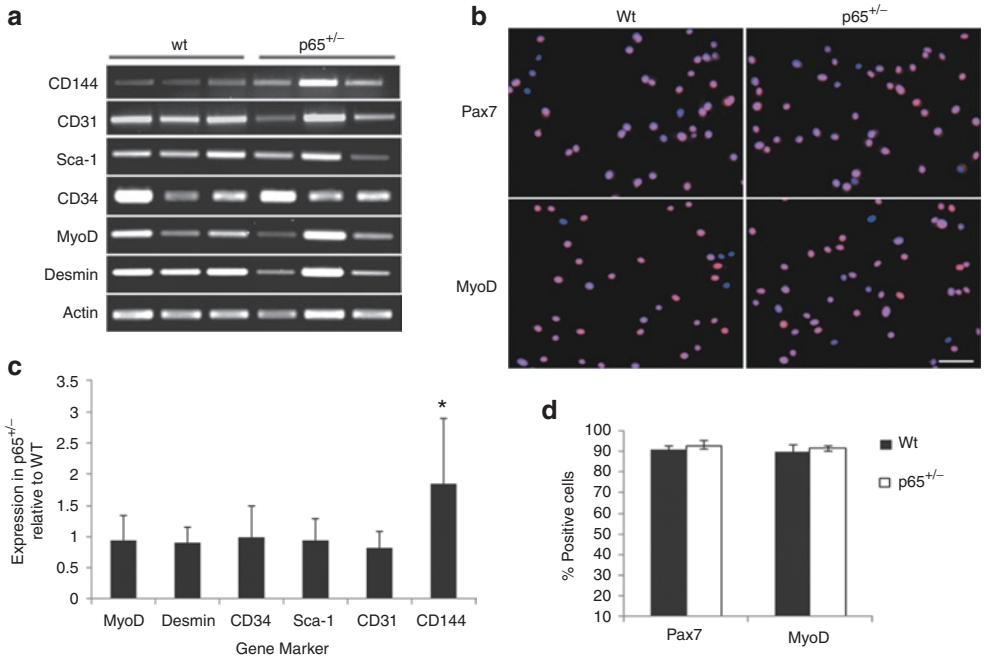

Figure 2 ***p65*$^{+/-}$ and wild-type (wt) muscle-derived stem cells (MDSCs) exhibit a similar molecular marker profile.** (**a**) RNA was isolated from three independent cell populations of each genotype. Reverse transcriptase-PCR (RT-PCR) was performed to characterize the MDSC populations for the expression of stem (CD34 and Sca-1), endothelial (CD31 and CD144) and myogenic (MyoD and desmin) cell markers. (**b**) Immunostaining for the muscle stem cell markers Pax7 and MyoD was also performed (bar = 25 µm). (**c**) Quantification of RT-PCR results. Error bars indicate "mean + SD" (n = 3 independent experiments). (**d**) Quantification of Immunostaining of Pax7 and MyoD.

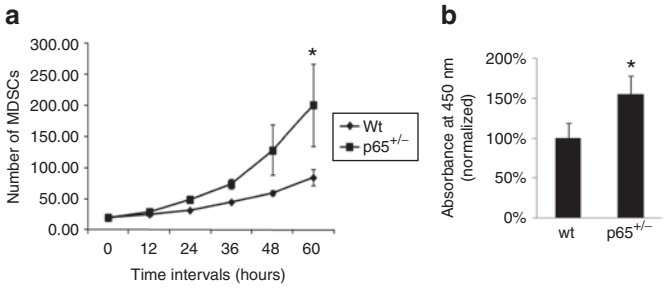

Figure 3 Muscle-derived stem cells (MDSCs) isolated from *p65*$^{+/-}$ mouse skeletal muscles (SKM) have a higher rate of proliferation than wild-type (wt) cells. (**a**) Cell proliferation rate was measured by Live Cell Imaging and (**b**) by an MTS assay ($P < 0.05$).

to that observed in wt cells treated with IKKi (Figure 5a). In order to verify that increased MyHC expression was concomitant with increased myotube formation, we treated wt MDSCs with 5 µmol/l IKKi. After 3 days, differentiation was assessed by immunofluorescence detection of MyHC. As shown in Figure 5e, compared to nontreated controls, the inhibitor caused a significant increase in myotube formation. The level of myogenic differentiation was comparable to that of *p65*$^{+/-}$ MDSCs ($P < 0.01$; Figure 5f). These results provide strong support that MDSC myogenic potential can be improved using NF-κB inhibition *ex vivo*.

p65$^{+/-}$ MDSCs have greater muscle regenerative capacity *in vivo*

To determine whether genetic depletion of p65 increases the engraftment and muscle regenerative capacity of MDSCs *in vivo*, we examined the ability of *p65*$^{+/-}$ and wt MDSCs to regenerate muscle fibers following their intramuscular implantation into an immunocompromised model of Duchenne muscular dystrophy. For these experiments, 3 × 10^5 *p65*$^{+/-}$ and wt MDSCs were injected into the gastrocnemius muscles of 8-week-old dystrophin-deficient SCID (mdx/SCID) mice. Fourteen days after implantation, significantly more dystrophin-positive myofibers were detected in the muscle injected with *p65*$^{+/-}$ MDSCs than in muscle injected with wt MDSCs ($P < 0.01$; Figure 6a,b). These results confirm our *in vitro* observations and may provide a novel mechanism as to why IKK inhibitors have been reported to improve muscle regeneration.[23]

Transplantation of *p65*$^{+/-}$ MDSCs postinjury reduces SKM inflammation and necrosis

The results above suggest that lowering basal levels of NF-κB activity increased the ability of MDSCs to engraft and differentiate following intramuscular injection (Figure 6). However, while it is possible this is mediated through enhanced proliferation and differentiation, the exact mechanism as to why more dystrophin-positive myofibers were found within the *p65*$^{+/-}$ MDSC engraftment sites remains unclear. Surrounding the engraftments of the wt MDSCs, we observed numerous cells positive for the macrophage marker CD14 as detected by immunofluorescent staining (data not shown), whereas the *p65*$^{+/-}$ MDSC engraftment sites were surrounded by fewer numbers of CD14+ cells (data not shown). As the mdx/SCID is an immunocompromised mouse model with a high level of background inflammation, we decided to further investigate this phenomenon using the well-established CTX muscle injury model in immunocompetent wt mice. In order

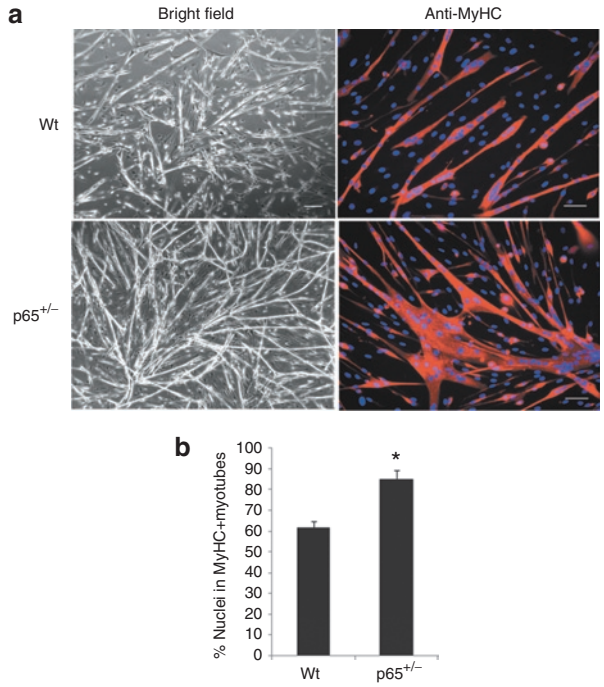

Figure 4 Myogenic differentiation is enhanced in muscle-derived stem cells (MDSCs) isolated from *p65*$^{+/-}$ mouse skeletal muscles (SKM) compared to wild-type (wt) MDSCs *in vitro*. (**a**) MDSCs were cultured in myogenic differentiation medium for 3 days, during which cell fusion into multinucleated myotubes was monitored using bright field microscopy and then confirmed by immunostaining for myosin heavy chain (MyHC-f). (**b**) Quantitation of MyHC-f positive myotubes. The percentage of differentiated myotubes was quantified as the number of nuclei in MyHC-f positive myotubes relative to the total number of nuclei. A total of three populations of *p65*$^{+/-}$ and wild-type (wt) MDSCs were tested ($P < 0.05$). In panel "**a**" all bars = 200 µm on bright field and all bars = 50 µm on MyHC immunostaining.

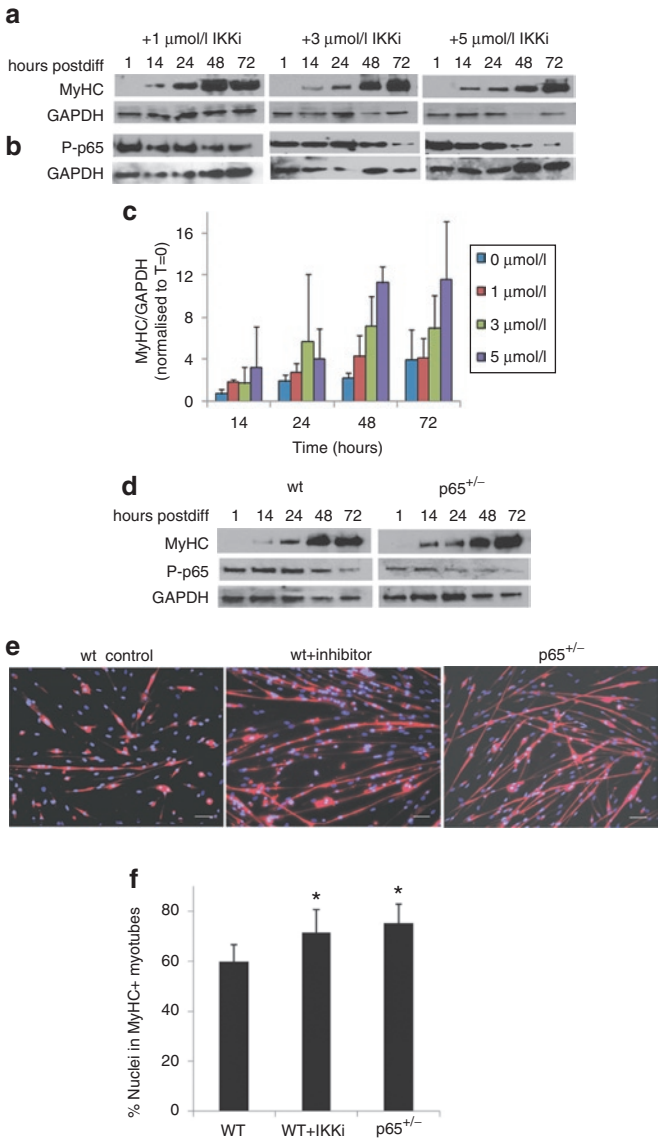

Figure 5 Muscle-derived stem cells (MDSCs) myogenic differentiation is enhanced by pharmacological inhibition of inhibitor of kappa B kinase β (IKKβ). (**a**) Western blot for myosin heavy chain (MyHC) over 72 hours of wild-type (wt) MDSCs treated with 1, 3, or 5 µmol/l IKKi during differentiation. (**b**) Western blot for P-p65 over 72 hours of wt MDSCs treated with 1, 3, or 5 µmol/l IKK inhibitor (IKKi) during differentiation. (**c**) Quantification of **b**, myosin heavy chain (MyHC-f) levels during differentiation ($n = 3$ independent experiments). (**d**) In parallel, wt and *p65*$^{+/-}$ MDSCs were cultured in differentiation medium and lysates were collected at the various time points indicated. Lysates were used for western blot for MyHC and P-p65 levels. (**e**) wt MDSCs, *p65*$^{+/-}$ MDSCs, and wt MDSCs treated with IKKi (5 µmol/l), were grown under fusion conditons for 72 hours and immunostained for MyHC-f expression (**f**) Quantification of MyHC-f staining ($P < 0.05$). In panel "**e**" all bars = 100 µm.

to confirm that transplanted *p65*$^{+/-}$ MDSCs are able to reduce inflammation in host skeletal muscle, we injected *p65*$^{+/-}$ and wt MDSCs into the gastrocnemius muscles of 8-week-old C57BL/6J mice 24 hours post-CTX injury. Six days post-transplantation, the wt MDSC engraftment area demonstrated a greater number of inflammatory cells surrounding the wt donor MDSCs than the *p65*$^{+/-}$ MDSCs. Furthermore, numerous centrally located nuclei, characteristic of regenerating muscle fibers, were found within the *p65*$^{+/-}$ MDSC injection sites. Consistent with observations made in mdx/SCID mice, the *p65*$^{+/-}$ MDSC engraftment area was associated with significantly fewer CD14+ cells than the wt MDSC engraftment area ($P < 0.01$; **Figure 7a,b**). There was also a significant (42%) reduction in tissue necrosis, as determined by quantification of mouse immunoglobulin G (IgG) staining ($P < 0.01$; **Figure 7a,c**). These results suggest that the improved engraftment and differentiation of *p65*$^{+/-}$ MDSCs is potentially due to their ability to attenuate the inflammation and necrosis that typically occurs after muscle injury.

DISCUSSION

NF-κB signaling has been implicated in the regulation of muscle degeneration and regeneration. The five mammalian NF-κB transcription factors are all expressed in skeletal muscle to modulate a variety of processes, including apoptosis, inflammation, and myoblast differentiation. Although there have been conflicting results reported as to whether NF-κB acts as a repressor or promoter of myogenesis,[8,24–29] recent results suggest that the classical NF-κB signaling pathway functions as a negative regulator of myogenesis.[14] In addition, NF-κB activation is associated with the degeneration and/or lack of regeneration of dystrophic

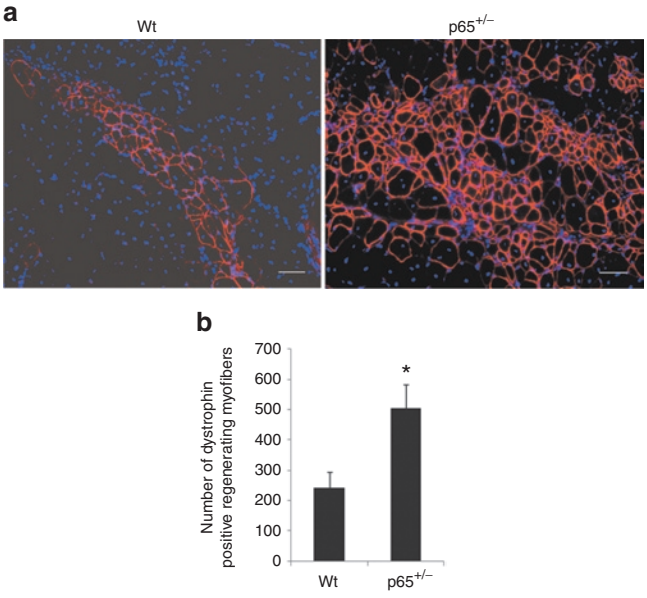

Figure 6 Heterozygous deletion of p65 promotes the regeneration capacity of muscle-derived stem cells (MDSCs). (**a**) Gastrocnemius cryosections from 8-week-old mdx/SCID mice in which $p65^{+/-}$ and wild-type (wt) MDSCs were implanted. Engraftment was determined by immunostaining for dystrophin (red). Three populations of $p65^{+/-}$ and wt MDSCs were transplanted into 12 mice in two independent experiments. (**b**) Quantitation of regenerated dystrophin-positive myofibers ($P < 0.05$). In panel "**a**" all bars = 50 µm. Error bars indicate "mean + SD" ($n = 12$).

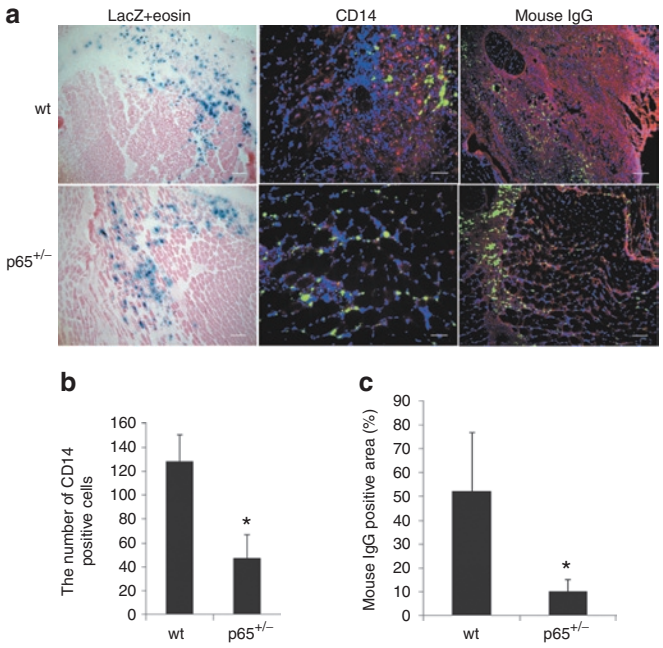

Figure 7 $p65^{+/-}$ muscle-derived stem cells (MDSCs) attenuate muscle inflammation and necrosis. (**a**) Gastrocnemius cryosections from 8-week-old C57BL/6J mice, which were injected with $p65^{+/-}$ or wild-type (wt) MDSCs 24 hours post-CTX injury. LacZ and eosin staining identified the injection area and immunostaining for CD14 (red) and mouse immunoglobulin G (IgG) (red) identified macrophages and necrotic tissue, respectively. In immunological stains, fluorescent green beads in C57BL/6J muscle sections confirmed the location of injection sites. (**b**) Quantitation of $CD14^+$ cells (the data represent six muscles per group). (**c**) Necrotic area in the gastrocnemius muscles was identified by IgG staining and quantified based on the total positive area per image (the data represent six muscles per group). In panel "**a**" all bars = 100 µm on LacZ+eosin and mouse IgG staining. All bars = 50 µm on CD14 staining.

muscle in mdx mice.[13] Thus, in this study, we examined the effect of NF-κB reduction on the proliferation and differentiation of MDSCs isolated from wt mice and mice heterozygous for p65. Although $p65^{+/-}$ MDSCs had more than a 30% reduction in p65/NF-kB levels compared to the wt MDSCs, the two genotypes expressed similar stem (CD34, Sca-1), myogenic (desmin, MyoD) and endothelial (CD144, CD31) cell markers. This result suggests that the reduction in NF-kB did not affect overall expression of MDSC markers, albeit there is some variability in stem cell marker expression between populations of the same genotype.

We observed that MDSCs with reduced p65 levels have improved proliferation compared to wt cells, suggesting that p65/NF-κB activity negatively controls MDSC expansion. More importantly, we also observed that both the rate and extent of myogenic differentiation was accelerated in MDSCs with reduced p65 and in wt MDSCs treated with an IKKβ inhibitor. Together, these data suggest that NF-κB inhibits muscle stem cell differentiation. Our results are in agreement with previous studies showing that regulation of myogenesis is dependent on p65 transcriptional activity, which is able to inhibit myogenesis.[14] It has been suggested previously that the negative effect of NF-κB on differentiation is mediated through the transcriptional activation of cyclin D1 and YinYang1 (YY1).[30,31] Interestingly, we have observed a reduction in the level of cyclin D1 in $p65^{+/-}$ MDSCs compared to wt cells, but found no difference in the level of YY1 expression (data not shown).

Recent genetic evidence supports the role of IKK/NF-κB in driving the pathogenesis of muscular dystrophy, identifying this signaling pathway a potential therapeutic target for the treatment of DMD.[13] The activity of NF-κB in dystrophic muscle is associated with not only immune cells, but also regenerative muscle fibers. Thus, we investigated whether the $p65^{+/-}$ MDSCs have a higher muscle regeneration potential than wt MDSCs after their intramuscular injection into dystrophic mdx/SCID skeletal muscles. Our results demonstrated that $p65^{+/-}$ MDSCs are more efficient at regenerating dystrophin-positive myofibers compared to wt MDSCs, which is consistent with the enhanced ability of the $p65^{+/-}$ MDSCs to differentiate in culture.

We also assessed inflammation around the engrafted site by immunofluorescent staining for CD14, a macrophage marker. While we found very few CD14+ cells within the injection sites of the $p65^{+/-}$ cells, many CD14+ cells were detected within the wt MDSC engraftment areas. As a decreased number of macrophages in the $p65^{+/-}$ cell engraftment area correlated with a reduction in necrosis, it is possible that a reduction in p65 enhances the local anti-inflammatory properties of MDSCs via regulation of paracrine factors. Several cytokines under the control of NF-κB, such as TNFα and interleukin-6 (IL-6), are potent inhibitors of myogenic differentiation.[8] Thus, taken together, these results suggest that inhibition of NF-κB/p65 may enhance myogenesis by reducing inflammation and necrosis.

During regeneration following injury, numerous paracrine factors such as myostatin, hepatocyte growth factor, and basic fibroblast growth factor play critical roles coordinating repair.[32] Other groups have demonstrated the importance of non-NF-kB proteins in muscle development and pathology. For example, myostatin acts independently of the classical TNFα and NF-kB pathway to inhibit MyoD expression and signal cachexia by reversing the IGF-1/PI3K/AKT hypertrophy pathway.[33] However, other factors, such as hepatocyte growth factor and IL-6, have been reported to activate NF-κB.[34] Given the numerous growth factors and cytokines present in damaged and regenerating muscle, the NF-κB pathway likely directs inflammation or regeneration in response to more than one factor. In summary, here we described a negative role for the p65/NF-κB signaling pathway in MDSC growth and differentiation *in vitro*, as well as muscle regeneration *in vivo*. Similarly, pharmacological inhibition of IKKβ identifies the IKK/NF-κB signaling pathway as a potential therapeutic target to improve the myogenic potential of MDSCs and muscle regeneration after injury and diseases.

MATERIALS AND METHODS

Animals. The C57BL/6J mice heterozygous for p65/RelA were originally described by Amer Beg (Cambridge, MA).[17] The mdx/SCID (C57BL/10ScSn DMD^{mdx}/J/CB17-Prkdc^{scid}/J) and C57BL/6J mice were obtained from the Jackson Laboratory (Bar Harbor, ME). All animal protocols used for these experiments were approved by the Children's Hospital of Pittsburgh's Institutional Animal Care and Use Committee.

Isolation of MDSCs from p65$^{+/-}$ mice. The mice were sacrificed at 5 months of age and muscle stem cell isolation was performed as previously described via a modified preplate technique.[18] Briefly, the SKM tissue was minced and processed through a series of enzymatic dissociations: 0.2% of collagenase type XI (Sigma-Aldrich, St Louis, MO) for 1 hour, 2.4 units/ml of dispase (Invitrogen, Carlsbad, CA) for 45 minutes, and 0.1% of trypsin-EDTA (Invitrogen) for 30 minutes at 37°C. After enzymatic dissociation, the muscle cells were centrifuged and resuspended in proliferation medium (Dulbecco's modified Eagle's medium supplemented with 10% fetal bovine serum, 10% horse serum, 0.5% chicken embryo extract, and 1% penicillin-streptomycin), and the resulting cell suspension from both $p65^{+/-}$ and wt muscle were plated in collagen type I coated flasks. Different populations of muscle-derived cells were isolated based on their adhesion characteristics. After 7 days, late preplate populations (slow-adhering cells) were obtained and cultured in proliferation medium. The slowly adhering fraction of muscle cells has been previously shown to contain MDSCs.[18] For all experiments, congenic $p65^{+/-}$ and $p65^{+/+}$ MDSCs of the same passage number were compared.

p65 staining and ArrayScan assay. Cells were fixed with 4% paraformaldehyde for 15 minutes at room temperature (RT), rinsed two times with phosphate-buffered saline (PBS), and the cells' membrane permeabilized for 10 minutes with 0.1% Triton X-100 in PBS. A 10% goat serum blocking solution was used for 1 hour and the cells were incubated with a 1:200 dilution of rabbit polyclonal anti-p65 (Abcam, Cambridge, MA) for 1 hour at RT. After washing three times, the cells were incubated for 30 minutes with Cy3-conjugated anti-rabbit IgG (1:500; Sigma-Aldrich). The nuclei were revealed by 4′,6-Diamidino-2-phenylindole (DAPI) staining. Nuclear localization of the NF-κB subunit p65 was measured via ArrayScan. This technique allows for the rapid, automated quantification of p65 and DAPI colocalization, as identified by immunocytochemistry in cells grown on a 96-well plate. Recordings were taken from multiple fields of view per well, generating data representative of each well.

Western blot assay. The cell populations isolated from $p65^{+/-}$ and wt mice were cultured in proliferation medium and stimulated with TNFα (10 ng/ml) for 30 minutes before harvesting. Cells were then lysed in Laemmli sample buffer (Bio-Rad, Hercules, CA), boiled for 5 minutes, and centrifuged at 4,000 r.p.m. for 5 minutes. Each sample was loaded on a 10% SDS-polyacrylamide gel, which was run for 2 hours and then transferred for 1.5 hours at 100 V while stirring on ice. The membrane was blocked with 5% bovine serum albumin (Sigma-Aldrich, St Louis, MO) in PBS for 1 hour and then incubated with rabbit anti-phospho-NF-κB/p65 monoclonal antibody (1:1,000; Cell Signaling, Danvers, MA) overnight at 4°C. After washing three times with Tris-buffered saline Tween-20, the membrane was incubated with goat anti-rabbit IgG (H+L) (1:5,000; Pierce, Rockford, IL) for 50 minutes at RT. Blots were developed by ECL solution (Pierce).

RT-PCR analysis. Total RNA was extracted from cells using Nucleo Spin RNA II column (Clontech, Mountain View, CA). Following isolation, complementary DNA was synthesized with SuperScript II reverse transcriptase (Invitrogen), according to the manufacturer's instructions. PCR was performed with Taq polymerase (Invitrogen) as per the manufacturer's instructions and PCR products were separated by electrophoresis with 1% agarose gels. The primers used for PCR are listed in **Table 1**. Each set of oligonucleotides was designed to span two different exons to avoid background amplification of genomic DNA. The data were quantified by densitometry using Adobe Photoshop 7.0.

Pax7 and MyoD staining. $P65^{+/-}$ and wt cells were fixed and permeabilized with 2% paraformaldehyde plus 1% Triton X-100 for 30 minutes at 4°C and rinsed two times with PBS. Cells were blocked with 5% horse serum and then incubated with a 1:100 dilution of mouse monoclonal anti-Pax7 (DSHB, Iowa City, IA) or anti-MyoD (Santa Cruz Biotechnology, Santa Cruz, CA) over night at 4°C. After washing three times, the cells were incubated for 1 hour with biotinylated anti-mouse IgG (1:300; Vector Lab, Burlingame, CA), which acted as a secondary antibody. Streptavidin 594 conjugate (1:500; Invitrogen) was added in the last step. The nuclei were revealed by DAPI staining. Negative control staining was performed by an identical procedure, with the exception that the primary antibody was omitted.

In vitro *assessment of cell proliferation.* In order to compare the proliferative potential of $p65^{+/-}$ MDSCs to wt MDSCs, we used a previously

Table 1 Primers used for RT–PCR

Gene	Forward primer	Reverse primer	Location
Sca-1	CCTACTGTGTGCAGAAAGAGC	CAGGAAGTCTTCACGTTGACC	89–331
CD34	GCAGCTTTGAGATGACATCACC	CTCAGCCTCCTCCTTTTCACA	498–715
MyoD1	ACAGTGGCGACTCAGATGCATC	GCTGCAGTCGATCTCTCAAAGC	708–1105
Desmin	AACCTGATAGACGACCTGCAG	GCTTGGACATGTCCATCTCCA	615–873
CD31	AGAGCTACGTCATTCCTCAG	GACCAAGTGTGTCACTTGAAC	474–988
CD144	CACCAACAAAAACCTGGAACA	CCACCACGATCTTGTATTCAG	425–729
β-Actin	TCAGAAGGACTCCTATGTGG	TCTTTGATGTCACGCACGAT	234–722

described Live Cell Imaging system (Kairos Instruments LLC, Pittsburgh, PA).[22] Bright field images were taken at a ×100 magnification at 10 minutes intervals over a 72-hour period in three fields of view per well, with three wells per population. The images were combined to generate a video using ImageJ software (NIH). Proliferation was assessed by counting the number of cells per field of view, over 12 hours. All six populations were also plated in 96-well plates in quadruplicate (500 cells/well) and cultured under normal conditions for 72 hours. At this time, 20 µl of CellTiter96 AQueous One Reagent (Promega, Madison, WI) was added to each well and incubated in 5% CO_2 at 37 °C. Following another 3-hour incubation, absorbance at 490 nm was read with a 96-well plate reader.

Myogenic differentiation assay and fast MyHC (MyHC-f) staining. After 15 passages, cells were plated on 24-well plates (30,000 cells/well) with Dulbecco's modified Eagle's medium supplemented with 2% fetal bovine serum to stimulate myotube formation. Three days later, immunocytochemical staining for fast skeletal MyHC was performed. After rinsing three times with PBS, cells were fixed for 2 minutes in cold methanol, blocked with 10% horse serum for 1 hour and then incubated with a mouse anti-MyHC-f (1:250; Sigma-Aldrich, clone MY-32) antibody for 2 hours at RT. The primary antibody was detected with a secondary anti-mouse IgG antibody conjugated with Cy3 (1:300; Sigma-Aldrich) for 15 minutes. The nuclei were revealed by DAPI staining. The percentage of differentiated myotubes was quantified as the number of nuclei in MyHC-f positive myotubes relative to the total number of nuclei. The myogenic differentiation was also monitored over a period of 5 days using Live Cell Imaging. The images were combined to create a video using ImageJ software (NIH).

Selective inhibition of IKKβ. To determine the effects of IKK/NF-κB inhibition on wt MDSCs during myogenic differentiation, we used IKK-2 inhibitor IV (IKKi), or 2-[(aminocarbonyl)amino]-5-(4-fluorophenyl)-3-thiophenecarboxamide (Calbiochem, San Diego, CA), a reversible competitive inhibitor of IKKβ ATP binding. Cells were plated at 10^5 cells/well in 6-well plates and exposed to IKK inhibitor in differentiation medium. Cells were treated with either 1, 3, or 5 µmol/l IKKi. Lysates were collected at 0 minute, 14, 24, 48, and 72 hours following treatment. NF-kB activity and myogenic differentation was assessed by western blot for phosphorylated NF-kB/p65 (1:1,000; Cell Signaling) and MyHC-f (1:500; Sigma-Aldrich, clone MY-32), as detailed above.

Cell implantation and dystrophin staining. MDSCs from $p65^{+/-}$ and wt muscle were grown in proliferation medium until the cell number was sufficient for injection. A total of 3×10^5 viable cells was suspended in 20 µl of Hank's balanced salts solution and injected into the gastrocnemius muscles of 8–12-week-old mdx/SCID mice using a Hamilton syringe. The same number of cells was injected into the gastrocnemius muscles of 8-week-old wt C57BL/6J mice that had been injured 1 day earlier by a 30 µl intramuscular injection of 2 µmol/l CTX (Sigma-Aldrich) in PBS. The cell suspension was mixed with green fluorescent-labeled beads before injection to detect the injection sites. Six or fourteen days after implantation, the mice were sacrificed and the gastrocnemius muscles were harvested and flash frozen in liquid nitrogen-cooled 2-methylbutane. Serial cryosections 10 µmol/l in thickness were obtained for immunohistochemical analyses. Cryosections were fixed with 5% formalin and blocked with 5% donkey serum in PBS for 1 hour, then incubated with rabbit anti-dystrophin (1:300; Abcam) for 2 hours at RT. The sections were exposed to secondary 594-conjugated anti-rabbit IgG (1:500; Invitrogen) in PBS for 30 minutes. The nuclei were revealed by DAPI staining. Immunostaining was visualized and images were taken by fluorescence microscopy (Nikon Eclipse E800; Nikon, Melville, NY). Northern Eclipse software was used for quantitative analysis of the regenerated dystrophin-positive myofibers. A series of pictures were taken, and Adobe Photoshop 7.0 was used to construct a composite picture of the dystrophin-positive myofibers, which were then manually counted.

Retroviral transduction of MDSCs. MDSCs were plated at an initial confluence of 30–40% and retrovirally transduced [in the presence of Polybrene (8 µg/ml)] to express the β-galactosidase gene (LacZ), as previously described.[35]

LacZ staining. The cryosections were fixed in 1% glutaraldehyde and incubated 3 hours with 5-bromo-4-chloro-3-indolyl β-D-galactopyranoside (X-gal) substrate at 37 °C. Sections were counterstained with Eosin.

CD14 staining. Cryosections were fixed with 5% formalin and blocked with 5% donkey serum in PBS for 1 hour, then incubated with rat anti-CD14 (1:200; Biolegend, San Diego, CA) overnight at 4 °C. This was followed by a 1-hour incubation with biotinylated anti-rat IgG (1:300; Vector Lab). Streptavidin Cy3 conjugate (1:500; Sigma-Aldrich) was added in the last step followed by several rinses in PBS. Following CD14 staining, five random pictures per slide were taken and the number of CD14+ cells was counted manually.

Mouse IgG staining and quantification of necrosis. Muscle sections were fixed with 5% formalin and blocked with 10% horse serum in PBS for 1 hour, then incubated with biotinylated anti mouse IgG (1:300; Vector Lab) for 1 hour at RT. This was followed by a 15-minute incubation with streptavidin Cy3 conjugate (1:500; Sigma-Aldrich). The nuclei were revealed by DAPI staining. The IgG positive area was measured and quantified as the percentage of mouse IgG expressing area per total area using Northern Eclipse software (Cheektowaga, NY).

Statistical analysis. All results are given as the mean ± SD. Means from $p65^{+/-}$ and wt or treated and untreated were compared using Students' *t*-test. Differences were considered statistically significant when the *P* value was < 0.05.

SUPPLEMENTARY MATERIAL

Video S1. $p65^{+/-}$ MDSC proliferation.
Video S2. wt MDSC proliferation.
Video S3. $P65^{+/-}$ MDSC differentiation.
Video S4. wt MDSC differentiation.

ACKNOWLEDGMENTS

The authors thank the members of the Huard Laboratory, especially Jenny Zhu and Bin Sun for discussions and technical advice. Special thanks go to Joseph Feduska and Bridget Deasy for live cell imaging advice. This work was supported in part by the Henry J. Mankin Endowed Chair for Orthopedic Research at the University of Pittsburgh, the William F. and Jean W. Donaldson Chair at Children's Hospital of Pittsburgh. L.J.N. is supported by NIEHS (ES016114) and NIA (AG033907). The authors do not have conflicts of interest to disclose other than the corresponding author who receives consulting fees from Cook MyoSite Inc.

REFERENCES

1. Verma, IM, Stevenson, JK, Schwarz, EM, Van Antwerp, D and Miyamoto, S (1995). Rel/NF-kappa B/I kappa B family: intimate tales of association and dissociation. *Genes Dev* **9**: 2723–2735.
2. Baeuerle, PA and Baltimore, D (1996). NF-kappa B: ten years after. *Cell* **87**: 13–20.
3. Baldwin, AS Jr (1996). The NF-kappa B and I kappa B proteins: new discoveries and insights. *Annu Rev Immunol* **14**: 649–683.
4. Li, Z and Nabel, GJ (1997). A new member of the I kappaB protein family, I kappaB epsilon, inhibits RelA (p65)-mediated NF-kappaB transcription. *Mol Cell Biol* **17**: 6184–6190.
5. Karin, M (1999). How NF-kappaB is activated: the role of the IkappaB kinase (IKK) complex. *Oncogene* **18**: 6867–6874.
6. Hayden, MS and Ghosh, S (2004). Signaling to NF-kappaB. *Genes Dev* **18**: 2195–2224.
7. Karin, M, Cao, Y, Greten, FR and Li, ZW (2002). NF-kappaB in cancer: from innocent bystander to major culprit. *Nat Rev Cancer* **2**: 301–310.
8. Langen, RC, Schols, AM, Kelders, MC, Wouters, EF and Janssen-Heininger, YM (2001). Inflammatory cytokines inhibit myogenic differentiation through activation of nuclear factor-kappaB. *FASEB J* **15**: 1169–1180.
9. Baghdiguian, S, Martin, M, Richard, I, Pons, F, Astier, C, Bourg, N *et al.* (1999). Calpain 3 deficiency is associated with myonuclear apoptosis and profound

perturbation of the IkappaB alpha/NF-kappaB pathway in limb-girdle muscular dystrophy type 2A. *Nat Med* **5**: 503–511.
10. Kumar, A, Lnu, S, Malya, R, Barron, D, Moore, J, Corry, DB *et al.* (2003). Mechanical stretch activates nuclear factor-kappaB, activator protein-1, and mitogen-activated protein kinases in lung parenchyma: implications in asthma. *FASEB J* **17**: 1800–1811.
11. Monici, MC, Aguennouz, M, Mazzeo, A, Messina, C and Vita, G (2003). Activation of nuclear factor-kappaB in inflammatory myopathies and Duchenne muscular dystrophy. *Neurology* **60**: 993–997.
12. Hunter, RB and Kandarian, SC (2004). Disruption of either the Nfkb1 or the Bcl3 gene inhibits skeletal muscle atrophy. *J Clin Invest* **114**: 1504–1511.
13. Acharyya, S, Villalta, SA, Bakkar, N, Bupha-Intr, T, Janssen, PM, Carathers, M *et al.* (2007). Interplay of IKK/NF-kappaB signaling in macrophages and myofibers promotes muscle degeneration in Duchenne muscular dystrophy. *J Clin Invest* **117**: 889–901.
14. Bakkar, N, Wang, J, Ladner, KJ, Wang, H, Dahlman, JM, Carathers, M *et al.* (2008). IKK/NF-kappaB regulates skeletal myogenesis via a signaling switch to inhibit differentiation and promote mitochondrial biogenesis. *J Cell Biol* **180**: 787–802.
15. Payne, TR, Oshima, H, Okada, M, Momoi, N, Tobita, K, Keller, BB *et al.* (2007). A relationship between vascular endothelial growth factor, angiogenesis, and cardiac repair after muscle stem cell transplantation into ischemic hearts. *J Am Coll Cardiol* **50**: 1677–1684.
16. Ambrosio, F, Ferrari, RJ, Distefano, G, Plassmeyer, JM, Carvell, GE, Deasy, BM *et al.* (2010). The synergistic effect of treadmill running on stem-cell transplantation to heal injured skeletal muscle. *Tissue Eng Part A* **16**: 839–849.
17. Beg, AA, Sha, WC, Bronson, RT, Ghosh, S and Baltimore, D (1995). Embryonic lethality and liver degeneration in mice lacking the RelA component of NF-kappa B. *Nature* **376**: 167–170.
18. Gharaibeh, B, Lu, A, Tebbets, J, Zheng, B, Feduska, J, Crisan, M *et al.* (2008). Isolation of a slowly adhering cell fraction containing stem cells from murine skeletal muscle by the preplate technique. *Nat Protoc* **3**: 1501–1509.
19. Wan, F and Lenardo, MJ (2009). Specification of DNA binding activity of NF-kappaB proteins. *Cold Spring Harb Perspect Biol* **1**: a000067.
20. Sacco, A, Doyonnas, R, Kraft, P, Vitorovic, S and Blau, HM (2008). Self-renewal and expansion of single transplanted muscle stem cells. *Nature* **456**: 502–506.
21. Jankowski, RJ, Haluszczak, C, Trucco, M and Huard, J (2001). Flow cytometric characterization of myogenic cell populations obtained via the preplate technique: potential for rapid isolation of muscle-derived stem cells. *Hum Gene Ther* **12**: 619–628.
22. Deasy, BM, Jankowski, RJ, Payne, TR, Cao, B, Goff, JP, Greenberger, JS *et al.* (2003). Modeling stem cell population growth: incorporating terms for proliferative heterogeneity. *Stem Cells* **21**: 536–545.
23. Tang, Y, Reay, DP, Salay, MN, Mi, MY, Clemens, PR, Guttridge, DC *et al.* (2010). Inhibition of the IKK/NF-?B pathway by AAV gene transfer improves muscle regeneration in older mdx mice. *Gene Ther* **17**: 1476–1483.
24. Lehtinen, SK, Rahkila, P, Helenius, M, Korhonen, P and Salminen, A (1996). Down-regulation of transcription factors AP-1, Sp-1, and NF-kappa B precedes myocyte differentiation. *Biochem Biophys Res Commun* **229**: 36–43.
25. Guttridge, DC, Albanese, C, Reuther, JY, Pestell, RG and Baldwin, AS Jr (1999). NF-kappaB controls cell growth and differentiation through transcriptional regulation of cyclin D1. *Mol Cell Biol* **19**: 5785–5799.
26. Kaliman, PA and Barannik, TV (1999). Regulation of delta-aminolevulinate synthase activity during the development of oxidative stress. *Biochemistry Mosc* **64**: 699–704.
27. Canicio, J, Ruiz-Lozano, P, Carrasco, M, Palacin, M, Chien, K, Zorzano, A *et al.* (2001). Nuclear factor kappa B-inducing kinase and Ikappa B kinase-alpha signal skeletal muscle cell differentiation. *J Biol Chem* **276**: 20228–20233.
28. Munz, B, Hildt, E, Springer, ML and Blau, HM (2002). RIP2, a checkpoint in myogenic differentiation. *Mol Cell Biol* **22**: 5879–5886.
29. Baeza-Raja, B and Muñoz-Cánoves, P (2004). p38 MAPK-induced nuclear factor-kappaB activity is required for skeletal muscle differentiation: role of interleukin-6. *Mol Biol Cell* **15**: 2013–2026.
30. Guttridge, DC, Mayo, MW, Madrid, LV, Wang, CY and Baldwin, AS Jr (2000). NF-kappaB-induced loss of MyoD messenger RNA: possible role in muscle decay and cachexia. *Science* **289**: 2363–2366.
31. Wang, H, Hertlein, E, Bakkar, N, Sun, H, Acharyya, S, Wang, J *et al.* (2007). NF-kappaB regulation of YY1 inhibits skeletal myogenesis through transcriptional silencing of myofibrillar genes. *Mol Cell Biol* **27**: 4374–4387.
32. Karalaki, M, Fili, S, Philippou, A and Koutsilieris, M (2009). Muscle regeneration: cellular and molecular events. *In Vivo* **23**: 779–796.
33. McFarlane, C, Plummer, E, Thomas, M, Hennebry, A, Ashby, M, Ling, N *et al.* (2006). Myostatin induces cachexia by activating the ubiquitin proteolytic system through an NF-kappaB-independent, FoxO1-dependent mechanism. *J Cell Physiol* **209**: 501–514.
34. Yao, P, Zhan, Y, Xu, W, Li, C, Yue, P, Xu, C *et al.* (2004). Hepatocyte growth factor-induced proliferation of hepatic stem-like cells depends on activation of NF-kappaB. *J Hepatol* **40**: 391–398.
35. Li, Y and Huard, J (2002). Differentiation of muscle-derived cells into myofibroblasts in injured skeletal muscle. *Am J Pathol* **161**: 895–907.

Appendix 5

Cell Transplantation, Vol. 21, pp. 1087–1093, 2012
Printed in the USA.

0963-6897/12 $90.00 + .00
DOI: http://dx.doi.org/10.3727/096368912X636876
E-ISSN 1555-3892
www.cognizantcommunication.com

Isolation of Myogenic Stem Cells From Cultures of Cryopreserved Human Skeletal Muscle

Bo Zheng,*[1] Chien-Wen Chen,*†[1] Guangheng Li,* Seth D. Thompson,*
Minakshi Poddar,* Bruno Péault,*‡§¶ and Johnny Huard*†

*Stem Cell Research Center, Department of Orthopaedic Surgery,
University of Pittsburgh School of Medicine and Children's Hospital of Pittsburgh of UPMC, Pittsburgh, PA, USA
†Department of Bioengineering, University of Pittsburgh Swanson School of Engineering, Pittsburgh, PA, USA
‡Department of Pediatrics, Children's Hospital of Pittsburgh of UPMC, Pittsburgh, PA, USA
§David Geffen School of Medicine, University of California at Los Angeles, Los Angeles, CA, USA
¶Center for Vascular Science and Center for Regenerative Medicine, University of Edinburgh, Edinburgh, UK

We demonstrate that subpopulations of adult human skeletal muscle-derived stem cells, myogenic endothelial cells (MECs), and perivascular stem cells (PSCs) can be simultaneously purified by fluorescence-activated cell sorting (FACS) from cryopreserved human primary skeletal muscle cell cultures (cryo-hPSMCs). For FACS isolation, we utilized a combination of cell lineage markers: the myogenic cell marker CD56, the endothelial cell marker UEA-1 receptor (UEA-1R), and the perivascular cell marker CD146. MECs expressing all three cell lineage markers ($CD56^+UEA\text{-}1R^+CD146^+/CD45^-$) and PSCs expressing only CD146 ($CD146^+/CD45^-CD56^-UEA\text{-}1R^-$) were isolated by FACS. To evaluate their myogenic capacities, the sorted cells, with and without expansion in culture, were transplanted into the cardiotoxin-injured skeletal muscles of immunodeficient mice. The purified MECs exhibited the highest regenerative capacity in the injured mouse muscles among all cell fractions tested, while PSCs remained superior to myoblasts and the unpurified primary skeletal muscle cells. Our findings show that both MECs and PSCs retain their high myogenic potentials after in vitro expansion, cryopreservation, and FACS sorting. The current study demonstrates that myogenic stem cells are prospectively isolatable from long-term cryopreserved primary skeletal muscle cell cultures. We emphasize the potential application of this new approach to extract therapeutic stem cells from human muscle cells cryogenically banked for clinical purposes.

Key words: Myogenesis; Human skeletal muscle; Myogenic endothelial cells (MECs); Perivascular stem cells (PSCs); Cell therapy

INTRODUCTION

Mammalian skeletal muscle harbors multiple stem/progenitor cell populations, which can repair and/or regenerate injured/defective tissues such as damaged/dystrophic skeletal muscles and ischemic hearts (1,2,5,7,8,10,12–19). In particular, we previously reported the identification of two subpopulations of multipotent stem cells within human skeletal muscle [i.e., myogenic endothelial cells (MECs) ($CD45^-CD34^+CD56^+CD144^+$) and perivascular stem cells (PSCs) ($CD34^-CD45^-CD56^-CD146^+$)], which exhibit multilineage mesodermal developmental potentials (6,20). These stem cell populations were specifically localized in situ within the walls of small blood vessels and can be prospectively purified by fluorescence-activated cell sorting (FACS) from fresh human skeletal muscle biopsies, through the use of a combination of positive and negative cell lineage markers (6,20). In vitro, purified MECs and PSCs displayed osteo-, chondro-, adipo-, and myogenic differentiation competence, and their high repair/regenerative capacities were not only demonstrated in injured mouse skeletal muscles but also in infarcted hearts (3,4,6,11,20). However, it has never been documented whether these stem cell fractions could persist and retain their high myogenic capacities after the cryopreservation of human primary skeletal muscle cell cultures (cryo-hPSMCs). Furthermore, MECs and PSCs have been shown to be superior to myoblasts for muscle regeneration in previously performed studies; however, it has

Received July 12, 2010; final acceptance July 10, 2011. Online prepub date: March 21, 2012.
[1]These authors provided equal contribution to this work.
Address correspondence to Johnny Huard, Ph.D., Stem Cell Research Center, Department of Orthopaedic Surgery, University of Pittsburgh School of Medicine, 206 Bridgeside Point II, 450 Technology Drive, Pittsburgh, PA, USA 15219, USA. Tel: (412) 648-2798; Fax: (412) 648-4066; E-mail: jhuard@pitt.edu

never been determined whether MECs isolated from cryopreserved, culture-expanded hPSMCs possessed the same superior regenerative capacity.

In order to identify and purify MECs and PSCs by FACS from in vitro expanded cryo-hPSMCs, we employed a collection of cell lineage markers reported in our previous studies, including the hematopoietic cell marker CD45, the myogenic cell marker CD56 (neural cell adhesion molecule; N-CAM), the perivascular cell marker CD146 (melanoma cell adhesion molecule; M-CAM/Mel-CAM/MUC18), and the endothelial cell marker UEA-1 receptor (*Ulex europaeus* agglutinin I receptor, UEA-1R) (6,20,21). UEA-1R was chosen as a substitute marker for CD34 and CD144 because these two endothelial cell markers are frequently lost during long-term culture whereas UEA-1 maintains consistent reactivity within endothelial cell lineage cultures (20,21). We hypothesized that MECs and PSCs (with and without culture expansion), purified from cryo-hPSMCs, retain their superior myogenic potential and exhibit a greater regeneration capacity of skeletal myofibers when compared to myoblasts.

MATERIALS AND METHODS

Human Muscle Biopsies and Animal Usage

In total, nine independent human skeletal muscle biopsies, from four female and five male donors (age range 4–75, mean 28), were used to obtain human primary skeletal muscle cells (hPSMCs). The procurement of human skeletal muscle biopsies from the National Disease Research Interchange (NDRI) was approved by the Institutional Review Board at the University of Pittsburgh Medical Center (UPMC). All the animal research experiments performed in this study were approved by the Animal Research and Care Committee at the Children's Hospital of Pittsburgh of UPMC (Protocol #34-05) and the University of Pittsburgh (Protocol #0810310-B2).

Cell Isolation and Cryopreservation

The human skeletal muscle biopsies were placed in Hank's Balanced Salt Solution (HBSS, Invitrogen) and transferred to the laboratory on ice. Briefly, tissues were finely minced and serially digested with 0.2% collagenase type XI, 0.25% dispase, and 0.1% trypsin, as previously described (20,21). Dispersed single cell suspensions were cultured in complete medium containing DMEM supplemented with 10% fetal bovine serum (FBS), 10% horse serum, 1% chicken embryo extract, and 1% penicillin/streptomycin (all from Invitrogen). After expansion, cells were cryopreserved at passages 2–8 in medium consisting of 50% complete culture medium and 50% freezing medium (80% FBS + 20% dimethyl sulfoxide) and stored in liquid nitrogen (21).

Flow Cytometry and Cell Sorting

To culture cryo-hPSMCs, cells were thawed and expanded for 2–6 passages. To perform flow cytometry analysis, cells were trypsinized, washed, and incubated with anti-human monoclonal antibodies/ligands: CD45-allophycocyanin-cyanine 7 (APC-Cy7), CD56-phycoerythrin-Cy7 (PE-Cy7), CD34-APC (all from Becton Dickinson), CD146-fluorescein isothiocyanate (FITC; Serotec), UEA-1-PE (Biomeda), von Willebrand factor (vWF)-FITC (US Biology), kinase insert domain receptor (also known as vascular endothelial growth factor receptor 2; VEGFR2) KDR-APC (R&D Systems), and CD144-PE (Beckman Coulter). Negative control samples received equivalent amounts of isotype-matched fluorophore-conjugated antibodies. For FACS purification, cells were incubated with CD45-APC-Cy7, CD56-PE-Cy7, CD146-FITC, UEA-1-PE, and with 7-amino-actinomycin D for dead cell exclusion. Sorted subpopulations were collected for immediate transplantation or transiently expanded in appropriate conditions as previously described (6,20).

Immunocytochemistry

For immunocytochemistry, cells were cytospun onto glass slides, fixed, and incubated with 10% serum. The following primary antibodies were used to detect cell lineage markers, including myogenic cell markers, CD56 (BD) and desmin (Sigma); perivascular cell markers, α-smooth muscle actin (Abcam) and CD146 (Cayman Chemical); endothelial cell markers/ligands, CD144 (Sigma), vWF (DAKO), CD34 (Novocastra), and biotinylated UEA-1 (Vector), followed by incubation with biotinylated secondary antibodies and/or Cy3-conjugated streptavidin (Sigma). Slides were observed and photographed on an epifluorescence microscope system (Nikon Eclipse E800).

Myogenesis In Vivo

To investigate whether the myogenic capacities of the cells were preserved, after cryopreservation, purified MECs, PSCs, myoblasts (Myos), endothelial cells (ECs), and unpurified muscle cells, without in vitro expansion, from six independent hPSMC samples were used for intramuscular injection. The newly sorted cells, on average, $11.8 \pm 5.8 \times 10^4$ $CD56^+$ Myo cells, $7.3 \pm 4.4 \times 10^4$ $CD146^+$ PSCs, $4.5 \pm 2.6 \times 10^4$ $UEA\text{-}1R^+$ ECs, and $2.9 \pm 1.7 \times 10^4$ $CD56^+UEA\text{-}1R^+CD146^+$ MECs as well as 30×10^4 corresponding unsorted cells, were resuspended in 20 μl of HBSS and used for transplantation.

To precisely measure the myogenic-regenerative capacity of each stem/progenitor cell subpopulation, newly sorted MECs, PSCs, and Myo cells were expanded in culture for 1–2 passages. Fifty thousand cells from each subpopulation as well as 5×10^4 corresponding

unsorted cells were trypsinized, washed, and resuspended in 20 μl of phosphate-buffered saline (PBS). Four individual animal experiments were performed, with each using cell populations purified from a single FACS sort of one independent cryo-hPSMC culture.

Cells were injected into a single site of the gastrocnemius muscles of severe combined immunodeficient (SCID) mice that were injured 24 h before by injecting 1 μg of cardiotoxin in 20 μl of HBSS. The untreated group received sham injections of 20 μl of HBSS or PBS only. Treated muscles were collected 2 weeks postinjection for immunohistochemical analyses. Anti-human spectrin was used to identify human cell-derived skeletal myofibers in the mouse muscles. In order to quantitatively evaluate the myogenic regenerative capacity of each subpopulation, the number of human spectrin-positive skeletal myofibers was averaged from six randomly selected sections at the site of injection in each specimen and presented as the regenerative index (per section).

Statistical Analysis

Data were summarized as average ± SE. Statistical comparison between the groups (purified cells after expansion in vitro) was performed using one-way ANOVA with a 95% confidence interval. Bonferroni pairwise multiple comparison test was performed for ANOVA post hoc analysis. Statistical analyses were performed with SigmaStat software.

RESULTS

Heterogenous Cell Composition of Human Primary Skeletal Muscle Cell Cultures (hPSMCs) After Cryopreservation and Long-Term Expansion

After expansion, the cryopreserved hPSMCs (cryo-hPSMCs) were examined by immunocytochemistry for cell surface marker expression. The majority of cryo-hPSMCs expressed desmin and CD56, and to a lesser extent, CD146 (Fig. 1). Only a fraction of cells expressed α-SMA, CD144, vWF, or UEA-1R. As predicted, the cultured human cryo-hPSMCs lacked CD34 expression. After excluding $CD45^+$ hematopoietic cells ($0.2 \pm 0.1\%$), flow cytometry analysis quantitatively confirmed the presence of cells with diverse expressions of cell lineage makers by cryo-hPSMCs: $77.1 \pm 5.7\%$ $CD56^+$, $66.9 \pm 8.1\%$ $CD146^+$, $11.2 \pm 2.5\%$ UEA-$1R^+$, $0.3 \pm 0.1\%$ $CD144^+$, 0.1% vWF^+, and null expression of CD34 and KDR (Fig. 1B). The number of cryo-hPSMCs positive for CD56, CD146, or UEA-1R decreased dramatically after passage 10 (Fig. 1C).

Isolation of Myogenic Stem/Progenitor Cells From Cryo-hPSMCs

After revealing the heterogeneous nature of cryo-hPSMCs, we analyzed these cells for the existence of previously defined subpopulations by multicolor flow cytometry, based on their expression of hematopoietic (CD45), myogenic (CD56), endothelial (UEA-1R), and perivascular (CD146) cell lineage markers (6,20). After exclusion of $CD45^+$ cells, four distinct cell fractions were identified, including myoblasts (Myo) ($CD56^+$/$CD45^-CD146^-$UEA-$1R^-$), endothelial cells (ECs) (UEA-$1R^+$/$CD45^-CD56^-CD146^-$), perivascular stem cells (PSCs) ($CD146^+$/$CD45^-CD56^-$UEA-$1R^-$), and myogenic endothelial cells (MECs), which expressed all three markers ($CD56^+$UEA-$1R^+CD146^+$/$CD45^-$). Long-term cultured cryo-hPSMCs included $22.58 \pm 6.32\%$ Myo, $0.58 \pm 0.23\%$ ECs, $5.92 \pm 4.66\%$ PSCs, and $1.16 \pm 0.19\%$ MECs (Fig. 2). These four cell subsets were subsequently fractionated by FACS, and on average we were able to recover the following number of each cell type: $25.61 \pm 9.16 \times 10^4$ $CD56^+$ Myo, $13.28 \pm 7.37 \times 10^4$ UEA-$1R^+$ ECs, $33.54 \pm 20.53 \times 10^4$ $CD146^+$ PSCs, and $3.84 \pm 0.96 \times 10^4$ $CD56^+$UEA-$1R^+CD146^+$ MECs (Fig. 2).

Purified Myogenic Stem/Progenitor Cells Retain High Myogenic Potentials In Vivo

To evaluate whether the myogenic capacity was preserved after cryopreservation, all sorted cells were immediately transplanted (without culture expansion) into the cardiotoxin-injured gastrocnemius muscles of SCID mice ($n = 6$ per cell fraction). Unpurified muscle cells and HBSS injections were employed as treated and untreated controls, respectively. Mouse muscles were harvested 2 weeks postinjection, cryosectioned, and examined by immunohistochemistry to detect muscle fiber regeneration. An antibody against human spectrin, a myofiber cytoskeletal protein, was used to identify human cell-derived skeletal myofibers in the tissue sections. All of the newly purified cell fractions regenerated human spectrin-positive myofibers in the injured mouse skeletal muscles; however, the purified fractions appeared to regenerate a greater number of muscle fibers than the unpurified cryo-hPSMCs (Fig. 3A). As expected, a lack of spectrin-expressing muscle fibers was observed in the HBSS-injected muscles (Fig. 3A).

To quantitatively measure the myogenic regenerative capacity of each purified stem/progenitor cell population, newly sorted MECs, PSCs, and Myo cells were transiently expanded in culture for 1–2 passages. Fifty thousand cells from each of the subpopulations as well as 5×10^4 corresponding unsorted cells were transplanted into the same type of muscle injury model described above ($n = 4$ per cell fraction). Phosphate-buffered saline (PBS) injections were used as negative controls. ECs were not included in this experiment due to their unstable phenotype in culture. Quantitative analyses revealed that the myogenic regenerative index,

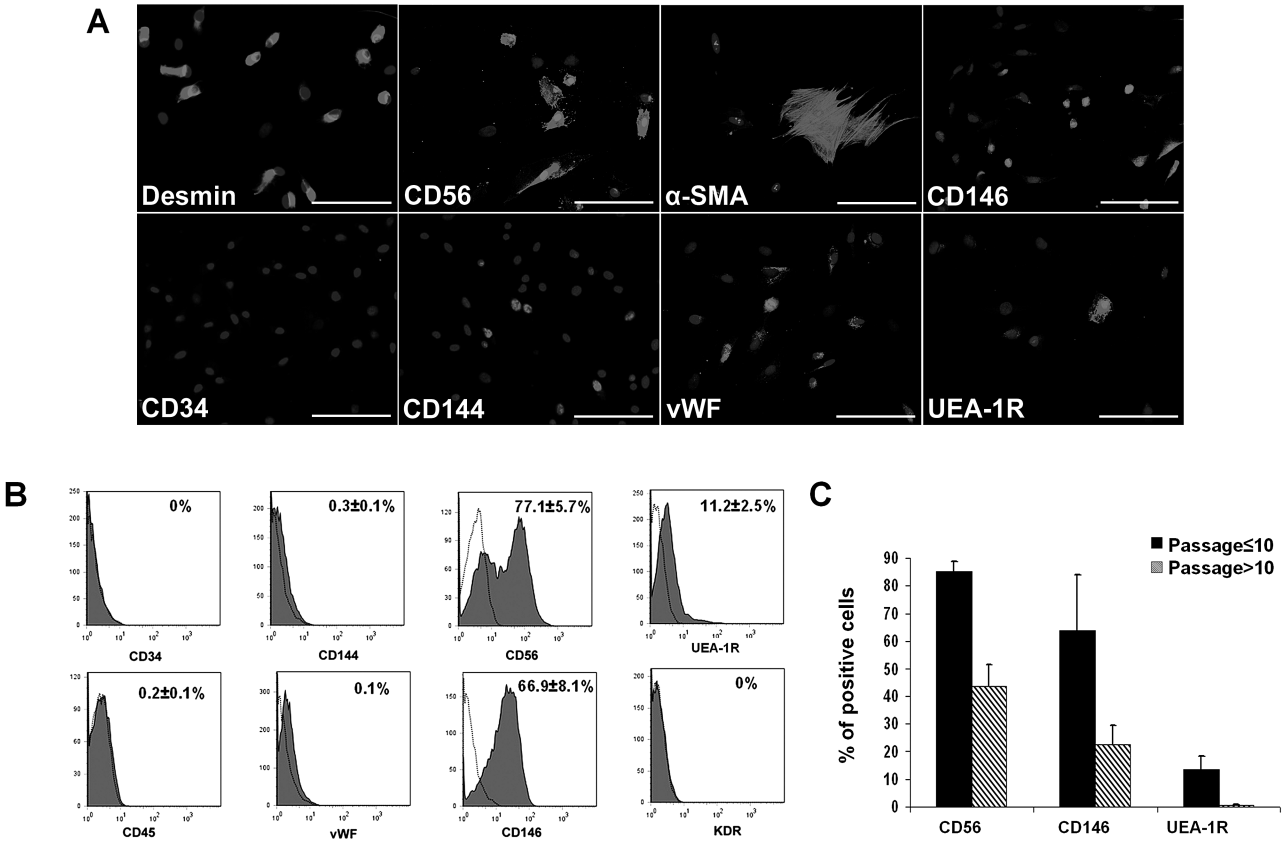

Figure 1. Expression of cell lineage markers by cryopreserved human primary skeletal muscle cells (cryo-hPSMCs). (A) Immunocytochemistry revealed the expression of various cell lineage markers (light gray) by cryo-hPSMCs after expansion. Nuclei were stained with DAPI (dark gray). (B) Flow cytometry analysis quantitatively confirmed the diverse cell composition of cryo-hPSMCs. (C) The number of cryo-hPSMCs positive for CD56, CD146, or UEA-1R decreased when cells were cultured beyond passage 10. Scale bars: 100 μm.

indicated by the average number of human spectrin-positive skeletal myofibers per muscle section, was 166.3 ± 19.2 for the MECs, 90.1 ± 8.0 for the PSCs, 45.7 ± 6.2 for the myoblasts (Myo), and 28.7 ± 8.4 for the unsorted muscle cells (Unsort) (Fig. 3B). The MECs exhibited the highest regeneration index of all four cell fractions tested ($p < 0.005$) (Fig. 3B) and the PSCs regenerated more myofibers than the Myo ($p > 0.05$) and the Unsort ($p = 0.017$) groups (Fig. 3B). Although the purified myoblasts displayed a trend of higher myogenic capacity than the unsorted cells, no statistically significant difference was observed ($p > 0.05$) (Fig. 3B).

DISCUSSION

Skeletal muscle is known to possess multiple stem/progenitor cell populations that are associated with muscle development, maintenance, and regeneration (13,18). Upon purification, muscle stem/progenitor cells in general display more robust myogenic regenerative capacities than unpurified muscle cells in animal disease models, suggesting the advantage of isolating stem cells for therapeutic purposes (6,10,13,20). More recent data have shown that there is a functional heterogeneity in myogenesis even among the muscle precursor cell pool (2).

In the present study, we demonstrated that even after in vitro expansion and cryopreservation, primary human muscle cell cultures include various subpopulations, as indicated by expression of diverse cell lineage markers. Using a modified collection of cell lineage markers (CD45, CD56, CD146, and UEA-1R), we identified and purified to homogeneity four distinct cell populations from cryo-hPSMCs, including two stem cell subpopulations: PSCs ($CD146^+/CD45^-CD56^-UEA\text{-}1R^-$) and MECs ($CD56^+CD146^+UEA\text{-}1R^+/CD45^-$) (6,20,21). Newly sorted MECs, PSCs, ECs, and Myo cells were immediately transplanted into the cardiotoxin-injured skeletal muscles of SCID mice to examine the preservation of their myogenic potential after FACS, all of which regenerated human spectrin-positive myofibers in the injured mouse

skeletal muscles. Quantitative analyses using sorted subpopulations that were minimally expanded in culture showed that the MECs displayed the highest muscle regenerative capacity among all cell subsets tested, and the PSCs were superior to myoblasts and unpurified cryo-hPSMCs.

These results were consistent with our previous observations from injections of cells isolated from fresh skeletal muscle biopsies (6,20). Taken together, our results suggest the presence of distinct subpopulations of highly myogenic stem/progenitor cells within culture-expanded, cryopreserved hPSMCs and support the feasibility of further purifying stem cell fractions from these unpurified cryopreserved human cells. Most importantly, these findings infer the practicability of prospective isolation of myogenic stem/progenitor cell populations from banked human skeletal muscle cells, highlighting a new technology to further enhance the availability and efficacy of cell-mediated therapies (9).

ACKNOWLEDGMENTS: This work was supported in part by grants to J.H from the National Institutes of Health (R01 DE013420-09) and the Department of Defense (W81XWH-09-1-0658) and from the William F. and Jean W. Donaldson Endowed Chair at the Children's Hospital of Pittsburgh, the Henry J. Mankin Endowed Chair for Orthopaedic Research at University of Pittsburgh, and by a grant to B.P. from the National Institutes of Health (R21 HL083057-01A2). The authors also wish to thank Allison Logar for her excellent technical assistance on the flow cytometry and the cell sorting and James H. Cummins for his editorial assistance in the preparation of this manuscript. The following author contributions are recognized: conception and design, collection and/or assembly of data, data analysis and interpretation, manuscript writing (B.Z.); conception and design, collection and/or

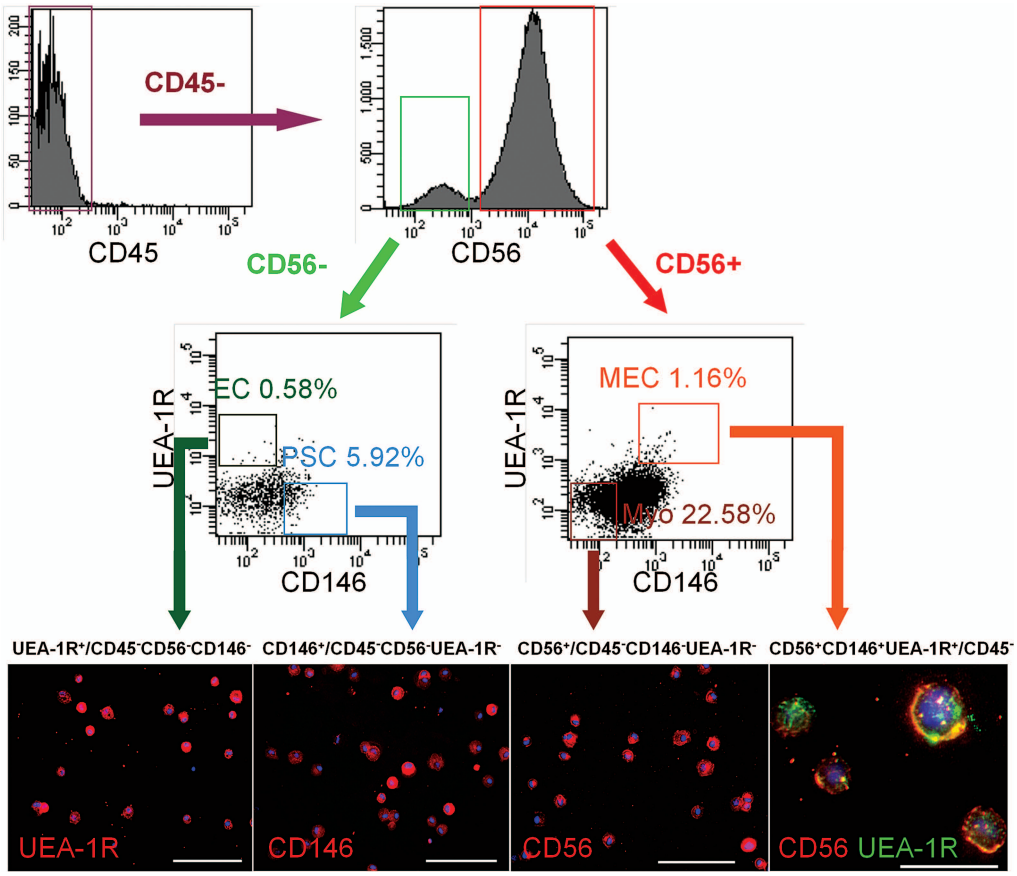

Figure 2. Identification and purification of myogenic stem cells within cryo-hPSMCs. After excluding $CD45^+$ hematopoietic cells, $CD45^-$ cells were separated based on CD56 expression. $CD56^+$ and $CD56^-$ populations were further gated on UEA-1R by CD146 to identify and/or sort four distinct cell populations: myogenic endothelial cells (MECs) ($CD56^+UEA\text{-}1R^+CD146^+/CD45^-$), myoblasts (Myos) ($CD56^+/CD45^-CD146^-UEA\text{-}1R^-$), perivascular stem cells (PSCs) ($CD146^+/CD45^-CD56^-UEA\text{-}1R^-$), and endothelial cells (ECs) ($UEA\text{-}1R^+/CD45^-CD56^-CD146^-$). The purities of the sorted populations were $90.73 \pm 4.82\%$, $92.94 \pm 1.23\%$, 93.86 ± 1.72, and 94.9 ± 0.64, respectively. Immunocytochemistry confirmed the expression of key cell lineage makers by freshly sorted cells: UEA-1R, CD146, and/or CD56. Nuclei were stained blue with DAPI. Scale bars: 100 µm; CD56/UEA-1R double staining: 20 µm.

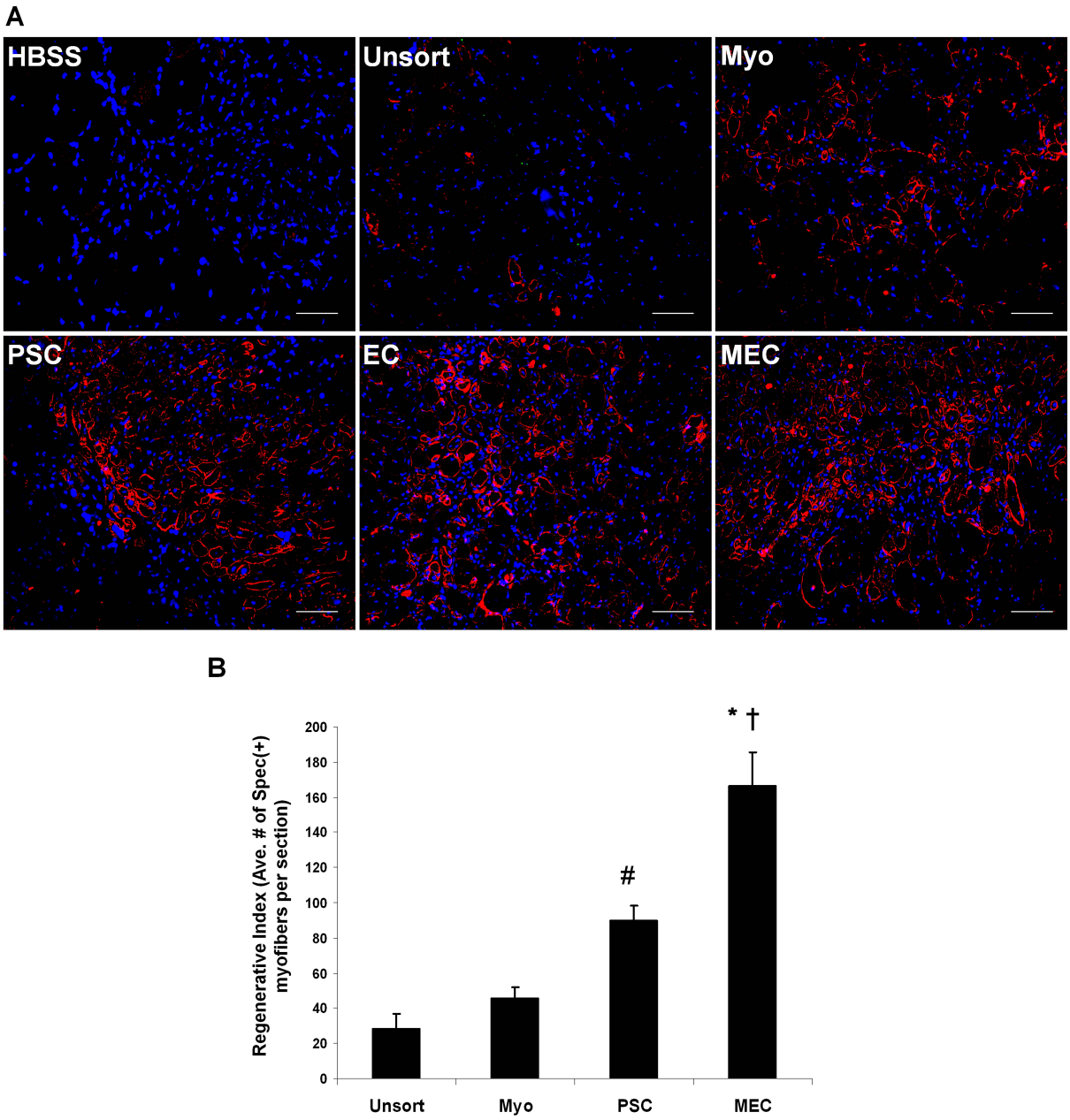

Figure 3. Comparison of myogenic regenerative capacities in vivo. (A) Representative pictures of regenerating human spectrin-positive myofibers in cardiotoxin-injured mouse skeletal muscles transplanted with newly sorted cell fractions from a single donor-derived cryo-hPSMC culture, including myogenic endothelial cells (MECs), perivascular stem cells (PSCs), endothelial cells (ECs), and myoblasts (Myos). Unsorted cryo-hPSMCs (Unsort) and HBSS were injected as treated and untreated controls respectively. Original magnification: 200×; scale bars: 50 µm. (B) Quantitative analyses of the myogenic regenerative capacities of sorted stem/progenitor cell populations. Fifty thousand cells from each cell fraction that was minimally expanded in culture were injected. Quantitative analyses of spectrin-positive human skeletal myofibers on tissue sections revealed that MECs mediated the highest myogenic regeneration among all four cell fractions tested (*$p < 0.001$ vs. Myo and Unsort; †$p = 0.004$ vs. PSC). Injection of PSCs regenerated more human myofibers than injections of Myos ($p > 0.05$) and Unsort (#$p = 0.017$). Finally, Myos displayed a trend of higher myogenic capacity than Unsort, but no significant difference was observed ($p > 0.05$).

assembly of data, data analysis and interpretation, manuscript writing (C.-W.C.); collection and/or assembly of data, data analysis, and interpretation (G.L.); collection and/or assembly of data, data analysis, and interpretation (S.D.T.); collection and/or assembly of data, data analysis and interpretation (M.P.); conception and design, financial support, data analysis and interpretation (B.P.); conception and design, financial support, data analysis and interpretation, manuscript writing, final approval of manuscript (J.H.). Dr. Johnny Huard has received remuneration from Cook Myosite, Inc. for consulting services and for royalties received from technology licensing during the period that the above research was performed. All other authors declare no conflicts of interst.

REFERENCES

1. Carr, L. K.; Steele, D.; Steele, S.; Wagner, D.; Pruchnic, R.; Jankowski, R.; Erickson, J.; Huard, J.; Chancellor, M. B. 1-year follow-up of autologous muscle-derived stem cell injection pilot study to treat stress urinary incontinence. Int. Urogynecol. J. Pelvic Floor Dysfunct. 19(6): 881–883; 2008.
2. Cerletti, M.; Jurga, S.; Witczak, C. A.; Hirshman, M. F.; Shadrach, J. L.; Goodyear, L. J.; Wagers, A. J. Highly efficient, functional engraftment of skeletal muscle stem cells in dystrophic muscles. Cell 134(1):37–47; 2008.
3. Chen, C. W.; Montelatici, E.; Crisan, M.; Corselli, M.; Huard, J.; Lazzari, L.; Péault, B. Perivascular multilineage progenitor cells in human organs: regenerative units, cytokine sources or both? Cytokine Growth Factor Rev. 20(5–6):429–434; 2009.
4. Chen, C. W.; Okada, M.; Tobita, K.; P?ault, B.; Huard, J. Purified human muscle-derived pericytes support formation of vascular structures and promote angiogenesis after myocardial infarction. Circulation 120(18 Suppl.):S1053; 2009.
5. Collins, C. A.; Zammit, P. S.; Ruiz, A. P.; Morgan, J. E.; Partridge, T. A. A population of myogenic stem cells that survives skeletal muscle aging. Stem Cells 25(4):885–894; 2007.
6. Crisan, M.; Yap, S.; Casteilla, L.; Chen, C. W.; Corselli, M.; Park, T. S.; Andriolo, G.; Sun, B.; Zheng, B.; Zhang, L.; Norotte, C.; Teng, P. N.; Traas, J.; Schugar, R.; Deasy, B. M.; Badylak, S.; Buhring, H. J.; Giacobino, J. P.; Lazzari, L.; Huard, J.; Péault, B. A perivascular origin for mesenchymal stem cells in multiple human organs. Cell Stem Cell 3(3):301–313; 2008.
7. Dellavalle, A.; Sampaolesi, M.; Tonlorenzi, R.; Tagliafico, E.; Sacchetti, B.; Perani, L.; Innocenzi, A.; Galvez, B. G.; Messina, G.; Morosetti, R.; Li, S.; Belicchi, M.; Peretti, G.; Chamberlain, J. S.; Wright, W. E.; Torrente, Y.; Ferrari, S.; Bianco, P.; Cossu, G. Pericytes of human skeletal muscle are myogenic precursors distinct from satellite cells. Nat. Cell Biol. 9(3):255–267; 2007.
8. Drowley, L.; Okada, M.; Payne, T. R.; Botta, G. P.; Oshima, H.; Keller, B. B.; Tobita, K.; Huard, J. Sex of muscle stem cells does not influence potency for cardiac cell therapy. Cell Transplant. 18(10):1137–1146; 2009.
9. Hirt-Burri, N.; de Buys Roessingh, A. S.; Scaletta, C.; Gerber, S.; Pioletti, D. P.; Applegate, L. A.; Hohlfeld, J. Human muscular fetal cells: A potential cell source for muscular therapies. Pediatr. Surg. Int. 24(1):37–47; 2008.
10. Jankowski, R. J.; Deasy, B. M.; Huard, J. Muscle-derived stem cells. Gene Ther. 9(10):642–647; 2002.
11. Okada, M.; Payne, T. R.; Zheng, B.; Oshima, H.; Momoi, N.; Tobita, K.; Keller, B. B.; Phillippi, J. A.; Péault, B.; Huard, J. Myogenic endothelial cells purified from human skeletal muscle improve cardiac function after transplantation into infarcted myocardium. J. Am. Coll. Cardiol. 52(23):1869–1880; 2008.
12. Oshima, H.; Payne, T. R.; Urish, K. L.; Sakai, T.; Ling, Y.; Gharaibeh, B.; Tobita, K.; Keller, B. B.; Cummins, J. H.; Huard, J. Differential myocardial infarct repair with muscle stem cells compared to myoblasts. Mol. Ther. 12(6):1130–1141; 2005.
13. Péault, B.; Rudnicki, M.; Torrente, Y.; Cossu, G.; Tremblay, J. P.; Partridge, T.; Gussoni, E.; Kunkel, L. M.; Huard, J. Stem and progenitor cells in skeletal muscle development, maintenance, and therapy. Mol. Ther. 15(5):867–877; 2007.
14. Pisani, D. F.; Dechesne, C. A.; Sacconi, S.; Delplace, S.; Belmonte, N.; Cochet, O.; Clement, N.; Wdziekonski, B.; Villageois, A. P.; Butori, C.; Bagnis, C.; Di Santo, J. P.; Kurzenne, J. Y.; Desnuelle, C.; Dani, C. Isolation of a highly myogenic CD34-negative subset of human skeletal muscle cells free of adipogenic potential. Stem Cells 28(4):753–764; 2010.
15. Rousseau, J.; Dumont, N.; Lebel, C.; Quenneville, S. P.; Côté, C. H.; Frenette, J.; Tremblay, J. P. Dystrophin expression following the transplantation of normal muscle precursor cells protects mdx muscle from contraction-induced damage. Cell Transplant. 19(5):589–596; 2010.
16. Seidel, M.; Borczyńska, A.; Rozwadowska, N.; Kurpisz, M. Cell-based therapy for heart failure: Skeletal myoblasts. Cell Transplant. 18(7):695–707; 2009.
17. Sherman, W.; He, K. L.; Yi, G. H.; Wang, J.; Harvey, J.; Lee, M. J.; Haimes, H.; Lee, P.; Miranda, E.; Kanwal, S.; Burkhoff, D. Myoblast transfer in ischemic heart failure: Effects on rhythm stability. Cell Transplant. 18(3):333–341; 2009.
18. Sherwood, R. I.; Christensen, J. L.; Conboy, I. M.; Conboy, M. J.; Rando, T. A.; Weissman, I. L.; Wagers, A. J. Isolation of adult mouse myogenic progenitors: Functional heterogeneity of cells within and engrafting skeletal muscle. Cell 119(4):543–554; 2004.
19. Torrente, Y.; Belicchi, M.; Marchesi, C.; Dantona, G.; Cogiamanian, F.; Pisati, F.; Gavina, M.; Giordano, R.; Tonlorenzi, R.; Fagiolari, G.; Lamperti, C.; Porretti, L.; Lopa, R.; Sampaolesi, M.; Vicentini, L.; Grimoldi, N.; Tiberio, F.; Songa, V.; Baratta, P.; Prelle, A.; Forzenigo, L.; Guglieri, M.; Pansarasa, O.; Rinaldi, C.; Mouly, V.; Butler-Browne, G. S.; Comi, G. P.; Biondetti, P.; Moggio, M.; Gaini, S. M.; Stocchetti, N.; Priori, A.; D'Angelo, M. G.; Turconi, A.; Bottinelli, R.; Cossu, G.; Rebulla, P.; Bresolin, N. Autologous transplantation of muscle-derived CD133^{+} stem cells in Duchenne muscle patients. Cell Transplant. 16(6):563–577; 2007.
20. Zheng, B.; Cao, B. H.; Crisan, M.; Sun, B.; Li, G. H.; Logar, A.; Yap, S.; Pollett, J. B.; Drowley, L.; Cassino, T.; Gharaibeh, B.; Deasy, B. M.; Huard, J.; Péault, B. Prospective identification of myogenic endothelial cells in human skeletal muscle. Nat. Biotechnol. 25(9):1025–1034; 2007.
21. Zheng, B.; Li, G. H.; Logar, A.; Péault, B.; Huard, J. Identification of CD56+CD146+UEA-1+ cell population within cryopreserved human skeletal muscle cells which endowed with a high myogenic potential in vivo. The Orthopaedic Research Society (ORS) 54th Annual Meeting, San Francisco, CA; 2008.

Appendix 6

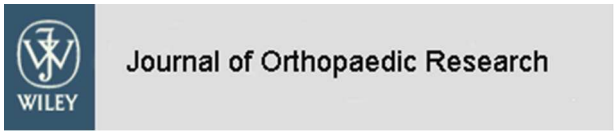

Human Myogenic Endothelial Cells Exhibit Chondrogenic and Osteogenic Potentials at the Clonal Level

Journal:	*Journal of Orthopedic Research*
Manuscript ID:	JOR-12-0639
Wiley - Manuscript type:	Research Article
Date Submitted by the Author:	29-Aug-2012
Complete List of Authors:	Zheng, Bo; Oregon Health & Science University, Li, Guangheng; University of Pittsburgh, Orthopedic Surgery Chen, William; University of Pittsburgh, Orthopedic Surgery; University of Pittsburgh, Bioengineering Deasy, Bridget; University of Pittsburgh, Orthopedic Surgery Pollett, Jonathan; Allegheny General Hospital, Cardiology Sun, Bin; University of Pittsburgh, Vascular Medicine Institute Drowley, Lauren; AstraZeneca, Gharaibeh, Burhan; University of Pittsburgh, Orthopedic Surgery Usas, Arvydas; University of Pittsburgh, Orthopedic Surgery Péault, Bruno; University of Edinburgh, Queens Medical Research Institute Huard, Johnny; Stem Cell Research Center, Dept. of Orthopaedic Surgery;
Keywords:	myogenic endothelial cells , muscle stem cells, clonal analysis, osteogenesis, chondrogenesis

Human Myogenic Endothelial Cells Exhibit Chondrogenic and Osteogenic Potentials at the Clonal Level

Bo Zheng[1,2], Guangheng Li[1,2,*], William CW Chen[1,3,*], Bridget M Deasy[1,2], Jonathan B Pollett[1], Bin Sun[1,4], Lauren Drowley[1], Burhan Gharaibeh[1], Arvydas Usas[1,2], Bruno Péault[1,4,5,6,7], Johnny Huard[1,2,5]

[1]Stem Cell Research Center, University of Pittsburgh School of Medicine

[2]Department of Orthopaedic Surgery, University of Pittsburgh School of Medicine

[3]Department of Bioengineering, University of Pittsburgh Swanson School of Engineering

[4]Department of Pediatrics, Children's Hospital of Pittsburgh of UPMC

[5]McGowan Institute for Regenerative Medicine, University of Pittsburgh

[6]David Geffen School of Medicine, University of California at Los Angeles

[7]Centre for Cardiovascular Science and MRC Centre for Regenerative Medicine, University of Edinburgh, UK

*These authors contributed equally to this work

Correspondence to:

Johnny Huard, PhD

Stem Cell Research Center, Department of Orthopaedic Surgery, School of Medicine, University of Pittsburgh, Bridgeside Point II, Suite 206, 450 Technology Drive, Pittsburgh, PA 15219

TEL: 1-412-648-2798

FAX: 1-412-648-4066

Email: jhuard@pitt.edu

Running Title: Clonal Myogenic Endothelial Cells Exhibit Osteogenic and Chondrogenic Potential

Key words: myogenic endothelial cells, muscle stem cells, clonal analysis, osteogenesis, chondrogenesis

Abstract

We have previously reported the high regenerative potential of murine muscle-derived stem cells (mMDSCs) that are capable of differentiating into multiple mesodermal cell lineages, including myogenic, endothelial, chondrocytic, and osteoblastic cells. Recently we described a putative human counterpart of mMDSCs, the myogenic endothelial cells (MECs), in adult human skeletal muscle, which efficiently repair/regenerate the injured and dystrophic skeletal muscle as well as the ischemic heart in animal disease models. Nevertheless it remained unclear whether human MECs, at the clonal level, preserve mMDSC-like chondrogenic and osteogenic potentials and classic stem cell characteristics including high proliferation and resistance to stress. Herein we demonstrated that MECs, sorted from fresh postnatal human skeletal muscle biopsies, can be grown clonally and exhibit robust resistance to oxidative stress with no tumorigeneity. MEC clones were capable of differentiating into chondrocytes and osteoblasts under inductive conditions in vitro and participated in cartilage and bone formation in vivo. Additionally, adipogenic and angiogenic potentials of clonal MECs (cMECs) were observed. Overall, our study showed that cMECs not only display typical properties of adult stem cells but also exhibit chondrogenic and osteogenic capacities in vitro and in vivo, suggesting their potential applications in articular cartilage and bone repair/regeneration.

INTRODUCTION

Recent studies suggest that stem/progenitor cell populations other than satellite cells repair/regenerate skeletal muscle.[1-7] Our group previously reported that murine muscle-derived stem cells (mMDSCs), a unique population of myogenic stem cells isolated from the slowly adhering fraction of primary muscle cells by the "preplate" technique, proliferate long-term, self-renew, and differentiate into diverse cell lineages.[8-13] mMDSCs express markers typically associated with stem cells, including CD34 and Sca-1. However, expression of these markers in mMDSCs is highly influenced by extended cell culture, leading to the difficulties of finding a valid marker profile for prospective identification and purification of native mMDSCs.

Recently, we have prospectively purified by cell sorting a unique stem cell population associated with the vasculature in the human skeletal muscle.[14] These myogenic endothelial cells (MECs) ($CD34^+/CD56^+/CD144^+/CD45^-$), which presumably represent the human counterpart of mMDSCs, can undergo long-term proliferation, multi-lineage differentiation, and repair skeletal and cardiac muscles with high efficiency, similar to mMDSCs.[14, 15] Although MECs have been characterized in our prior studies,[14, 15] the true capacity of these cells to function as multi-lineage regenerative units has not yet been fully disclosed, especially in chondrogenesis and osteogenesis. One major limitation in characterizing their multipotent potential is the likely heterogeneous nature in stemness. In the present study, we investigated whether MECs, freshly sorted from adult human skeletal muscle based on their unique cell surface marker profile, preserve chondrogenic and osteogenic potentials at the clonal level.

Our results showed that MEC clones possess stem cell characteristics equivalent to mMDSCs, including long-term proliferation with no karyotypic abnormalities and high resistance to stress. The robust ability of clonal MECs (cMECs) to differentiate into

chondrogenic and osteogenic cell lineages in vitro and in vivo was demonstrated. This clonal study of human MECs highlights their regenerative potential for integrated musculoskeletal repair and regeneration.

METHODS

Human Muscle Biopsy Procurement and Animal Research

The procurement of adult human skeletal muscle biopsies from the National Disease Research Interchange (Philadelphia, PA, USA) was approved by the Institutional Review Board at the University of Pittsburgh Medical Center (UPMC). After procurement, biopsies were immediately transported to our laboratory in Hanks' Balanced Salt Solution (HBSS) (Invitrogen, Grand Island, NY, USA) on ice. Animal experiments were approved by the Animal Research and Care Committee of the Children's Hospital of Pittsburgh of UPMC (Protocol #42-04).

Cell Isolation and Cloning

Muscle biopsies were finely minced and digested with collagenases and dispase to obtain single cell suspension as previously described.[14] Cells were immunofluorescently labeled and subject to cell sorting.[14] Details are documented in Supplementary Material.

Gene Expression Profiling

Total RNA was extracted from the 1×10^6 cells using Nucleospin RNA kit (Clontech, Mountain View, CA, USA). Details are listed in Supplementary Material. Primer sequences used for PCR are listed in Supplemental Table 1.

Cell Proliferation Analysis and Cell Survival under Oxidative Stress

For the single cell proliferation assay, cMECs were transduced with lentiviral eGFP reporter and further sorted to homogeny by FACS as previously reported.[16] To test the capacity of cMECs against oxidative stress, MEC clones were plated onto collagen-coated plates and

cultured with proliferation medium containing 400μM hydrogen peroxide (H_2O_2) and 2μl propidium iodide (1:500, PI, Sigma-Aldrich). Bright-field and fluorescent images were taken in a time-lapsed microscopic imaging system. Details are summarized in Supplementary Material.

Tumorigenesis Assay and Karyotype Analysis

To examine the tumorigenic property of cMECs in vitro, we monitored the growth of cMECs plated at different densities on 1% agar in proliferation medium. For karyotype analysis, cMEC clones were cultured for 8 weeks and harvested. The cell pellets were processed for chromosome analysis. Detail procedures are listed in Supplementary Material.

Chondrogenic and Osteogenic Differentiation in Culture and in Vivo

The details of in vitro chondrogenesis and osteogenesis are documented in Supplementary Material. To track donor cells after implantation, cMECs and unsorted cells were co-transduced with retroviral nuclear LacZ (nLacZ) reporter and subsequently with retroviral BMP4 gene as previously reported.[17] After expansion, 5×10^6 cells were seeded onto a 6×6-mm piece of Gelfoam, incubated overnight, and implanted into the gluteofemoral muscle pockets of SCID mice (8-week-old male; The Jackson Laboratory, Bar Harbor, ME, USA).

Adipogenesis in Culture and Angiogenesis in Vitro/in Vivo

The details of in vitro adipogenesis and angiogenesis as well as in vivo angiogenesis are summarized in Supplementary Material.

RESULTS

Isolation and characterization of myogenic endothelial cell clones

MECs ($CD34^+CD56^+CD144^+CD45^-$) were isolated by fluorescence activated cell sorting (FACS) from dissociated muscle biopsies as previously reported.[18] Single sorted MEC was then automatically seeded by the autoclone system of the FACSAria sorter into each well of a

collagen-coated 96-well plate (seeding density: 1 cell/well). Wells that did not contain exactly 1 cell/well were excluded from the study. A total of six MEC clones from 2 distinct muscle biopsies were obtained from 576 single-cell seeded wells. The average cloning efficiency was 1.04 %, with MECs of donor #1 and #2 having the cloning efficiency of 0.69% and 1.39% respectively. Clonal MECs (cMECs) at passage 6-15 were analyzed for their phenotypes, single cell proliferation, and multi-lineage differentiation capacity and subsequently used for transplantation experiments. Six MEC clones were individually analyzed for gene expression by RT-PCR. The results showed that genes of the lineage-specific markers were expressed in all clones at similar levels (**Figure 1A**). Notably, in addition to the late myogenic markers: desmin, m-cadherin, and CD56, we also detected expression of the early myogenic transcription factors, Pax3, Pax7, and Myf5 in all 6 clones (**Figure 1A**).

Single cells derived from MEC clones undergo clonogenic proliferation

To precisely quantitate the clonogenic potential and long-term proliferation of cMECs in culture, we performed sub-cloning analysis. MEC clones were lentivirally transduced at passage 15 to express enhanced green fluorescence protein (eGFP). Sub-cloning analysis was performed with eGFP+ cMECs individually sorted into each well of a 384-well plate by the FACSAria autoclone system (**Supplemental Figure 1**). Approximately 1/3 of all wells received exactly one cell per well; the remaining 2/3 received none. Proliferation of sub-cloned cMECs was monitored by a time-lapsed microscopic imaging system. The results showed that 73% of sub-cloned cMECs expanded to more than 8 cells, 14% divided into 2-4 cells, 12% did not divide, and 1% eventually died (**Figure 1B**). Cell doubling time and averaged cell division time were 28.1 ± 5.5 hours and 16.8 ± 2.1 hours respectively (mean±SD, n=4) (**Figure 1C**). A video of single sub-cloned cMEC proliferation was presented (**Supplemental Video**).

Gene expression, tumorigenesis, karyotype analysis, and resistance to oxidative stress

Gene expression analyses revealed that cMECs express genes associated with undifferentiated cells (GABRB3 and DNMT3B), and the stemness gene, IL6ST when compared to the unsorted human primary skeletal muscle cells (hPSMCs) (**Supplemental Table 2**). In contrast, hPSMCs expressed genes associated with myogenic differentiation including: Runx-2, Noggin, MYF5, MyoD1, Des and Actc (**Supplemental Table 2**). To assess their tumorigenesis, cMECs cultured for 2 months were analyzed for anchorage independent growth, a hallmark of transformed tumor cells. Cells were plated on a layer of 1% agar at different densities, and colony growth was scored at 2 and 3 weeks post-seeding. Non-adherent cell growth was only observed when cMECs were plated at a very high density of 2.5×10^4 cells/cm^2. Cells plated at low densities (25 and 250 cells/cm^2) and regular culture density (2,500 cells/cm^2) did not grow in an anchorage-independent manner and eventually died (**Supplemental Figure 2**). Furthermore, tumorigenesis in vivo was examined by implanting expanded cMECs into skeletal muscle pockets in the hind limbs of SCID mice. No evidence of tumor growth at 12 weeks post-transplantation was observed physically and histologically (data not shown). Finally, karyotype analyses revealed little-to-no structural (data not shown) and numerical (**Figure 1D**) abnormalities in the chromosome of all long-term cultured MEC clones.

Non-clonal MECs displayed a superior regenerative capacity in both skeletal and cardiac muscles when compared to myoblasts and/or endothelial cells, a behavior hypothesized to be associated with MECs' ability to withstand oxidative stress.[18, 19] Whether cMECs retain the resistance to oxidative stress was examined by culturing the cells in 400μM H_2O_2 and analyzing their survival every 12 hours over a 72-hour period.[20] Among five MEC clones tested, four withstood the oxidative stress to a similar or better level as non-clonal MECs, which had a

survival rate of 30.6% at 72 hours (**Supplemental Table 3**). This result suggested that cMECs in general have high resistance to extended exposure of oxidative stress.

cMECs undergo chondrogenic differentiation in vitro and in vivo

To induce chondrogenic differentiation, cMECs and hPSMCs were pellet-cultured in chondrogenic induction medium supplemented with BMP4 and TGF-β3 for up to 3 weeks. Gross morphology of pellets was compared (**Figure 2A**). The average volume of the pellets formed by cMECs was significantly larger than those formed by hPSMCs at day 7 and 21 (n=3 per group, $p<0.01$, two-tailed unpaired t test) (**Figure 2B**). Pellets were then sectioned and stained specifically for the cartilaginous matrix with Alcian blue (pH=1). cMEC pellets displayed denser blue staining when compared to hPSMC ones at all 3 time points, suggesting a robust chondrogenic potential of cMECs (**Figure 2C**). To investigate their chondrogenic potential in vivo, we co-transduced cMECs with retroviruses encoding BMP4 and nuclear LacZ (nLacZ) genes. The transduction efficiency was near 80%, revealed by the positive β-gal staining (blue) localized to the nuclei of cMECs (**Figure 2D.a**). The presence of round chondrocytes with LacZ+ nuclei (**Figure 2D.b**) and positive immunostaining for collagen type II (**Figure 2D.c**) were observed within the implanted scaffold. A few collagen type II-positive cells co-expressed β-galactosidase, confirming the presence of functional chondrogenic cells originated from donor cMECs (**Figure 2D.d**). Together these data suggest that cMECs were able to differentiate into chondrocytes in vitro and in vivo, albeit to a different extent.

cMECs undergo osteogenic differentiation in vitro and in vivo

To assay the production of mineralized extracellular matrix, cMECs were pellet-cultured in osteogenic induction medium supplemented with BMP4. Osteogenic differentiation was revealed by von Kossa staining after 7 and 21 days in culture. Compared with hPSMCs, pellets

formed by cMECs exhibited more intense mineralization (**Figure 3A**). cMEC pellets maintained in control proliferation medium with no BMP4 remained negative for von Kossa staining, suggesting no spontaneous osteogenic differentiation of cMECs without a proper inductive signal (**Figure 3A**). Mineralization within the pellet was detected by micro-computerized tomography (μCT) at 7 and 21 days (**Figure 3B**). μCT images showed that cMECs produced a significantly higher volume (**Figure 3C**) and density (**Figure 3D**) of mineralized matrix when compared to hPSMCs at both time points (n=3 per group, both $p<0.01$, two-tailed unpaired t test).

To evaluate their osteogenic potential in vivo, cMECs or hPSMCs were co-transduced with retroviruses encoding nLacZ and BMP4 genes and seeded onto a gelatin sponge (5×10^6 cells), followed by implantation into an intramuscular pocket of SCID mice. μCT imaging revealed that transduced cMECs form dense ectopic bone consistently at 2, 4, 8 and 16 weeks post-implantation while transduced hPSMCs fail to form any organized structure (**Figure 3E**). A significant difference in mineralized tissue volume between the two groups was observed at all time points (n=3 per group, all $p<0.01$, two-tailed unpaired t test) (**Figure 3F**). To track donor cMECs undergoing osteogenic differentiation, β-gal/eosin co-staining was performed on the sections of the cMEC-formed ectopic bone structure (**Figure 3G.a**). Osteogenic differentiation of donor cMECs was also confirmed by co-localization of the positive immunohistochemical signals of nLacZ and osteocalcin (**Figure 3G.b**) as well as the positive immunofluorescent signals of β-galactosidase and osteocalcin (**Figure 3G.c)**. Collectively, cMECs exhibited robust osteogenic differentiation capacity under appropriate inductive signals in vitro and in vivo.

cMECs differentiate into adipocytes and remain angiogenic in vitro and in vivo

To understand whether cMECs are able to differentiate into other mesodermal cell lineages, we examined their adipogenic potential in vitro. cMECs cultured in adipogenic induction medium were subsequently stained positive by Oil Red O, revealing the accumulated cytoplasmic lipid droplets **(Supplemental Figure 3A)**. cMECs maintained in control medium were not adipogenic **(Supplemental Figure 3B)**.

To investigate the angiogenic capacity of cMECs, Matrigel culture was used to observe the formation of capillary-like structures.[21] After incubation for 16 hours, cMECs cultured in Matrigel formed capillary-like network **(Supplemental Figure 3C)** while hPSMCs failed to form similar structures under the same condition **(Supplemental Figure 3D)**. Next we subcutaneously implanted Matrigel plugs encapsulating 1.0×10^6 cMECs, hPSMCs, or no cells into the back of SCID mice (n=4 per group). Capillary formation within the implanted plug was determined by anti-CD31 immunostaining **(Supplemental Figure 3E-G)**. The cMEC-plugs displayed significantly higher capillary density than the hPSMC-plugs ($p<0.01$, two-tailed unpaired t test) **(Supplemental Figure 3H)**. Implants with no cells exhibited no presence of CD31-positive structures. To confirm the human origin of the newly formed microvessels within the Matrigel plugs, Lamin A/C, a human nuclear specific antigen, was used to identify donor cMECs. A fraction of microvascular endothelial cells within the cMEC plugs indeed co-expressed CD31 and Lamin A/C, indicative of their human origin **(Supplemental Figure 3I-L).** These results suggest that human cMECs are not only capable of differentiating into major mesenchymal cell lineages but also retain their angiogenic capacity and participate in neovascularization in vivo after long-term culture.

DISCUSSION

Our group has previously demonstrated that mMDSCs differentiate into diverse cell lineages including bone, cartilage, muscle, endothelial, and blood cells.[8-11, 13, 22] mMDSCs repair skeletal and cardiac muscles more efficiently than myoblasts and vascular endothelial cells.[9, 11] Recently we have purified myogenic endothelial cells (MECs) from adult human skeletal muscle that co-express cell surface markers of both myogenic and endothelial cell lineages and exhibit superior regenerative capacities in injured skeletal and cardiac muscle, similar to mMDSCs.[14, 15] Nevertheless, the osteogenic and chondrogenic potentials of MECs were not fully examined at the clonal level. The present study employed the clonogenic assay to evaluate the osteogenic and chondrogenic capacities of single MEC and further characterize their stem cell properties.

We herein established a protocol that enable us to prospectively purify MEC clones from fresh human muscle biopsies directly by FACS sorting, using the previously reported combination of cell surface markers for MEC isolation.[14] RT-PCR analysis revealed that all of the MEC clones expressed genes of myogenic (desmin, CD56, Pax3, Pax7, m-cadherin and MYf5), endothelial (CD34, CD144 and vWF), smooth muscle/vascular mural (α-smooth muscle actin, PDGFR-β, NG2 and CD146), and mesenchymal stem/stromal (CD90 and CD105) cell lineages, showing consistency between clones from the two donor sources. cMECs displayed robust multipotency in vitro and in vivo, including chondrogenesis, osteogenesis, adipogenesis and angiogenesis/vasculogenesis, in addition to myogenesis reported previously.[14] Nevertheless, cMECs could not differentiate into hematopoietic cells in vitro under inductive conditions, even with the presence of OP9 stromal cells (data not shown).

MEC clones were shown to resist oxidative stress efficiently, to a similar or better level of that of non-clonal MECs. cMECs up-regulated genes associated with early progenitor cells, GABRB3 and DNMT3B, and a gene correlated to stemness, IL6ST. When compared to hPSMC,

cMECs expressed much lower level of genes associated with advanced myogenic differentiation, including Runx-2, Noggin, MyoD1, MYF5, Desmin and α-actin. The tumorigenic assay and karyotype analysis revealed no tumorigeneity in long-term expanded cMECs, suggesting the safety of this novel multi-lineage stem cell population in regenerative applications.

Our previous studies of mMDSCs indicated that these cells reside in areas that are normally occupied by capillaries running alongside myofibers.[8, 9] Similarly, MECs are associated with the vasculature in human skeletal muscle, specifically the capillaries located within the interstitial space between myofibers. The hypothesis that MECs represent a developmental intermediate between myogenic and endothelial cells was further supported by the evidence suggesting that muscle satellite cells and endothelial cells are close neighbors and privileged developmental partners.[23] Despite the unclear developmental relationship between MECs and other blood-vessel-associated stem/progenitor cells such as mesoangioblasts[24-26] and pericytes[16, 27], our data suggest that cMECs are indeed one of the multi-lineage mesodermal stem cell populations residing in a vascular niche within the adult skeletal muscle[1, 28, 29] and likely represent a human counterpart of mMDSCs.[30] Overall, these cells not only represent a promising cell source for an integrative application in musculoskeletal repair but also provide more evidence to the involvement of vasculature in post-natal musculoskeletal regeneration.

ACKNOWLEDGEMENTS

The authors wish to thank Alison Logar for her expert assistance in flow cytometry and James H. Cummins for his editorial assistance. This work was supported in part by grants from the National Institutes of Health (R01-AR049684; RO1-DE13420-06; IU54AR050733-01) and the Department of Defense (AFIRM grant W81XWH-08-2-0032) and by the William F. and Jean W. Donaldson Endowed Chair at the Children's Hospital of Pittsburgh, the Henry J. Mankin

Endowed Chair at the University of Pittsburgh, the Orris C. Hirtzel and Beatrice Dewey Hirtzel Memorial Foundation, and the Lemieux Foundation at the University of Pittsburgh. Johnny Huard received remuneration as a consultant for Cook MyoSite, Inc. during the period of this investigation. No other authors have any conflict of interest to disclose.

REFERENCES

1. Peault B, Rudnicki M, Torrente Y, Cossu G, Tremblay JP, Partridge T, et al. Stem and Progenitor Cells in Skeletal Muscle Development, Maintenance, and Therapy. Mol Ther. 2007; **15**(5): 867-77.
2. De Angelis L, Berghella L, Coletta M, Lattanzi L, Zanchi M, Cusella-De Angelis MG, et al. Skeletal myogenic progenitors originating from embryonic dorsal aorta coexpress endothelial and myogenic markers and contribute to postnatal muscle growth and regeneration. J Cell Biol. 1999; **147**(4): 869-78.
3. Ferrari G, Cusella-De Angelis G, Coletta M, Paolucci E, Stornaiuolo A, Cossu G, et al. Muscle regeneration by bone marrow-derived myogenic progenitors. Science. 1998; **279**(5356): 1528-30.
4. Sampaolesi M, Torrente Y, Innocenzi A, Tonlorenzi R, D'Antona G, Pellegrino MA, et al. Cell therapy of alpha-sarcoglycan null dystrophic mice through intra-arterial delivery of mesoangioblasts. Science. 2003; **301**(5632): 487-92.
5. Dellavalle A, Sampaolesi M, Tonlorenzi R, Tagliafico E, Sacchetti B, Perani L, et al. Pericytes of human skeletal muscle are myogenic precursors distinct from satellite cells. Nat Cell Biol. 2007; **9**(3): 255-67.
6. Crisan M, Yap S, Casteilla L, Chen C-W, Corselli M, Park TS, et al. A Perivascular Origin for Mesenchymal Stem Cells in Multiple Human Organs. Cell Stem Cell. 2008; **3**(3): 301-13.
7. Dellavalle A, Maroli G, Covarello D, Azzoni E, Innocenzi A, Perani L, et al. Pericytes resident in postnatal skeletal muscle differentiate into muscle fibres and generate satellite cells. Nat Commun. 2011; **2**: 499.
8. Lee JY, Qu-Petersen Z, Cao B, Kimura S, Jankowski R, Cummins J, et al. Clonal isolation of muscle-derived cells capable of enhancing muscle regeneration and bone healing. J Cell Biol. 2000; **150**(5): 1085-100.
9. Qu-Petersen Z, Deasy B, Jankowski R, Ikezawa M, Cummins J, Pruchnic R, et al. Identification of a novel population of muscle stem cells in mice: potential for muscle regeneration. J Cell Biol. 2002; **157**(5): 851-64.
10. Cao B, Zheng B, Jankowski RJ, Kimura S, Ikezawa M, Deasy B, et al. Muscle stem cells differentiate into haematopoietic lineages but retain myogenic potential. Nat Cell Biol. 2003; **5**(7): 640-6.
11. Payne TR, Oshima H, Sakai T, Ling Y, Gharaibeh B, Cummins J, et al. Regeneration of dystrophin-expressing myocytes in the mdx heart by skeletal muscle stem cells. Gene Ther. 2005; **12**(16): 1264-74.

12. Gharaibeh B, Lu A, Tebbets J, Zheng B, Feduska J, Crisan M, et al. Isolation of a slowly adhering cell fraction containing stem cells from murine skeletal muscle by the preplate technique. Nat Protocols. 2008; **3**(9): 1501-9.
13. Kuroda R, Usas A, Kubo S, Corsi K, Peng H, Rose T, et al. Cartilage repair using bone morphogenetic protein 4 and muscle-derived stem cells. Arthritis Rheum. 2006; **54**(2): 433-42.
14. Zheng B, Cao B, Crisan M, Sun B, Li G, Logar A, et al. Prospective identification of myogenic endothelial cells in human skeletal muscle. Nat Biotech. 2007; **25**(9): 1025-34.
15. Okada M, Payne TR, Zheng B, Oshima H, Momoi N, Tobita K, et al. Myogenic Endothelial Cells Purified From Human Skeletal Muscle Improve Cardiac Function After Transplantation Into Infarcted Myocardium. Journal of the American College of Cardiology. 2008; **52**(23): 1869-80.
16. Crisan M, Yap S, Casteilla L, Chen CW, Corselli M, Park TS, et al. A perivascular origin for mesenchymal stem cells in multiple human organs. Cell Stem Cell. 2008; **3**(3): 301-13.
17. Zheng B, Cao B, Li G, Huard J. Mouse adipose-derived stem cells undergo multilineage differentiation in vitro but primarily osteogenic and chondrogenic differentiation in vivo. Tissue Eng. 2006; **12**(7): 1891-901.
18. Zheng B, Cao B, Crisan M, Sun B, Li G, Logar A, et al. Prospective identification of myogenic endothelial cells in human skeletal muscle. Nat Biotechnol. 2007; **25**(9): 1025-34.
19. Okada M, Payne TR, Zheng B, Oshima H, Momoi N, Tobita K, et al. Myogenic endothelial cells purified from human skeletal muscle improve cardiac function after transplantation into infarcted myocardium. J Am Coll Cardiol. 2008; **52**(23): 1869-80.
20. Drowley L, Okada M, Payne TR, Botta GP, Oshima H, Keller BB, et al. Sex of muscle stem cells does not influence potency for cardiac cell therapy. Cell Transplant. 2009; **18**(10): 1137-46.
21. Wang ZZ, Au P, Chen T, Shao Y, Daheron LM, Bai H, et al. Endothelial cells derived from human embryonic stem cells form durable blood vessels in vivo. Nat Biotechnol. 2007; **25**(3): 317-8.
22. Gharaibeh B, Lu A, Tebbets J, Zheng B, Feduska J, Crisan M, et al. Isolation of a slowly adhering cell fraction containing stem cells from murine skeletal muscle by the preplate technique. Nat Protoc. 2008; **3**(9): 1501-9.
23. Christov C, Chretien F, Abou-Khalil R, Bassez G, Vallet G, Authier FJ, et al. Muscle satellite cells and endothelial cells: close neighbors and privileged partners. Mol Biol Cell. 2007; **18**(4): 1397-409.
24. Minasi MG, Riminucci M, De Angelis L, Borello U, Berarducci B, Innocenzi A, et al. The meso-angioblast: a multipotent, self-renewing cell that originates from the dorsal aorta and differentiates into most mesodermal tissues. Development. 2002; **129**(11): 2773-83.
25. Cossu G, Bianco P. Mesoangioblasts--vascular progenitors for extravascular mesodermal tissues. Curr Opin Genet Dev. 2003; **13**(5): 537-42.
26. Sampaolesi M, Blot S, D'Antona G, Granger N, Tonlorenzi R, Innocenzi A, et al. Mesoangioblast stem cells ameliorate muscle function in dystrophic dogs. Nature. 2006; **444**(7119): 574-9.
27. Dellavalle A, Sampaolesi M, Tonlorenzi R, Tagliafico E, Sacchetti B, Perani L, et al. Pericytes of human skeletal muscle are myogenic precursors distinct from satellite cells. Nat Cell Biol. 2007; **9**(3): 255-67.
28. Kuang S, Gillespie MA, Rudnicki MA. Niche regulation of muscle satellite cell self-renewal and differentiation. Cell Stem Cell. 2008; **2**(1): 22-31.

29. Voog J, Jones DL. Stem cells and the niche: a dynamic duo. Cell Stem Cell. **6**(2): 103-15.
30. Chen C-W, Corselli M, Péault B, Huard J. Human Blood-Vessel-Derived Stem Cells for Tissue Repair and Regeneration. Journal of Biomedicine and Biotechnology. 2012: Epub Feb 2.

FIGURE LEGENDS

Figure 1. Characterization of clonal myogenic endothelial cells (cMECs) in culture. (A) RT-PCR analysis was performed on all six FACS-sorted MEC clones and compared with HUVECs, cultured unsorted hPSMCs (Unsorted), and fresh skeletal muscle cell lysate (Fresh total cells). All MEC clones consistently expressed myogenic (desmin, CD56, Pax7, m-cadherin, Pax3 Myf5), endothelial (CD34, VE-cadherin, vWF), smooth muscle/vascular mural (α-smooth muscle actin, PDGFR-β, NG2, CD146), and mesenchymal stem/stromal (CD90 and CD105) cell markers. **(B)** Analysis of cMEC clonogenic proliferation capacity by sub-cloning single cells from GFP-transduced MEC clones. A total of 80 sub-cloned single GFP-positive cMEC cells (31% of 258 seeded wells) were tracked. Among them, 1% died, 12% did not divide, 14% divided to 2-4 cells, and 73% were able to form colonies (> 8 cells). **(C)** Colony growth rate (n=4) after 17 days in culture showed that the population doubling time was 28.1±5.5 hours, and the cell division time was 16.8 ±2.1 hours. **(D)** After 10 passages in culture, the majority of cMEC metaphases analyzed possess an euploid number (46) of chromosomes.

Figure 2. Chondrogenic differentiation in vitro and in vivo. (A) Gross morphology of cartilage-like pellets formed by cMECs and unsorted muscle cells after being pellet-cultured in chondrogenic medium for 3 weeks. **(B)** cMEC pellets had significantly larger volume than unsorted hPSMC pellets at day 7 and 21 (**p<0.01, Student's t-test). Data were shown as mean ± SD (n=3). **(C)** Chondrogenic differentiation is revealed by Alcian blue/nuclear fast red staining

of pellets cultured in chondrogenic medium supplemented with BMP4 and TGFβ3 at different time points (day 7, 14 and 21) (10X magnification, scale bar represents 25μm). **(D.a)** cMECs were genetically engineered to express nLacZ reporter gene. Positive staining (blue) is localized to the nuclei of the cells (scale bar represents 25μm). **(D.b)** Three weeks after transplantation, chondrogenesis in vivo by cMECs was demonstrated by co-localization of round chondrocytes with blue nuclei (arrow) after staining for β-galactosidase/eosin (scale bar represents 50μm) **(D.c)** Chondrogenesis of cMECs was also revealed by positive immunostaining for collagen type-II (red) (scale bar represents 25μm), and (**D.d**) Co-localization of collagen type-II (red) and β-galactosidase (green, arrow) signals was also detected (scale bar represents 50μm).

Figure 3. Osteogenic differentiation in vitro and in vivo. (A) von Kossa staining of cell pellets cultured in the osteogenic inductive conditions at different time points. Compared to unsorted cell pellets, cMEC pellets cultured in the osteogenic inductive medium containing BMP4 appear to display more extensive mineralization at day 7 and 21. Nevertheless, control cMEC pellets maintained in proliferation medium exhibited no mineralization (scale bar represents 250μm). **(B)** MicroCT images showed that cMEC pellets have a significantly higher **(C)** mineralized matrix volume and (**D)** mineralized matrix density when compared with unsorted cell pellets at day 7 and 21 (**$p<0.01$, Student t-test). Data were shown as mean ± SD (n=3). **(E)** cMECs or unsorted hPSMCs were retrovirally transduced to express BMP4, seeded onto Gelfoam, and implanted into the intramuscular pocket of SCID mice. MicroCT imaging demonstrated that cMEC implants appear to give rise to larger and more organized ectopic mineralized tissue than unsorted cells at all time points. **(F)** There is a significant difference of mineralized tissue volume between the two groups ($p<0.01$ at all time points, Student's t-test). Data were shown as mean ± SEM (n=3). Osteogenesis in vivo by cMECs was also confirmed by co-localization of

(G.a) β-galactosidase-positive nuclei (blue) within eosin-positive cells and **(G.b)** positive immunohistochemical staining for β-galactosidase (blue) and osteocalcin (brown) in the newly formed mineralized tissue as well as **(G.c)** co-localized immunofluorescent staining of osteocalcin (red) and β-galactosidase (green, arrow) (scale bar represents 50μm).

Figure 1

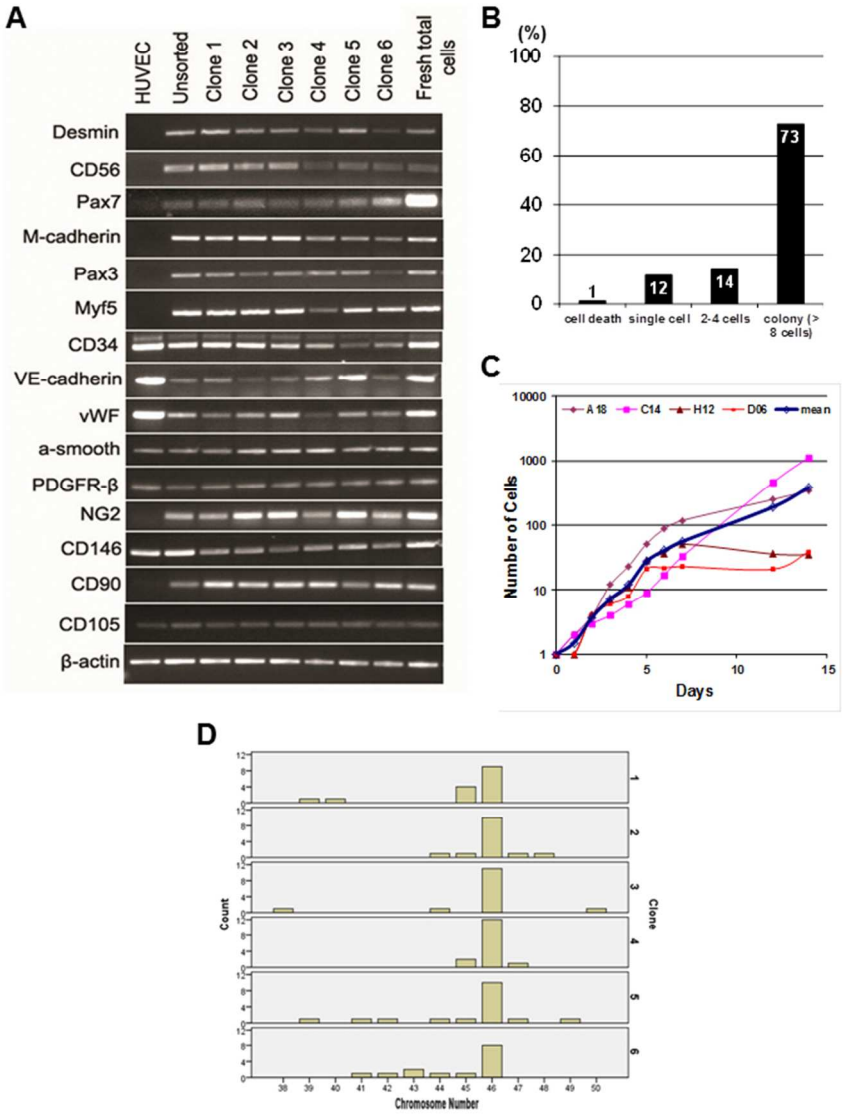

190x254mm (96 x 96 DPI)

Figure 2

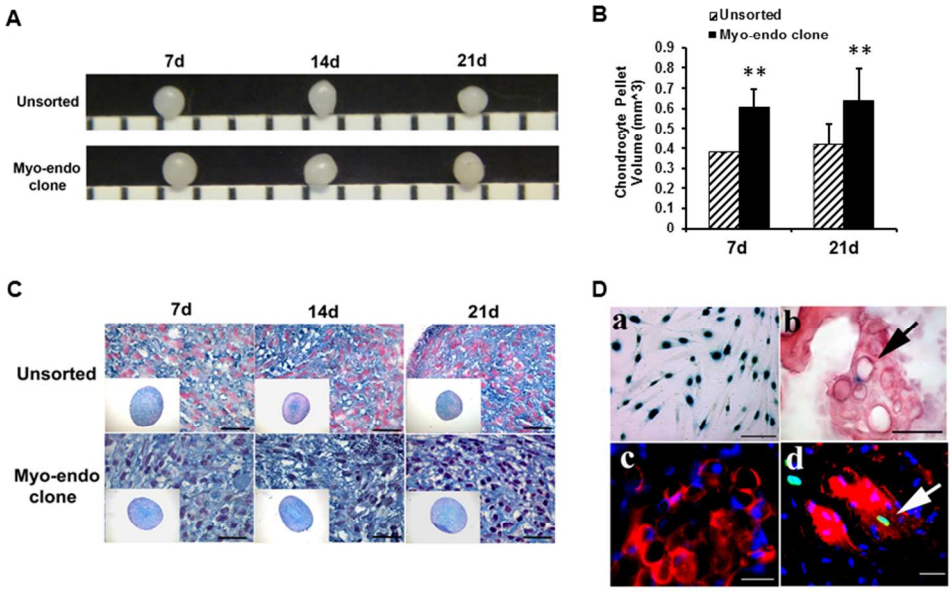

246x168mm (96 x 96 DPI)

Figure 3

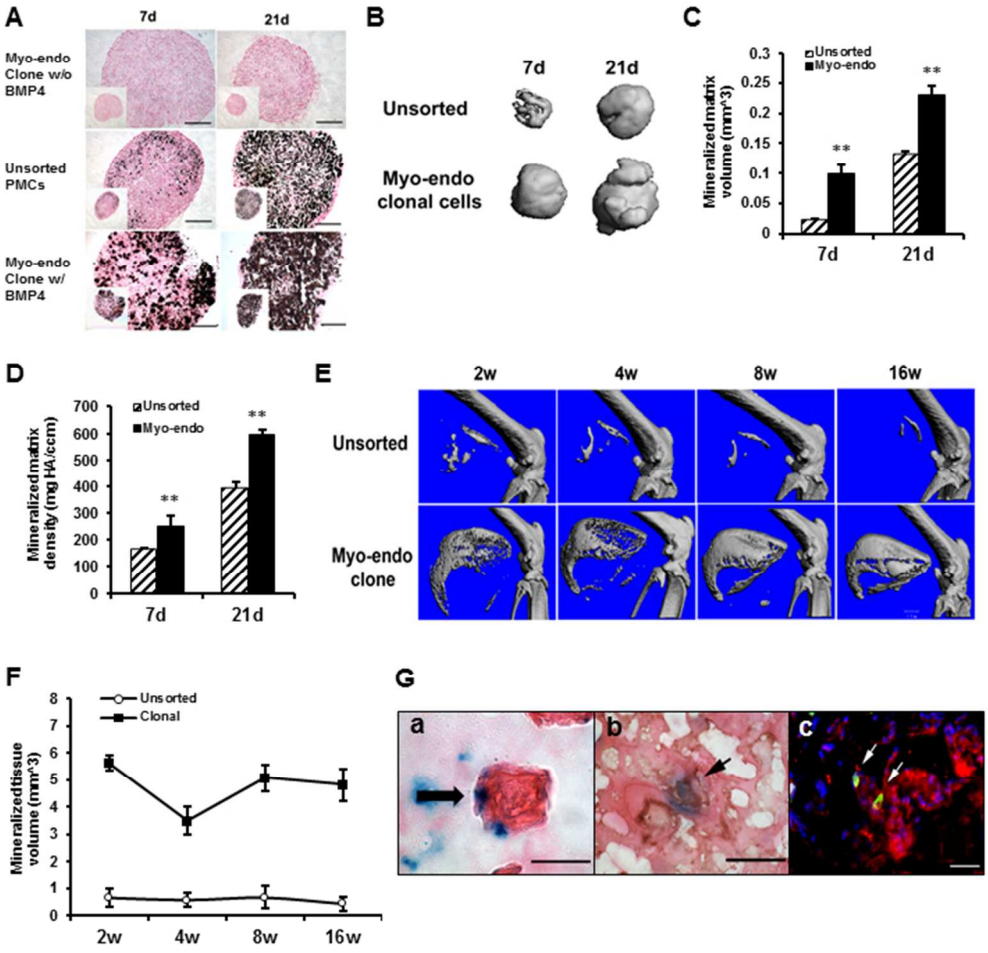

190x194mm (96 x 96 DPI)

Progression of muscular dystrophy in dystrophin/utrophin-/- mice is associated with rapid muscle progenitor cell exhaustion

Aiping Lu; Jonathan Proto; Xiaodong Mu; Ying Tang; Minakshi Poddar; Bing Wang; Johnny Huard
Stem Cell Research Center, Department of Orthopaedic Surgery, University of Pittsburgh, Pittsburgh, PA

Introduction

Duchenne muscular dystrophy (DMD) is a deadly genetic disease characterized by a lack of dystrophin expression and progressive weakening and wasting of the skeletal muscles. Researchers have observed that despite the lack of dystrophin at birth, the histopathological signs of muscle weakness do not become apparent until 4-8 years of age, which happens to coincide with the exhaustion of the muscle progenitor cell (MPC) pool (1).In this study we isolated MPCs from the skeletal muscle of young (2 weeks) and old (6 weeks) dKO (dystrophin/utrophin double knock out) mice, which have a maximum lifespan of 6 to 8 weeks and is a mouse model of DMD that closely recapitulates the disease progression observed in DMD patients. We found that MPCs isolated from old dKO mice have a reduced ability to proliferate and differentiate compared to MPCs isolated from young dKO mice. In addition, Pax7 staining (a muscle progenitor cell marker) indicated that the MPC population significantly decreased during disease progression. These observations suggest that blocking the exhaustion of the MPC pool could be a new approach to improve muscle weakness in DMD patients, despite their continued lack of dystrophin expression.

Methods

1. Cell Isolation: MPCs were isolated from dKO mice at 2 and 6 weeks of age, as previously described via a modified preplate technique (2).

2. Cell proliferation: Proliferation behavior of the MPCs isolated from the skeletal muscle of dKO mice was examined and compared by using a robotic time-lapsed live-cell imaging system (LCI).

3. ***Immunohistocytochemistry:***

Cryosections were stained for mouse Pax7 and the nuclei were revealed by DAPI staining.

4. Myogenic differentiation assay: Myogenic differentiation capacity of the MPCs was assessed by switching the proliferation medium to fusion medium (DMEM containing 2% fetal bovine serum). After 3 days, the cells were stained for fast myosin heavy chain (MyHCf), which is a marker of terminal myogenic differentiation. Myogenic differentiation levels were quantified as the percentage of the number of nuclei in MyHCf positive myotubes relative to the total number of nuclei.

5. Single fiber isolation: Skeletal muscle tissue isolated from 6 week old dKO and 9 week old WT control mice were incubated in a solution of 0.2% collagenase type I for 40 minutes at 37°C. When the muscle was sufficiently digested the muscles were triturated with heat polished glass pipettes to liberate single fibers and then transferred to a matrigel coated 12 well plate with proliferation medium.

Results

1. MPCs isolated from aged dKO mice display limited proliferation ability.

We examined the proliferation kinetics of both populations *in vitro* using LCI (3) and we observed a significant reduction in the proliferation capacity of the old dKO MPCs compared to young dKO MPCs (**Figure 1**)

2. Pax7 positive cells undergo a rapid decline in the skeletal muscle of dKO mice during aging and disease progression.

The results from the Pax7 staining showed that there is a rapid statistically significant decline in the population of Pax7 positive cells in the skeletal muscle of dKO mice from 4 to 8 weeks of age in contrast to that observed in *mdx* skeletal muscle ($p<0.05$) (**Figure 2A**).

3. Isolated muscle fibers from dKO mice show a reduction in muscle progenitor cells.

The single muscle fibers were isolated from 6 weeks old dKO and WT control mice. We observed that there were more cell nuclei in the WT muscle fibers compared to the dKO muscle fibers. In addition, 5 days post-culturing, the WT muscle fibers were able to release myogenic progenitor cells forming new myotubes, in contrasts to that observed with the dKO muscle fibers. These results support both a reduction in the number and myogenic potential of the MPCs derived from the dKO mice when compared to the WT MPCs (**Figure 2B**)

***4. MPCs isolated from aged dKO mice display a limited myogenic differentiation ability*.**
We observed that the MPCs isolated from young dKO mice formed numerous, large multi-nucleated myotubes compared to the MPCs isolated from the old dKO mice. The degree of myogenic differentiation was significantly reduced in the old dKO MPCs relative to the MPCs isolated from young dKO mice ($P < 0.001$).(**Figure 3**)

Discussion:
It is interesting to note that despite the lack of dystrophin at birth, the initiation of any signs of muscle weakness does not occur in DMD patients until later in childhood which happens to coincide with the exhaustion of the muscle progenitor cell pool (1). In this study we demonstrated that MPCs isolated from the skeletal muscle of old dKO mice have a reduced ability to proliferate and differentiate compared to MPCs isolated from young mice. Moreover, the numbers of Pax7 positive cells *in vivo* undergo a rapid decline in the skeletal muscle of dKO mice during aging and disease progression. Since dKO mice can only live 6-8 weeks, stem cell exhaustion could represent the main mechanism for the rapid progress of this disease. Blocking the exhaustion of muscle progenitor cells and stem cell-mediated therapy may represent a potential strategy for treating these muscle diseases.

Significance:
This study suggested that the exhaustion of stem cells contributes to the histopathology associated with DMD and that blocking the exhaustion of muscle progenitor cells and stem cell-mediated therapy could be used as a potential clinical strategy to treat muscle disease.

Figure 1

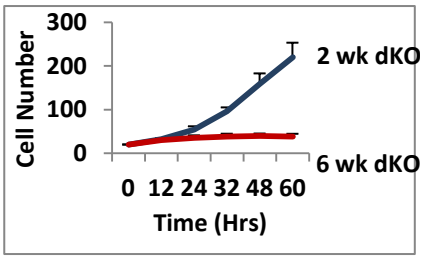

Figure 2A

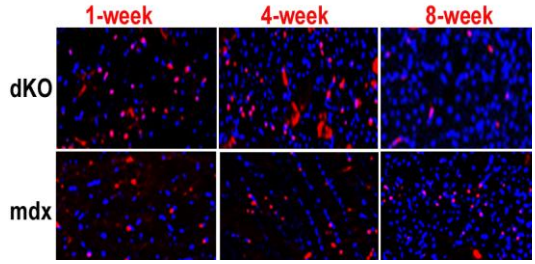

Figure 2B

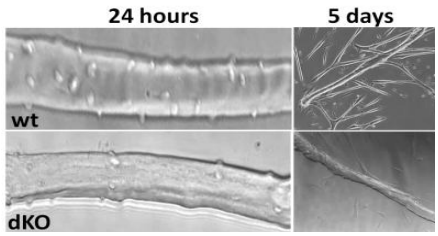

Figure 3

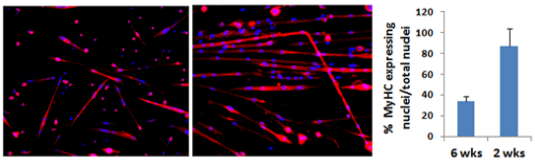

Reference

1. McLoon LK. Focusing on fibrosis: halofuginone-induced functional improvement in the mdx mouse model of Duchenne muscular dystrophy. Am J Physiol Heart Circ Physiol. 2008;294(4):H1505-7.
2. Gharaibeh B, Lu A, Tebbets J, Zheng B, Feduska J, Crisan M, et al. Isolation of a slowly adhering cell fraction containing stem cells from murine skeletal muscle by the preplate technique. Nat Protoc. 2008;3(9):1501-9.
3. Deasy BM, Jankowski RJ, Payne TR, Cao B, Goff JP, Greenberger JS, et al. Modeling stem cell population growth: incorporating terms for proliferative heterogeneity. Stem Cells. 2003;21(5):536-45.

TITLE:
Muscle-derived cells (MDCs) responsible for myogenesis differ from MDCs involved in adipogenesis in dystrophin/utrophin-/- mice

AUTHORS:
Jihee Sohn, Ying Tang, Bing Wang, Aiping Lu, +Johnny Huard
Department of Orthopaedic Surgery, University of Pittsburgh, Pittsburgh, Pennsylvania, United States, 15260 and [2]Department of Bioengineering and McGowan Institute for Regenerative Medicine, University of Pittsburgh, Pittsburgh, Pennsylvania, United States, 15260.
jhuard@pitt.edu

ABSTRACT BODY:
INTRODUCTION: Duchenne muscular dystrophy (DMD) is a genetic disease characterized by progressive weakening of the skeletal and cardiac muscles. The predominant symptoms seen in advanced cases of DMD are sarcopenia and pseudohypertrophy with fatty infiltration in skeletal muscle. Ectopic fat accumulation in skeletal muscle can be seen not only in myopathies but also in several disorders, including obesity and ageing-related sarcopenia; however, the origin of ectopic adipocytes, nor the stimulus that trigger their formation in disease, is known. In our lab, we utilize utrophin/dystrophin double knockout (dys-/-utro-/-, dKO) mice, which better emulates the phenotype seen in DMD patients. Several types of cells, including satellite cells, can be isolated from skeletal muscle and based on a previously published preplate technique (1) we isolated two types of cells; rapidly adhering cells (RACs) ,which are PDGFRα + mesenchymal progenitor cells, and slowly adhering cells (SACs), which are Pax7+ myogenic progenitor cells, from skeletal muscle of dKO and wild type (wt) mice. Previously, we have shown that dKO-SACs have reduced proliferation and myogenic and adipogenic differentiation abilities compared to wt-SACs. These observations suggested that SACs in dKO mice are exhausted and potentially are the main mechanism for the rapid progress of sarcopenia; however, the cells involved in pseudohypertrophy in dKO mice remains unclear. In this study, we examined the proliferation and adipogenic differentiation capabilities of RACs since adipose cells are thought to be derived from mesenchymal stem cells. We observed increased proliferation and adipogenic differentiation capabilities in dKO-RACs compared to wt-RACs. Our results suggest that muscle progenitor cells, SACs, may be more involved in muscle fiber regeneration or degeneration while mesenchymal progenitor cells, RACs, may be the origin of the cell population that is involved in adipogenesis in dKO muscle.

METHODS:

Cell Isolation: Cells were isolated from dKO (dys-/-utro-/-) and wild type (wt) mice at 6 weeks of age, as previously described via a modified preplate technique [1]. After 24hrs, the RACs were obtained and after 7 days, the SACs were obtained. Both cells were cultured in proliferation medium (DMEM supplemented with 10% fetal bovine serum, 10% horse serum, 0.5% chicken embryo extract and 1% penicillin-streptomycin).

Cell proliferation: Proliferation behavior of the dKO-SACs, dKO-RACs, wt-SACs, and wt-RACs were examined by using a robotic time-lapsed microscopic live-cell imaging system (LCI) and MTT assay.

Flow cytometry analysis and Immunofluorescent staining: 100,000 RACs and SACs were used to analyze their PDGFRα expressions. Cells were harvested and stained with PDGFRα-PE (eBioscience) antibody. 10,000 cells/well RACs and SACs were seeded on 24 well collagen type-1 coated plates and stained with mouse-monoclonal primary Pax7 antibody (1:400).

Multi-lineage Differentiation:

Adipogenic: 25,000 cells were cultured on 24 well plates for 21days in adipogenic induction media (Lonza) and then tested for adipogenesis with an AdipoRed reagent.

Myogenic: Myogenic differentiation capacity of the MDSCs was assessed by switching the proliferation medium into fusion medium (DMEM containing 2% fetal bovine serum). After 3 days, we analyzed myotube formation.

RESULTS:

dKO-RACs had increased PDGFRα expression compared to dKO-SACs. Flow cytometry analysis was used to evaluate the expression of PDGFRα, a marker for mesenchymal cells, of the RACs and SACs from both dKO and wt mice. dKO-RACs were about 98% positive for the PDGFRα surface protein, while much lower expression levels were detected in the SACs (Figure 1).

dKO-RACs displayed increased proliferation ability. The proliferation of the RACs and SACs were examined in vitro using an LCI system and MTT assay. We observed a significant increase in the proliferation of the dKO-RACs compared to the wt-RACs.

Increased in vitro adipogenic potential was detected in dKO-RACs. RACs and SACs from both dKO and wt mice were cultured in adipogenic differentiation medium for 21 days. AdipoRed staining was observed in the cytoplasm of the cells, around the nuclei. The degree of adipogenic differentiation was significantly increased in PDGFRα+ dKO-RACs compared to the dKO-SACs (Figure 2).

DISCUSSION: In dKO mice, an animal model of DMD, we observed severe peri-muscular adipose tissue on the surface of the gastrocneminus muscles (GM) as well as lipid accumulation inside of skeletal muscle myofibers. Intramyocellular lipid accumulation could be observed in the cardiac muscle of dKO mice; however, the source of the ectopic fat tissue within the skeletal muscle is unknown. In this study, we provide evidence that the RACs, PDGFRα + mesenchymal progenitor cells, are responsible for increased fat cell formation in the skeletal muscle of dKO mice. We observed that dKO-RACs had increased proliferation and adipogenic differentiation capabilities. This result suggests that dKO-RACs are prone to form adipocytes in skeletal muscle.

SIGNIFICANCE: This study suggests that dKO-RACs, mesenchymal progenitor cells in skeletal muscle, may contribute to adipogenesis and are responsible for ectopic fat cell formation within skeletal muscle in pathological conditions such as DMD. Therefore, targeting RACs to block adipogenesis in skeletal muscle may open new opportunities to treat muscle diseases.

REFERENCE:
[1] Gharaibeh, et al. Nat Protoc. 2008; 3:1501-9
[2] Uezumi, et al. Nat Cell biology. 2010; 2:143-152

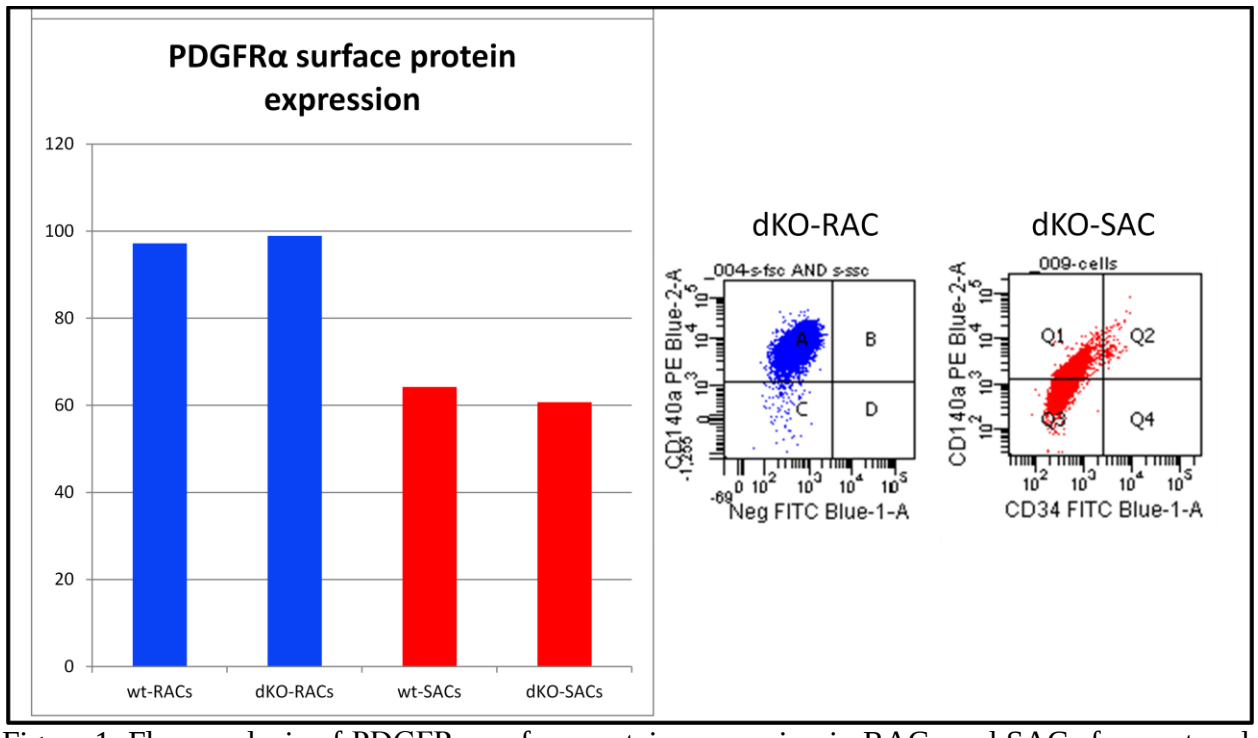

Figure 1. Flow analysis of PDGFRα surface protein expression in RACs and SACs from wt and dKO mice.

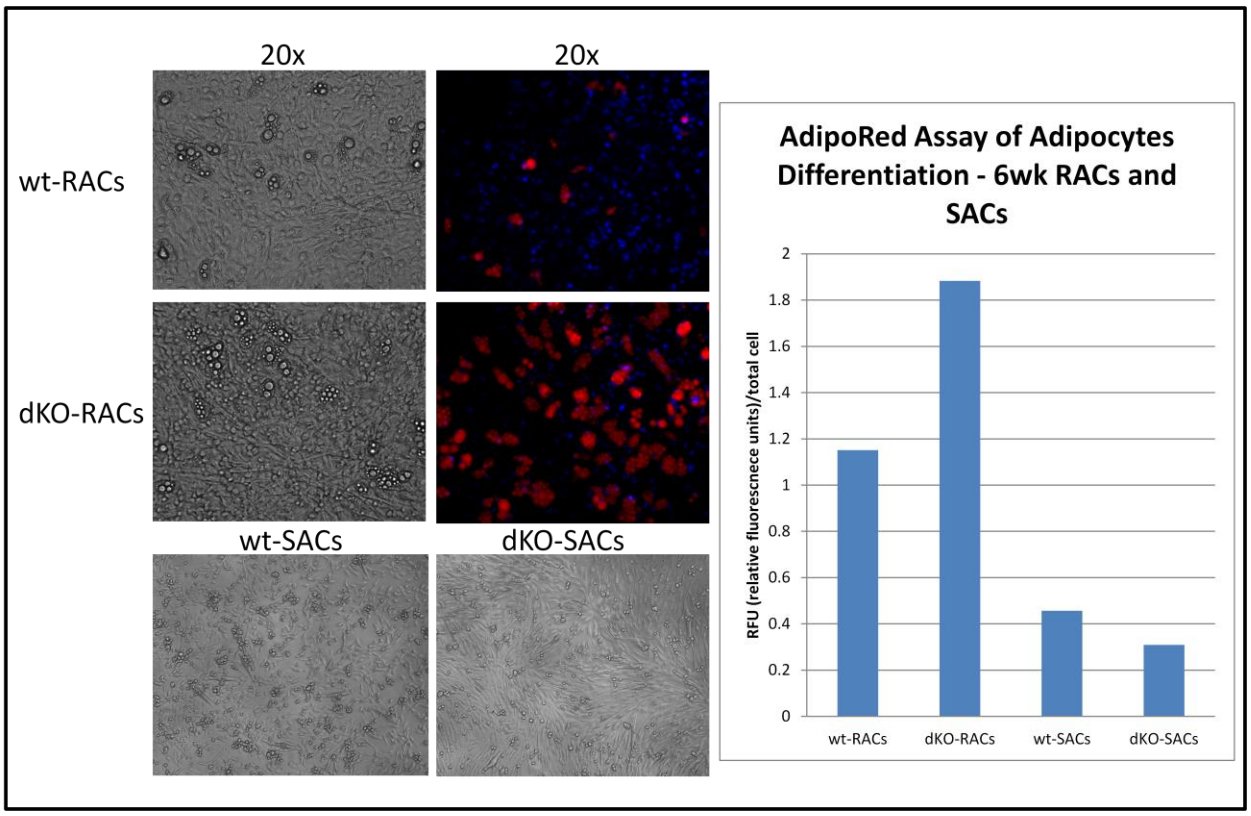

Figure 2. Adipogenesis of RACs and SACs. Bright field pictures and AdipoRed staining. Quantification of AdipoRed assay is shown.

RhoA signaling regulates heterotopic ossification and fatty infiltration in dystrophic skeletal muscle

Xiaodong Mu, Arvydas Usas, Ying Tang, Aiping Lu, Jihee Sohn, Bing Wang, Kurt Weiss, and Johnny Huard
Stem Cell Research Center, Department of Orthopaedic Surgery, University of Pittsburgh

Introduction: Frequent heterotopic ossification (HO) or fatty infiltration is observed in the dystrophic muscle of many animal models of human Duchenne muscular dystrophy (DMD); however, little is known about the correlated molecular mechanisms involved in the process. The RhoA-Rho kinase (ROCK) signaling pathway has been shown to function as a commitment switch of the osteogenic and adipogenic differentiation of mesenchymal stem cells (MSCs). Activation of RhoA-ROCK signaling in cultured MSCs *in vitro* induces their osteogenesis but inhibits the potential of adipogenesis, while the application of Y-27632, a specific inhibitor of ROCK, reversed the process. Inflammation has been shown to be one of main contributors to HO, while the role of RhoA signaling in inflammation reaction has been demonstrated. The objective of the current study is to investigate the potential role of RhoA signaling in regulating HO and fatty infiltration in dystrophic skeletal muscle.

Methods: 1.Mice models**:** Animal experiments were approved by IACUC of University of Pittsburgh. mdx mice (dystrophin-deficient) and dKO (Dystrophin/Utrophin double knockout) mice are both important mouse models of DMD; however, in contrast to the mild phenotype of mdx mice, dKO mice display a far more severe phenotype as is observed in human DMD patients, including a much shorter life span (~ 8 weeks compared to 2 years), more necrosis and fibrosis in the skeletal muscle, etc. 2. Tissue histological analysis: The gastrocnemius muscles (GM) of the mice were used for histological analysis. Alizarin red stain shows calcium deposition caused by HO or during osteogenic differentiation, Oil Red O stain shows fatty infiltration in muscle or fat cells, and Trichrome stain shows fibrosis. 3. Statistics: N >=6 for each group in animal study. Student's T-test was used to evaluate the significance.

Results: 1. Skeletal muscle of dKO mice features more HO but less fatty infiltration than mdx mice (Fig. 1). Both μ-CT scan of animals (**Fig. 1A**) and Alizarn Red stain (**Fig. 1B**) of the muscle tissues revealed greatly enriched HO in the dystrophic muscles of the dKO mice. While, Oil Red O stain (**Fig. 1C**) and Trichrome stain **(Fig. 1D)** of the muscle tissues revealed reduced fatty infiltration and a number of normal muscle fibers in the muscle of dKO mice.

2. RhoA signaling is more activated in both skeletal muscle and muscle-derived stem cells (MDSCs) from dKO mice. Both semi-quantitative PCR and immunohistochemistry study demonstrated that RhoA signaling is more activated in the muscles of dKO mice, as well as dKO MDSCs.

3. *In vitro* RhoA inactivation of cultured MDSCs from dKO mice decreases the osteogenesis potential and increases adipogenesis and myogenesis potential (Fig. 2). Semi-quantitative PCR study showed that Y27632 treatment *(*10 μM) of dKO-MDSCs down-regulated the expression of RhoA, BMP2 and 4, and inflammatory factors such as TNF-α and IL-6 (**Fig. 2A**). Osteogenesis potential was repressed while the adipogenesis and myogenesis potential of the dKO-MDSCs were increased by Y27632 (**Fig. 2B**).

4. RhoA inactivation in the skeletal muscle of dKO mice decreased HO and increased both fatty infiltration and muscle regeneration. GM muscles of 6 dKO mice were injected with Y27632 (5mM in 20μL of DMSO) (left limb) or control (20μL of DMSO) DMSO (right limb). Injections were conducted 3 times a week for 3 weeks. The skeletal muscles that received Y27632 injection demonstrated much slower development of HO and improved muscle regeneration, as well as reduced fibrosis formation.

Discussion: Our current results revealed that DMD mouse models featuring different severity of muscular dystrophy may have varied potentials for developing HO or fatty infiltration in the dystrophic muscle, and RhoA signaling might be a critical mediator of the determining these differential fates, including the progression towards HO, fatty infiltration, or normal muscle regeneration. RhoA inactivation is shown to have a great potential to repress HO and improve the phenotypes of dystrophic muscle. The status of RhoA activation in the skeletal muscle of human DMD patients and the potential effect of RhoA inactivation in human dystrophic muscle requires further investigation.

Significance: Our data reveals the involvement of RhoA signaling in regulating the process of heterotopic ossification, and indicates that RhoA may serve as a potential target for repressing injury-induced and congenital heterotopic ossification in humans.

Fig 1

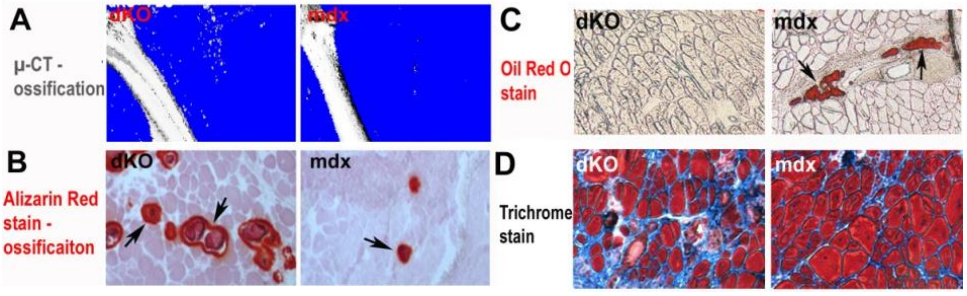

Fig 2

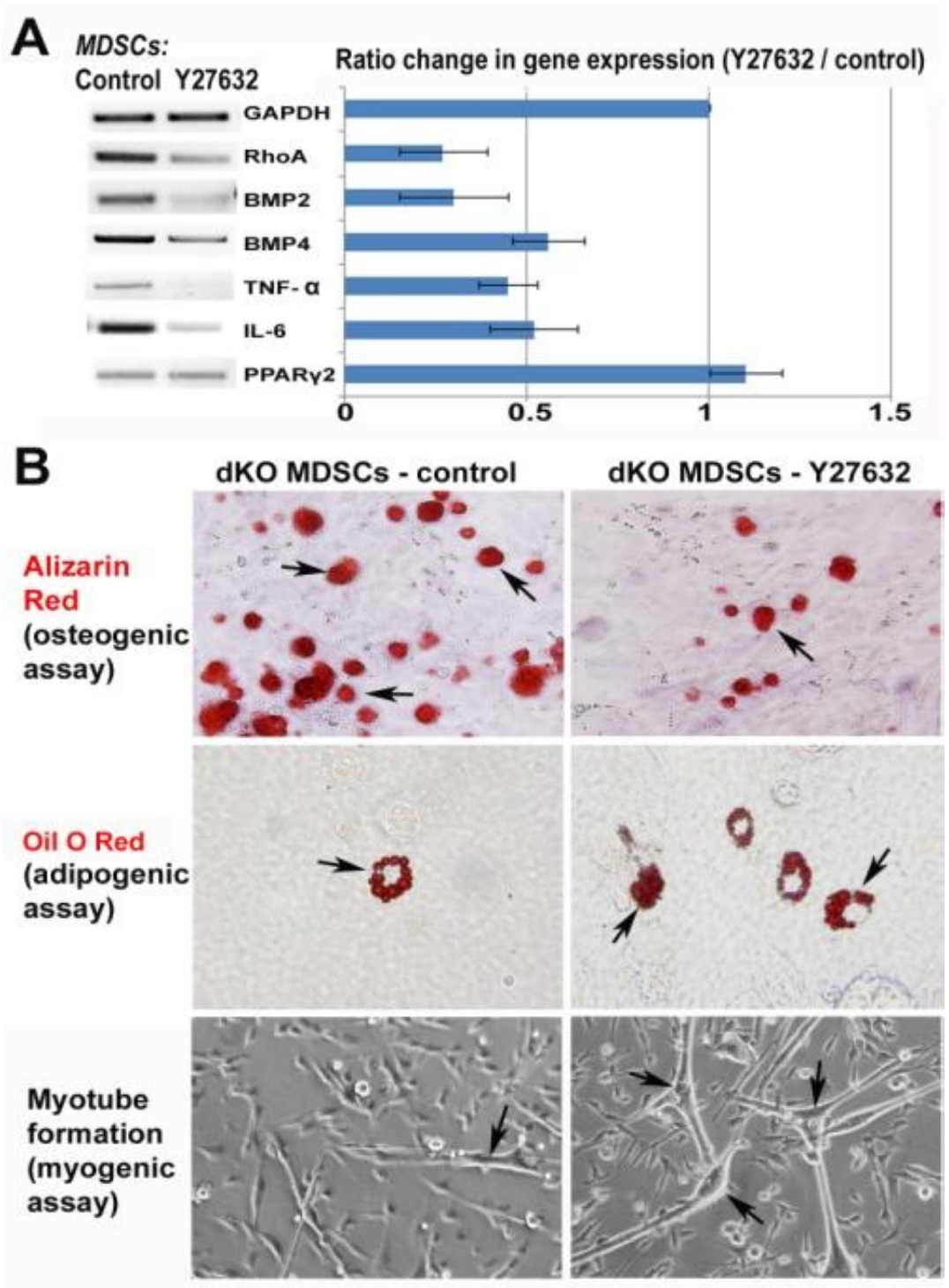
A
MDSCs:
Control Y27632
GAPDH
RhoA
BMP2
BMP4
TNF-α
IL-6
PPARγ2
Ratio change in gene expression (Y27632 / control)
0
0.5
1
1.5
B
dKO MDSCs - control
dKO MDSCs - Y27632
Alizarin Red (osteogenic assay)
Oil O Red (adipogenic assay)
Myotube formation (myogenic assay)

Suppression of skeletal muscle inflammation by muscle stem cells is associated with hepatocyte growth factor in wild type and *mdx*;p65$^{+/-}$ mice

[1]Proto, J.; [1]Tang, Y; [1]Lu, A.; [2]Robbins, P.D.; [1]Wang, B. [1]+Huard, J.
[1]+ Stem Cell Research Center, Children's Hospital of Pittsburgh, and Department of Orthopedic Surgery;
[2]Department of Metabolism and Aging, The Scripps Research Institute, Jupiter, FLA
jhuard@pitt.edu

INTRODUCTION

Persistent, unresolved inflammation can lead to secondary tissue damage. Recently, we reported that intramuscular (i.m.) injection of muscle-derived stem cells (MDSCs) heterozygous for the NF-kB subunit p65 (p65$^{+/-}$) reduced host inflammation and fiber necrosis seven days following muscle injury, relative to wild type (WT) MDSC injection [1]. In this investigation, we looked closer at the role of secreted factors in this observation. Using a murine cardiotoxin muscle injury model, we observed that delivery of p65$^{+/-}$ MDSCs accelerated the resolution of inflammation, relative to WT MDSCs. *In vitro* inflammation assays demonstrated that MDSCs secrete factors that modulate cytokine expression in LPS-activated macrophages, and genetic reduction of p65 enhanced this effect. Finally, deletion of one p65 allele in a murine model of Duchenne muscular dystrophy (mdx) increased the expression of the anti-inflammatory factor hepatocyte growth factor (HGF) and was associated with disease improvement.

MATERIALS AND METHODS

Mice: C57Bl/6 (WT) mice were purchased from the Jackson Laboratory (Bar Harbor, ME). P65$^{+/-}$ mice were bred with *mdx* mice to produce mdx/p65$^{+/-}$ and mdx/p65$^{+/+}$ mice. PCR analysis of tail samples was used for genotyping.

Cell Isolation: MDSCs were isolated from five month old (n=3) *p65*$^{+/+}$ or *p65*$^{+/-}$ mice via a modified preplate technique [2]. A population of slowly adhering cells was obtained and expanded in proliferation medium (PM, DMEM containing 10% fetal bovine serum (FBS), 10% horse serum, 1% penicillin-streptomycin, and 0.5% chick embryo extract).

In vivo regeneration assay: Muscle injury was induced in C57Bl/6J mice by the injection of cardiotoxin (4uM) into the gastrocnemius muscle. One day later, MDSCs were injected into the injured muscles. Muscles were harvested 1, 3, and 7 days post-injury. Serial cryosections were prepared and immunohistochemistry was performed to assess inflammation (F480, Gr-1). Gross tissue histology was performed by hematoxylin and eosin (H&E) staining.

In vitro Inflammation Model: MDSCs were grown for 24 hours in proliferation medium, after which the medium was collected and sterile filtered. RAW264.7 cells, immortal murine macrophage-like cells, were activated by exposure to 100 ng/mL LPS in either PM, *p65*$^{+/+}$-, or *p65*$^{+/-}$- conditioned medium for 30 min, 3 hours, and 24 hours. At each time point, RNA was collected for real time RT-PCR analysis or lysates were collected for western blot.

RESULTS

Confirming our previous report [1], we found that by 7 days, p65$^{+/-}$ cell engraftments were associated with reduced numbers of F4/80+ cells, compared to WT cell engraftments (Fig 1A). This can be further demonstrated histologically by H&E staining, revealing a reduction in mono-nuclear cells at sites of injury one week post injection (Fig 1B).

To look at the direct effects of MDSC-secreted factors, we performed *in vitro* inflammation assays. Briefly, RAW264.7 macrophages were activated with LPS (100ng/mL) in normal PM or WT or p65$^{+/-}$ conditioned medium (CM) (Fig 2A). The expression of the cytokines IL-1β and IL-6 was determined by real time (RT-PCR). Our results demonstrated that MDSC-CM significantly attenuates cytokine expression (Fig 2B).

Figure 1.

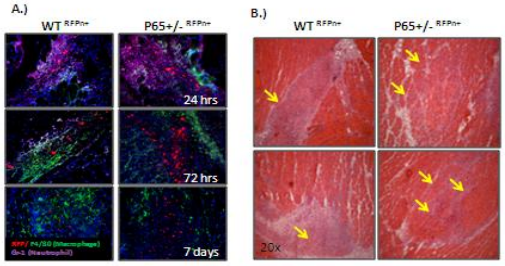

Although WT and p65$^{+/-}$ CM had a similar effect, we found that p65$^{+/-}$ CM exerted a stronger suppression of IL-6 expression. Previous reports have found that the activation of inflammatory macrophages is attenuated by the phosphorylation and subsequent inactivation of GSK3β [3]. By western blot, we found that upon treatment with LPS in WT-CM, the fraction of pS9-GSK3beta modestly increased within 30mins and was maintained through 24 hours. Furthermore, p65$^{+/-}$-CM demonstrated an even stronger induction of phosphorylation.

Figure 2.

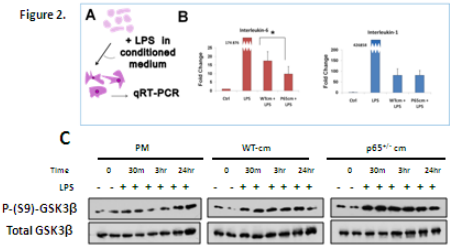

Hepatocyte growth factor (HGF) is one of the factors previously demonstrated to modulate inflammation via pS9-GSK3beta. We examined HGF expression in MDSCs and found elevated levels in p65$^{+/-}$ cells compared to the WT cells. Acharyya and colleagues have reported that haploinsufficiency of p65 in an mdx background improves dystrophic pathology [4]. As we had hypothesized, HGF expression was significantly increased. Based on our *in vitro* and *in vivo* inflammatory studies, HGF could be one of the contributing factors to disease improvement.

Figure 3.

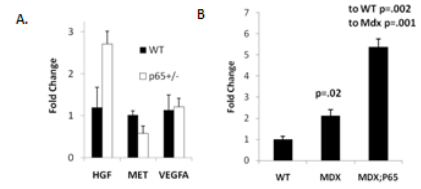

DISCUSSION

These findings indicate that NF-kB has a broader role in muscle stem and progenitor cells than previously thought, and that the anti-inflammatory molecules secreted by stem cells, such as HGF, could potentially be harnessed to control secondary pathologies of muscle diseases such as DMD.

REFERENCES

[1]Lu, A., et al, Mol Ther 2012, 20(3);661-68. [2] Gharaibeh, et al. Nat Protoc. 2008; 3:1501-9. [3] Beurel, E., et al, Trends Immunol 2010; 3-(1):24-31 [4]Acharyya, S., et al., J Clin Invest 2007, 117:889-901.

Improved muscle histology in old dystrophic mice exposed to young dystrophic peripheral circulation: a parabiotic paring study

Aiping Lu, Hongshuai Li, ying Tang, Xiaodong Mu, Minakshi Poddar, Bing Wang, Johnny Huard
Stem Cell Research Center, Department of Orthopaedic Surgery, University of Pittsburgh, Pittsburgh, PA

Introduction

Researchers have observed that in Duchenne muscular dystrophy (DMD), despite the lack of dystrophin at birth, the histopathological signs of muscle weakness do not become apparent until patients reach 4-8 years of age. This happens to coincide with the exhaustion of the muscle progenitor cell (MPC) pool. Our previous results demonstrated that MPCs isolated from old dystrophin/utrophin double knock-out (dKO) mice (a reliable mouse model of DMD), are defective in their proliferation and differentiation capacities, however, it remains unclear if the disease-related loss of adult stem cell function is primarily driven by cell autonomous (a direct stem cell defect) and/or non-autonomous mechanisms (aged microenvironment or circulating factors). The parabiotic approach has been useful for revealing the striking ability of circulating factors in young mice to rejuvenate the muscle regenerative potential in old animals (1). In this study, we preformed heterochronic parabiosis between old dKO-hetero with young mdx mice. We tested whether muscle histopathology can be improved by blood-borne factors in vivo using a parabiotic system to enable constant exchange of peripheral blood between the mice. We found that there was decreased fibrosis, calcium deposition and improved histology of skeletal muscle, and decreased intramyocardial lipid accumulation in the old dKO-hetero mice after parabiotic pairing for 3 months. The results suggested that the defect in the MPCs might be related to the dystrophic microenvironment or circulating factors. These observations suggest that changing the dystrophic microenvironment could be a new approach to improve muscle weakness in DMD patients, despite their continued lack of dystrophin expression.

Methods

Animals and parabiosis: Two animal models of DMD were used in this study, the 1st was the mdx mouse which has mild skeletal muscle defects and potent regenerative capacity and the 2nd was the dKO mouse which is a more severely affected model of DMD. Since dKO-homo mice (dystrophin$^{-/-}$utrophin$^{-/-}$) are too sick and unable to survive surgical pairing, we choose to use old dKO-hetero mice (dystrophin$^{-/-}$utrophin$^{+/-}$) which have a similar phenotype to the dKO-homo mice, albeit at a later stage of life. The parabiotic surgery was conducted following procedures previously described (2).Two animals of the same age (old dKO-hetero-to-old dKO-hetero) were the control isochronic pairs, while young mdx-to-old dKO-hetero pairs were the experimental heterochronic parabionts. An intravascular dye (Evan's Blue) was injected into one of the mouse's tail veins prior to sacrifice.

Flow cytometry analysis: The MPCs isolated from normal mice were transduced with GFP and then injected into the tail vein of the young mdx mice. Blood was then drawn from both mice and GFP positive cells were analyzed by flow cytometry to demonstrate the mice had a shared circulatory system.

Histology: 3 months after parabiosis the mice were sacrificed, and the muscle and heart were harvested. H&E, Alizarin red and Trichrome staining were preformed according to the manufacturer's instructions. Intramyocellular lipid accumulation was detected by AdipoRed assay.

Results:

1. Peripheral blood cross-circulation and the redistribution of circulating cells were established between the two parabiotic mice. To verify the development of cross-circulation between animals, we examined the distribution of an intravascular dye (Evan's Blue) across the adjoining wounds. After injecting one of the paired mice, the Evan's Blue dye immediately

flushed the same animal and progressively spread through the common vascular tree at the junction to its partner, as shown in **Figure1**. We also found that MPCs could travel from one mouse to its parabiotic partner by the intravenous injection of GFP positive MPCs (**Figure1**).

2. *Improved muscle histology in old dKO-hetero mice exposed to young mdx peripheral circulation.* We performed parabiosis between young mdx mice (3-5 months) and old dKO-hetero mice (12-14 months)**.** These heterochronic pairs were compared to the old isochronic paired mice. The H&E results indicated that the skeletal muscles were greatly improved in their histopathological appearance in the old dKO-hetero mice sutured with young mdx mice when compared to old isochronic paired mice. Alizarin red and Trichrome results also showed there was less calcium deposition and decreased fibrotic muscle fibers in the old heterochronic mice compared to old isochronic paired mice (**Fig.2A**).The AdipoRed staining of the cardiac muscle of the parabiotic mice also revealed reduced intramyocardial lipid accumulation in the cardiac muscle cells of the old heterochronic mice compared to the old isochronic paired mice (**Fig.2B**).

Discussion:

In order to determine if disease-related loss of MPCs function is primarily driven by cell autonomous and/or non-autonomous mechanisms and to further develop a new approach to improve the quality of life of DMD patient's without restoring dystyophin. These experiments were motivated by the question of whether blood-borne factors from young healthy mdx mice could influence the dystrophic microenvironment and improve the histopathology of old dKO-hetero mice. Our results indicated that the skeletal muscles were greatly improved in their histopathological appearance in the old dKO-hetero mice and decreased intramyocardial lipid accumulation in cardiac muscle when sutured with young mdx mice compared to old isochronic paired mice. These parabiosis results provided some evidence which suggested that the defect in the MPCs is driven by the dystrophic microenvironment which might be, in part, attributable to changes in the blood-borne factors passed on from the young mdx mice to the old dKO-hetero mice. Moreover, these histological improvements may relate to a beneficial effect on the dystrophic MPCs due to circulating factors in the blood of the young mdx mice. These observations demonstrated that changes to the dystrophic microenvironment could be a new approach to improving muscle weakness in DMD patients, despite their continued lack of dystrophin expression.

Significance:

We believe that the information gained from these experiments highlight potential treatment regimes that could rescue the stem cell defect in muscular dystrophy and could prove to be highly successful in delaying the disease progression in DMD.

Figure1

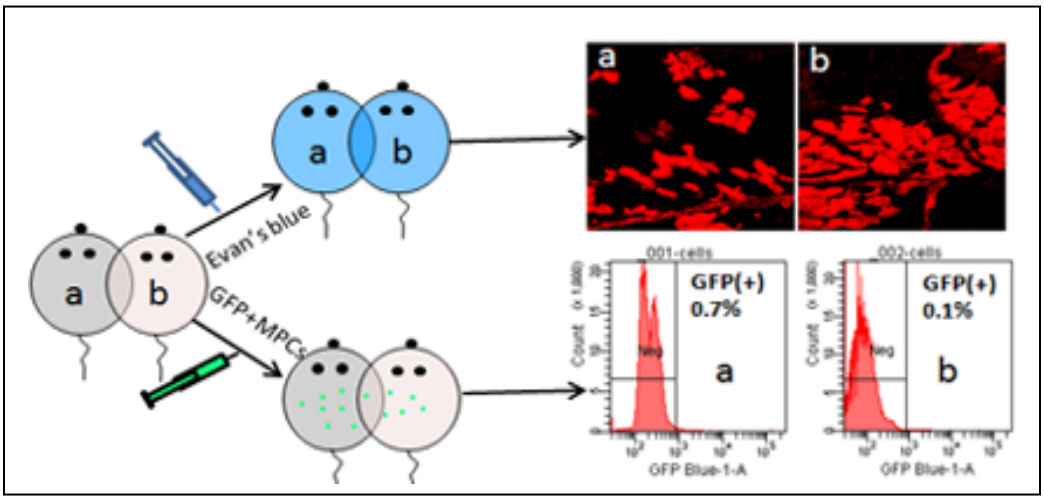

Figure 2

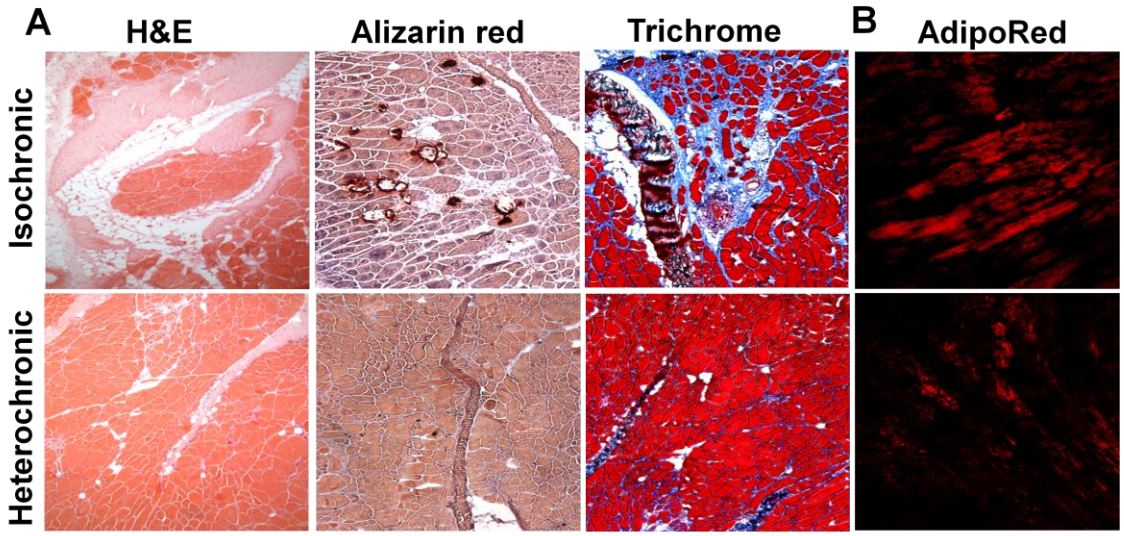

Reference

1. Conboy IM, Conboy MJ, Wagers AJ, Girma ER, Weissman IL, Rando TA. Rejuvenation of aged progenitor cells by exposure to a young systemic environment. Nature. 2005;433(7027):760-4.

2. Boban I, Barisic-Dujmovic T, Clark SH. Parabiosis and transplantation models show no evidence of circulating dermal fibroblast progenitors in bleomycin-induced skin fibrosis. J Cell Physiol. 2008;214(1):230-7.